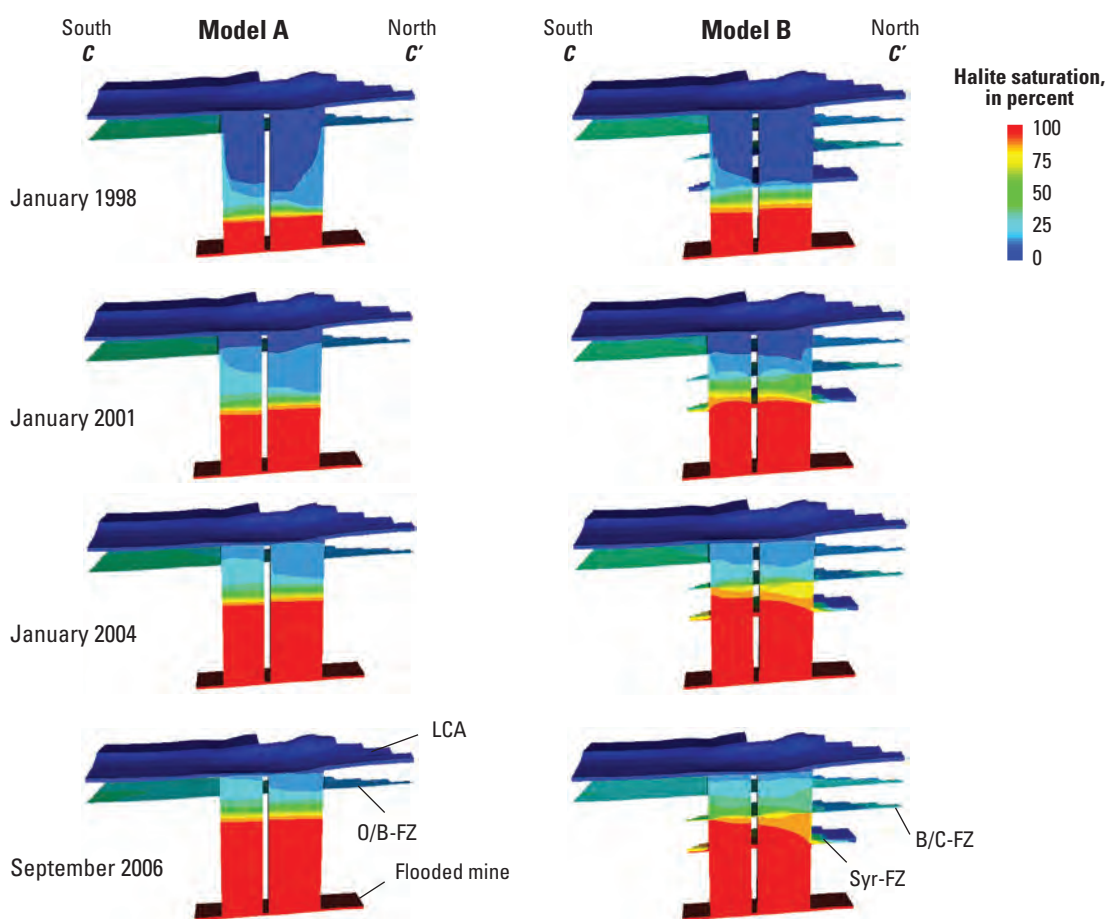**Prepared in cooperation with the
Office of the New York State Attorney General**

Brine Migration from a Flooded Salt Mine in the Genesee Valley, Livingston County, New York: Geochemical Modeling and Simulation of Variable-Density Flow

Professional Paper 1767

**U.S. Department of the Interior
U.S. Geological Survey**

Brine Migration from a Flooded Salt Mine in the Genesee Valley, Livingston County, New York: Geochemical Modeling and Simulation of Variable-Density Flow

By Richard M. Yager, Paul E. Misut, Christian D. Langevin, and David L. Parkhurst

Professional Paper 1767

U.S. Department of the Interior
U.S. Geological Survey

U.S. Department of the Interior
KEN SALAZAR, Secretary

U.S. Geological Survey
Suzette M. Kimball, Acting Director

U.S. Geological Survey, Reston, Virginia: 2009

Contents

Figures

Tables

Conversion Factors and Datum

Multiply	By	To obtain
Length		
centimeter (cm)	0.3937	inch (in.)
millimeter (mm)	0.03937	inch (in.)
meter (m)	3.281	foot (ft)
meter (m)	1.094	yard (yd)
kilometer (km)	0.6214	mile (mi)
kilometer (km)	0.5400	mile, nautical (nmi)
Area		
square meter (m^2)	0.0002471	acre
hectare (ha)	2.471	acre
hectare (ha)	0.003861	square mile (mi^2)
square kilometer (km^2)	247.1	acre
square centimeter (cm^2)	0.001076	square foot (ft^2)
square meter (m^2)	10.76	square foot (ft^2)
square centimeter (cm^2)	0.1550	square inch (ft^2)
square kilometer (km^2)	0.3861	square mile (mi^2)
Volume		
cubic meter (m^3)	6.290	barrel (petroleum, 1 barrel = 42 gal)
liter (L)	33.82	ounce, fluid (fl. oz)
liter (L)	2.113	pint (pt)
liter (L)	1.057	quart (qt)
liter (L)	0.2642	gallon (gal)
liter (L)	61.02	cubic inch (in^3)
cubic meter (m^3)	264.2	gallon (gal)
cubic meter (m^3)	0.0002642	million gallons (Mgal)
cubic centimeter (cm^3)	0.06102	cubic inch (in^3)
cubic meter (m^3)	35.31	cubic foot (ft^3)
cubic meter (m^3)	1.308	cubic yard (yd^3)
cubic meter (m^3)	0.0008107	acre-foot (acre-ft)
Flow rate		
meter per day (m/d)	3.281	foot per day (ft/d)
cubic meter per day (m^3/d)	35.31	cubic foot per day (ft^3/d)
liter per second (L/s)	15.85	gallon per minute (gal/min)
cubic meter per day (m^3/d)	264.2	gallon per day (gal/d)
centimeter per year (cm/yr)	0.3937	inch per year (in/yr)
Mass		
gram (g)	0.03527	ounce, avoirdupois (oz)
kilogram (kg)	2.205	pound avoirdupois (lb)
metric ton per year (t/yr)	1.102	ton per year (ton/yr)
Density		
gram per cubic centimeter (g/cm^3)	62.4220	pound per cubic foot (lb/ft^3)
Hydraulic conductivity		
meter per day (m/d)	3.281	foot per day (ft/d)
Transmissivity*		
meter squared per day (m^2/d)	10.76	foot squared per day (ft^2/d)

Temperature in degrees Celsius (°C) may be converted to degrees Fahrenheit (°F) as follows:

$$°F = (1.8 \times °C) + 32$$

Temperature in degrees Fahrenheit (°F) may be converted to degrees Celsius (°C) as follows:

$$°C = (°F - 32) / 1.8$$

Vertical coordinate information is referenced to the North American Vertical Datum of 1988 (NAVD 88).

Horizontal coordinate information is referenced to the North American Datum of 1983 (NAD 83).

Elevation, as used in this report, refers to distance above or below the vertical datum.

*Transmissivity: The standard unit for transmissivity is cubic foot per day per square foot times foot of aquifer thickness [$(ft^3/d)/ft^2$]ft. In this report, the mathematically reduced form, foot squared per day (ft^2/d), is used for convenience.

Specific conductance is given in millisiemens per centimeter at 25 degrees Celsius (mS/cm at 25°C).

Concentrations of chemical constituents in water are given in either milligrams per liter (mg/L) or micrograms per liter (µg/L).

THIS PAGE INTENTIONALLY LEFT BLANK

Brine Migration from a Flooded Salt Mine in the Genesee Valley, Livingston County, New York: Geochemical Modeling and Simulation of Variable-Density Flow

By Richard M. Yager, Paul E. Misut, Christian D. Langevin, and David L. Parkhurst

Abstract

The Retsof salt mine in upstate New York was flooded from 1994 to 1996 after two roof collapses created rubble chimneys in overlying bedrock that intersected a confined aquifer in glacial sediments. The mine now contains about 60 billion liters of saturated halite brine that is slowly being displaced as the weight of overlying sediments causes the mine cavity to close, a process that could last several hundred years. Saline water was detected in the confined aquifer in 2002, and a brine-mitigation project that includes pumping followed by onsite desalination was implemented in 2006 to prevent further migration of saline water from the collapse area. A study was conducted by the U.S. Geological Survey using geochemical and variable-density flow modeling to determine sources of salinity in the confined aquifer and to assess (1) processes that control movement and mixing of waters in the collapse area, (2) the effect of pumping on salinity, and (3) the potential for anhydrite dissolution and subsequent land subsidence resulting from mixing of waters induced by pumping.

The primary source of salinity in the collapse area is halite brine that was displaced from the flooded mine and transported upward by advection and dispersion through the rubble chimneys and surrounding deformation zone. Geochemical and variable-density modeling indicate that salinity in the upper part of the collapse area is partly derived from inflow of saline water from bedrock fracture zones during water-level recovery (January 1996 through August 2006). The lateral diversion of brine into bedrock fracture zones promoted the upward migration of mine water through mixing with lower density waters. The relative contributions of mine water, bedrock water, and aquifer water to the observed salinity profile within the collapse area are controlled by the rates of flow to and from bedrock fracture zones. Variable-density simulations of water-level recovery indicate that saline water has probably not migrated beyond the collapse area, while simulations of pumping indicate that further upward migration of brine and saline water is now prevented by groundwater withdrawals under the brine-mitigation project. Geochemical modeling indicates that additional land subsidence as a result of anhydrite dissolution in the collapse area is not a concern, as long as the rate of brine pumping is less than the rate of upward flow of brine from the flooded mine.

The collapse area above the flooded salt mine is within a glacially scoured bedrock valley that is filled with more than 150 meters of glacial drift. A confined aquifer at the bottom of the glacial sediments (referred to as the lower confined aquifer, or LCA) was the source of most of the water that flooded the mine. Two rubble chimneys that formed above the roof collapses in 1994 hydraulically connect the flooded mine to the LCA through 180 meters of sedimentary rock. From 1996 through 2006, water levels in the aquifer system recovered and the brine-displacement rate ranged from 4.4 to 1.6 liters per second, as estimated from land-surface subsidence above the mine. A zone of fracturing within the bedrock (the deformation zone) formed around the rubble chimneys as rock layers sagged toward the mine cavity after the roof collapses. Borehole geophysical surveys have identified three saline-water-bearing fracture zones in the bedrock: at stratigraphic contacts between the Onondaga and Bertie Limestones (O/B-FZ) and the Bertie Limestone and the Camillus Shale (B/C-FZ), and in the Syracuse Formation (Syr-FZ). The only outlets for brine displaced from the mine are through the rubble chimneys, but some of the brine could be diverted laterally into fracture zones in the rocks that lie between the mine and the LCA.

Inverse geochemical models developed using PHREEQC indicate that halite brine in the flooded mine is derived from a mixture of freshwater from the LCA (81 percent), saline water from bedrock fracture zones (16 percent), and an hypothesized bromide-rich brine (3 percent) assumed to originate from salt-bearing rocks above the flooded mine. Geochemical modeling results also indicate that halite brine entering the rubble chimneys is diluted by both bedrock water and aquifer water, and that water from the mine has not reached the bedrock surface. Forward geochemical models indicate that

additional land subsidence could occur if pumping from the brine-mitigation project were to introduce either freshwater or bedrock water that is undersaturated with respect to anhydrite into the lower part of the rubble chimneys. In this unlikely scenario, the maximum subsidence rates are predicted to range from 0.6 to 1.1 centimeters per year—subsidence rates would be lower (0.1 to 0.6 centimeters per year) if ion-exchange reactions affect the water chemistry.

Variable-density, transient groundwater-flow models were constructed using SEAWAT to simulate the movement of saline water, aquifer water, bedrock water, and brine within the rubble chimneys and surrounding deformation zone during the 10.7-year period following flooding of the salt mine. Two three-dimensional models reproduced the profile of halite saturation with depth measured in September 2006 reasonably well, and neither model indicated that saline water had migrated beyond the collapse area. The models differed in the number of fracture zones represented: one zone in model A (O/B-FZ) and three zones in model B (O/B-FZ, B/C-FZ, and Syr-FZ). It is unknown whether model A or model B better represents current conditions because the lateral extents of the B/C-FZ and Syr-FZ have not been delineated beyond the collapse area.

In model A, the salinity of water in the upper part of the rubble chimneys is derived mainly from the inflow of bedrock water from the O/B-FZ, as indicated by geochemical models. Bedrock water that was pushed upward by brine during the 10.7-year simulation period formed a diffuse front above a nearly horizontal brine level in both chimneys. In model B, some of the salinity in the upper part of the rubble chimneys is derived from mine water. The rate of bedrock-water inflow from the O/B-FZ was lower in model B than in model A, and mixing with waters from the Syr-FZ and B/C-FZ transported mine water higher in the water column than in model A. Simulated brine levels in both chimneys sloped northward, reflecting lateral diversion of brine into the B/C-FZ, and less aquifer water was displaced from the collapse area than in model A.

Models A and B were used to simulate changes in water levels and salinity produced by pumping for the brine-mitigation project from September 2006 through February 2008. Both simulations indicated that current pumping rates are sufficient to offset upward migration of brine and saline water through the collapse area and, therefore, to further prevent contamination of the LCA. A greater decrease in salinity was simulated in model B, however, because the porosity of the rubble chimneys was lower (6 percent compared to 10 percent in model A), and some brine and saline waters were diverted through the B/C-FZ. Model B better simulates the influent saturation to the desalination plant, the amount of halite produced, and the observed declines in saturations than model A, which is more consistent with results of geochemical modeling. Sensitivity analyses indicate that the actual brine-displacement rate could be lower than estimated because simulated declines in saturations

underpredict the observed decline from September 2006 through February 2008.

Although halite saturations within the upper part of the collapse area are predicted to decrease with continued pumping, brine displacement from the flooded mine is expected to continue for hundreds of years. Simulations of a shutdown of the brine-mitigation project indicate southward migration of saline water through the LCA, extending 700 meters to the model boundary within 10 years. Continued migration of saline water would eventually form a pool in the LCA in a bedrock depression 8 kilometers south of the collapse area near Sonyea, but the large relative density of the saline water would likely prevent it from reaching overlying aquifers. Simulations also indicate that brine will migrate through bedrock fracture zones—some brine could possibly emerge updip to the north where the subcrop area of the Bertie Limestone intersects the bedrock surface near Avon, but the projected time of travel is unknown.

Introduction

Salt-mine flooding is a common occurrence worldwide and is typically caused by water inflow through improperly sealed shafts or wells, sometimes with catastrophic results (Berest and others, 2004). A mine in a domal salt formation at Jefferson Island, Louisiana (USA), was penetrated by an oil exploration borehole, drained an overlying lake, and was flooded in a few hours (Thoms and Gehle, 1994). Although mined salt is relatively impermeable, pathways created by mining operations between a mine and adjacent aquifers or surface water can provide avenues for flow—small inflow rates can increase substantially over time as undersaturated water dissolves salt and enlarges the pathway. A potash mine operated at Ronneberg, Germany, from 1905 to 1973 was abandoned in 1975 after inflow rates increased by three orders of magnitude to more than 15 m^3/min (250 L/s) (Rolleke, 2000).

Flooding of abandoned salt mines has also caused catastrophic failures, for example, in Ireland and Kansas, USA (Berest and others, 2004). Abandoned salt mines have been intentionally flooded and sealed to minimize the potential for collapse (Berest and others, 2004). Salt-mine cavities generally close gradually over a period of centuries as salt pillars that support the roof deform and contract, causing the mine roof to sag. Inundating the mine with brine or even freshwater can increase the stability of the mine by increasing the formation pressure within the mine cavity, thereby reducing the mine-closure rate (Van Sambeek and Thoms, 2000).

The Retsof salt mine in upstate New York (fig. 1) was one of the world's largest salt mines (26 km^2) and historically dry, but had to be abandoned after roof collapses in the spring of 1994 triggered flooding by water from overlying aquifers. The roof collapses propagated upward through 180 m of
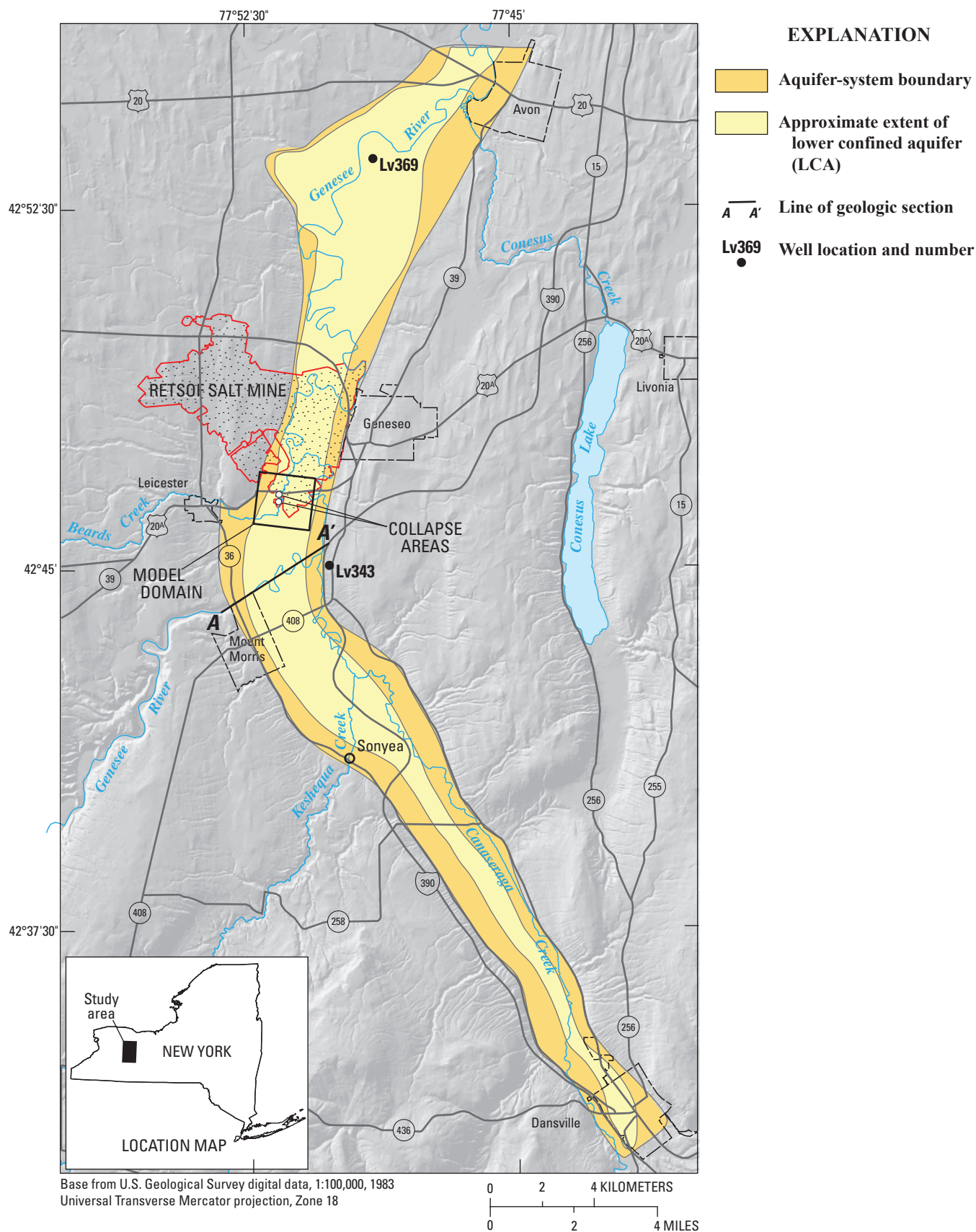
Figure 1. Location of aquifer system and Retsof salt mine in Livingston County, N.Y.

bedrock and formed two sinkholes filled with fractured rock (hereinafter referred to as "rubble chimneys") that connected the mine to water-bearing fracture zones in the bedrock and a confined aquifer in the glacial drift (LCA, fig. 2). Two depressions as much as 150 m in diameter and 18 m deep appeared at land surface above the rubble chimneys after glacial sediments slumped into cavities that formed in the underlying bedrock. Groundwater flowed from the aquifer through the rubble chimneys and into the mine at an average rate of 76 m^3/min (1,300 L/s), until the mine was completely flooded in January 1996. Flooding of the mine caused widespread drawdown, causing water levels in the LCA to decline by as much as 120 m near the collapse area by January 1996 (Yager and others, 2001). Water-level declines in the LCA also caused exsolution of methane gas from groundwater, which migrated to land surface (Yager and Fountain, 2001). Dissolution of salt pillars within the mine cavity increased the rate of mine closure, causing land subsidence that ranged from 0.3 to 5 m over different areas of the mine by February 1996 (New York State Department of Environmental Conservation, 1997). Additional subsidence also occurred beyond the extent of the mined area as thick clay confining units were partially dewatered in response to water-level drawdown.

By 2005, water levels in the LCA had nearly recovered to pre-collapse conditions when the rate of land subsidence had decreased to 1 cm/yr, but the hydraulic connection that was created between the mine cavity and the aquifer through the two rubble chimneys is still present. About 60 billion L of saturated halite brine now resides in the mine cavity, which is expected to close slowly over a period of several hundred years as the unmined salt deforms under the weight of overlying rock (John T. Boyd Company, 1995). As the mine cavity closes, about 80 percent of the brine could be displaced and migrate upward through the rubble chimneys toward the LCA (L.L. Van Sambeek, RE/SPEC, Inc., written commun., 2007). Although not currently used as a water supply, the aquifer represents a significant potential resource of potable water that could be damaged by the intrusion of saline water. In 2002, the chloride concentration of water sampled from the LCA near the collapse area was about 20,000 mg/L, indicating that saline water migrating through the rubble chimneys had reached the aquifer.

There are two possible sources of saline water that could migrate through the rubble chimneys and contaminate freshwater in the LCA: (1) saline water (chloride concentration of 29,000 mg/L) flowing through carbonate rocks between the mine and the aquifer, and (2) saturated halite brine (greater than 90-percent halite saturation) displaced from the flooded mine cavity. A brine-mitigation project that includes pumping and desalination of saline

water and brine from the collapse area was implemented in 2006 to limit contamination of the LCA (Alpha Geoscience, 2007). Pumping will cause mixing of three different waters: saturated halite brine from the mine, saline water from carbonate bedrock, and freshwater from the LCA. Mixing of high-salinity fluids with fresher waters could alter water chemistry and induce chemical reactions that might dissolve or precipitate minerals in the collapse area. A particular concern is that mixing could create waters that would dissolve anhydrite in the rubble chimneys. This possibility is indicated by the solubility curve in figure 3 (modified from Runnells, 1969), which shows that a mixture of freshwater and brine (represented by points A and B) would be undersaturated with respect to anhydrite (point C) and, therefore, cause dissolution of the mineral. Dissolution of anhydrite would enhance void formation and further destabilize the rubble chimneys, leading to additional land subsidence.

An understanding of the hydraulic and chemical processes that control the movement of saline water and brine in the collapse area will greatly improve the likelihood of success of the brine-mitigation project. In October 2006, the U.S. Geological Survey (USGS) began a cooperative study with the Office of the New York State Attorney General to assess the significance of the potential sources of salinity and to examine the factors that control the movement and mixing of waters in the collapse area through the application of geochemical and variable-density flow models. A further objective of the study was to assess the potential for dissolution and land subsidence as a result of pumping and migration of saline water.

This report describes the hydrogeologic setting and the effects of mine flooding and water-level recovery on the aquifer system in the Genesee Valley. The report also describes current conditions in the collapse area and the brine-mitigation project. The application of geochemical modeling is discussed, including (1) inverse models used to identify mixing proportions of initial waters and water-rock reactions that explain the observed water chemistry in the collapse area, and (2) forward models used to assess the potential for mineral dissolution and land subsidence resulting from mixing induced by pumping from the brine-mitigation project. The report documents the design and application of variable-density flow models that were used to simulate migration of brine and saline water during the 10.7-year period while water levels recovered after the mine flooding. Additional model simulations are also presented to predict changes in salinity in response to pumping from the brine-mitigation project. Finally, the implications of model results for future mitigation plans are discussed.
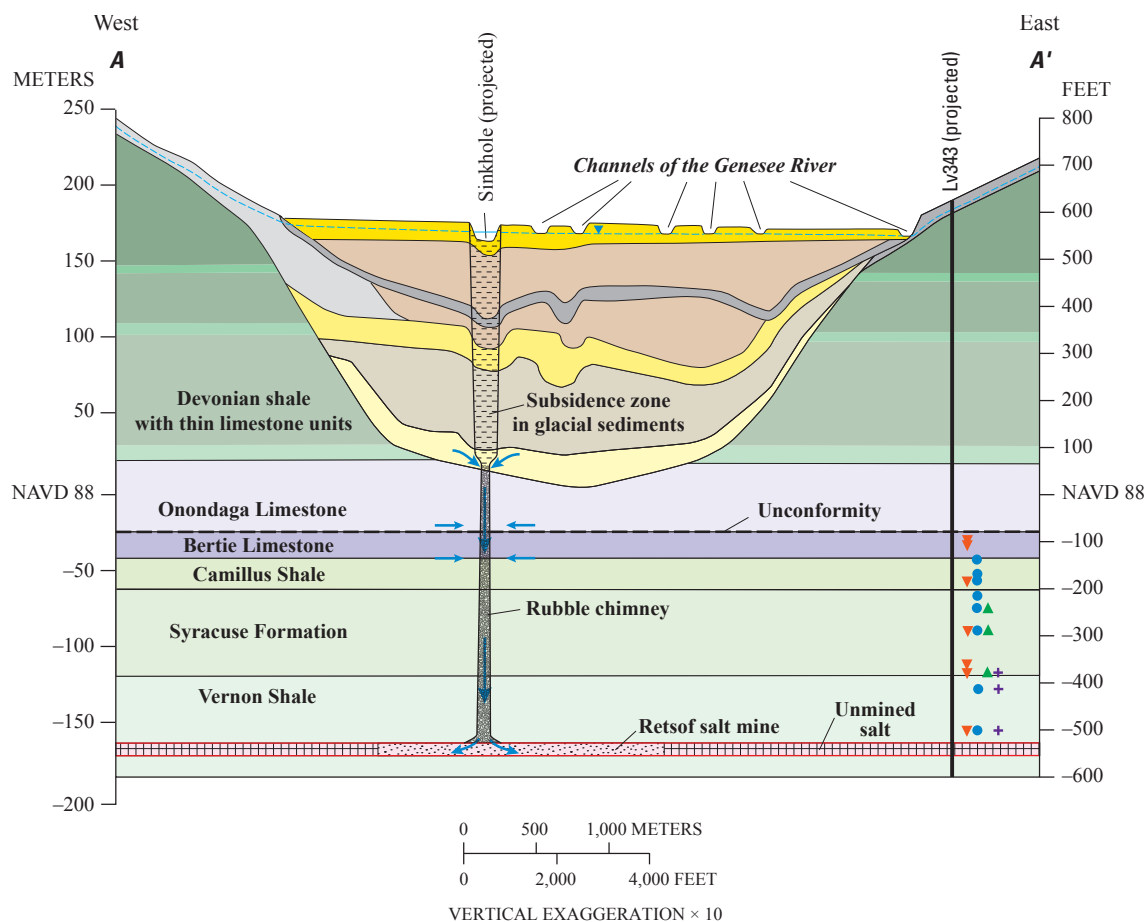
Figure 2. Stratigraphic section A-A' depicting rubble chimney above collapsed room in salt mine, Livingston County, N.Y.
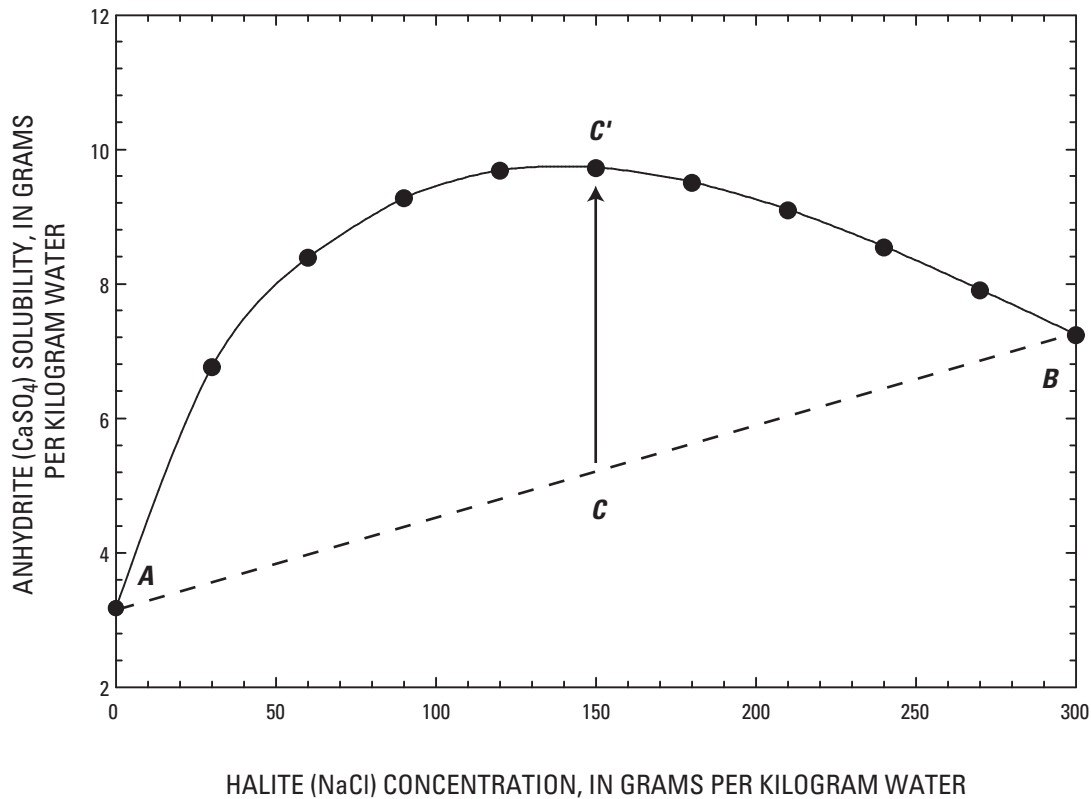
Figure 3.   Solubility of anhydrite ($CaSO_4$) at 10°C as a function of halite content (NaCl) in solution (solid line). Mixing equal volumes of freshwater *(A)* with brine *(B)* produces a mixture *(C)* that is undersaturated with respect to anhydrite (dashed line), resulting in dissolution to attain equilibrium (C′). (Modified from Runnells, 1969).

Hydrogeologic Setting

The collapse area overlying the flooded Retsof salt mine is within a bedrock valley that was deepened and widened by ice during the Pleistocene Epoch. The bedrock valley is partly filled with glacial drift more than 150 m thick deposited during the last deglaciation. The distribution of coarse-grained and fine-grained sediments in the glacial drift has created a flow system that consists of three aquifers separated by two confining layers (fig. 2). The uppermost (unconfined) aquifer consists of alluvial sediments 6 to 8 m thick, the middle confined aquifer consists of glaciofluvial sand and gravel 3 to 5 m thick, and the lower confined aquifer consists of glaciofluvial sand and gravel about 8 m thick overlying the bedrock valley floor (Yager and others, 2001). The two confining layers are each as much as 75 m thick and consist primarily of lacustrine sediments. The LCA was the principal source of water that flooded the mine.

The Onondaga Limestone of Devonian age forms the bedrock valley floor in the collapse area and is overlain by younger Devonian rock (primarily shale) that forms the valley walls and uplands. The bedrock units below the Onondaga Limestone are of Silurian age and include the Bertie Limestone and the salt-bearing shale and dolostone in the upper part of the Salina Group. The flooded salt mine is located in the Vernon Shale and about 180 m of rock separates the mined salt bed from the bedrock surface (fig. 2). All bedrock units dip to the south at less than 1° and are largely undeformed. A regional unconformity separates the late Silurian Bertie Limestone from the Middle Devonian Onondaga Limestone. A fracture zone at this stratigraphic contact is an extensive water-bearing zone that discharged 4.1 L/s of water in 1986 to a shaft in the Retsof salt mine 2 km northwest of the collapse area (R.F. Langill and Associates, 1990).

The mineralogy of 15 bedrock samples was identified using quantitative x-ray diffraction by a USGS laboratory in Boulder, CO. The samples were taken from rock core collected in borehole Lv343 located 3 km southeast of the collapse area (fig. 1). The principal minerals present in the Silurian rocks (Bertie Limestone and Salina Group) were Fe-dolomite, anhydrite, and halite, with lesser amounts of calcite, K-feldspar, and quartz (fig. 2). Significant quantities of clay minerals (>20 percent by weight) also were present in the Syracuse Formation of the Salina Group. Fe-dolomite and anhydrite are present throughout the Silurian rocks above the flooded mine, whereas halite is found in the lower part of the Syracuse Formation and in the Vernon Shale.

Mine Flooding and Aftermath

Flooding and Formation of Rubble Chimneys

Roof collapses in two panels (mining areas) within the salt mine (2YS and 11YW, fig. 4) propagated upward through 180 m of overlying bedrock in stages from March 12 through April 14, 1994. Inflow from water-bearing fracture zones intersected by the expanding rubble chimneys (fig. 2) discharged 20 m^3/min (330 L/s) of 98-percent halite-saturated brine to the mine after the first collapse in panel 2YS on March 12 (Gowan and Trader, 2000b). The rate of inflow increased to 49 m^3/min (820 L/s) of saline water (62 percent saturated) by April 2 and increased again to 76 m^3/min (1,300 L/s) by April 14 once the bedrock surface was breached, allowing freshwater from the LCA to flow through the rubble chimneys and into the mine. Two large sinkholes appeared above the collapse panels at land surface on April 6 and May 25 (fig. 4). Mining was halted in September 1995 and the mine was completely inundated in January 1996, by which time the access shafts to the mine had been sealed.

Gowan and Trader (2000b) concluded that the rubble chimneys formed as voids were created through dissolution of evaporites within the collapsing rock column. This void formation would account for the offset of more than 13 m in the bedrock surface detected by seismic-reflection surveys (Dobecki Earth Sciences, Inc., 1994); in contrast, the ceiling height in the mined salt panels was only 3.7 m. The overlying unconsolidated sediments slumped into the depression formed in the bedrock surface, causing the sinkholes at land surface, but no direct connection was created in the collapse area between the LCA and the overlying aquifers. Drilling and borehole geophysical surveys conducted in 2004 indicated that the rubble chimneys are surrounded by a zone of fracturing within the bedrock that probably formed as the rock layers sagged toward the mine cavity after the roof collapses (Alpha Geoscience, 2005). This zone of fracturing is referred to as the "deformation zone" in this report, and the rubble chimneys and surrounding deformation zone are collectively referred to as the "collapse area."

Several borehole geophysical surveys were conducted by the USGS in 1994 immediately following the collapse of the two panels and prior to the formation of the second sinkhole above 11YW (Williams, 1996). The survey results indicated that water flowing through two fracture zones in the bedrock toward the rubble chimneys resulted in downward flow through wells. The largest flows (7 to 13 L/s) measured in three wells exited at the stratigraphic contact between the Onondaga and Bertie Limestones that coincides with the unconformity between Devonian and Silurian rocks. A smaller flow (0.9 L/s) measured in one well exited at a lower contact between the Bertie Limestone and the Camillus Shale. The geophysical logging also measured the specific conductance of water in the following water-bearing zones: (1) LCA, 1 to 2.5 mS/cm (Lv309, Lv326, and Lv328); (2) Onondaga Limestone, 10 mS/cm (Lv305); and (3) Bertie/Camillus contact, 50 mS/cm (Lv305) (Williams, 1996).

Flowmeter logs in well Lv309 (located between the rubble chimneys; see appendix for information on wells and boreholes referenced in this report) indicated that three water-bearing zones intersected the well (1) at the bottom of the casing at 160-m depth, (2) at the Onondaga/Bertie contact (O/B-FZ) at 183-m depth, and (3) at the Bertie/Camillus contact (B/C-FZ) at 206-m depth (fig. 5). These water-bearing zones corresponded to deflections on the caliper log that indicated enlargements in the borehole diameter. The flowmeter log indicated that water entered the well below the casing at the bedrock surface, flowed downward, and exited at the O/B-FZ, indicating hydraulic connection between the fracture zone and the rubble chimneys. The specific-conductance log indicated that freshwater (<6 mS/cm) occupied nearly the entire well as the result of downward flow from below casing, and also detected a small fracture zone in the Syr-FZ.

Well Lv309 was logged again by the USGS in March 2004, more than 8 years after the mine was inundated. Detailed comparison of gamma logs from before (April 1994) and after (March 2004) formation of the rubble chimneys indicates that the thickness of the Bertie Limestone in the collapse area had increased by about 3 m, indicating that parts of this unit broke apart during formation of the rubble chimneys. This conclusion is consistent with caliper and acoustic televiewer logs that show broken zones and voids in the lower 6 m of the Bertie Limestone in March 2004 (fig. 5). The 2004 flowmeter log indicates that downward flow entered the well from below the casing and upward flow entered from the bottom of the well. Both flows exited the well through the broken zones in the lower part of the Bertie Limestone.
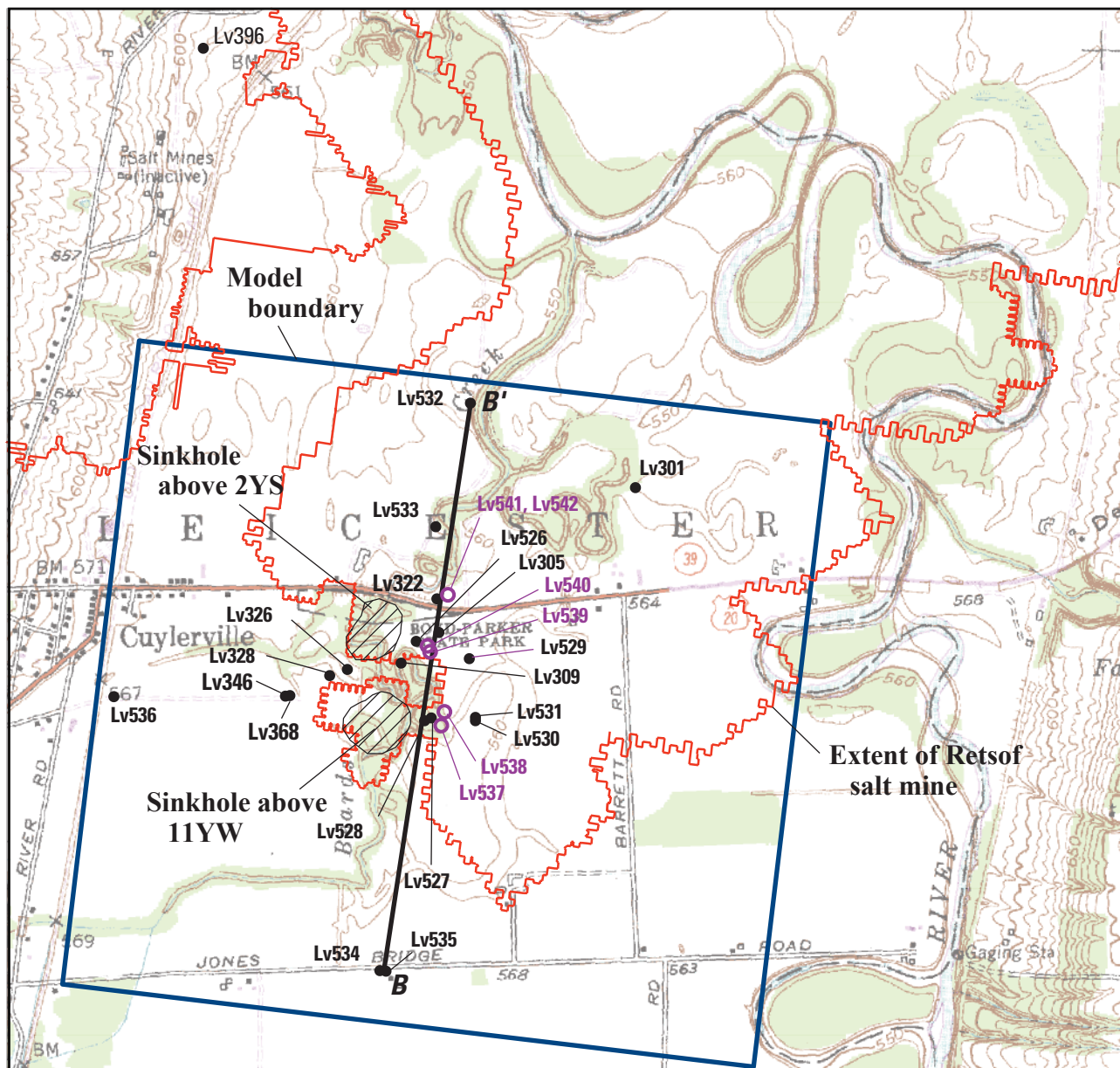
Base from U.S. Geological Survey, Digital Raster Graphic, 1998, 1:24,000
Universal Transverse Mercator projection, Zone 18

0   500   1,000 METERS

0   2,000   4,000 FEET

EXPLANATION

$\overline{B \quad B'}$ **Line of geologic section**

Lv301   **Monitoring well and identifier**
  •

Lv540   **Pumped well and identifier**
  ○

Figure 4.   Location of sinkholes, and pumped and monitoring wells in the collapse area above the flooded salt mine, Livingston County, N.Y. 2YS and 11YW are panels (mining areas).
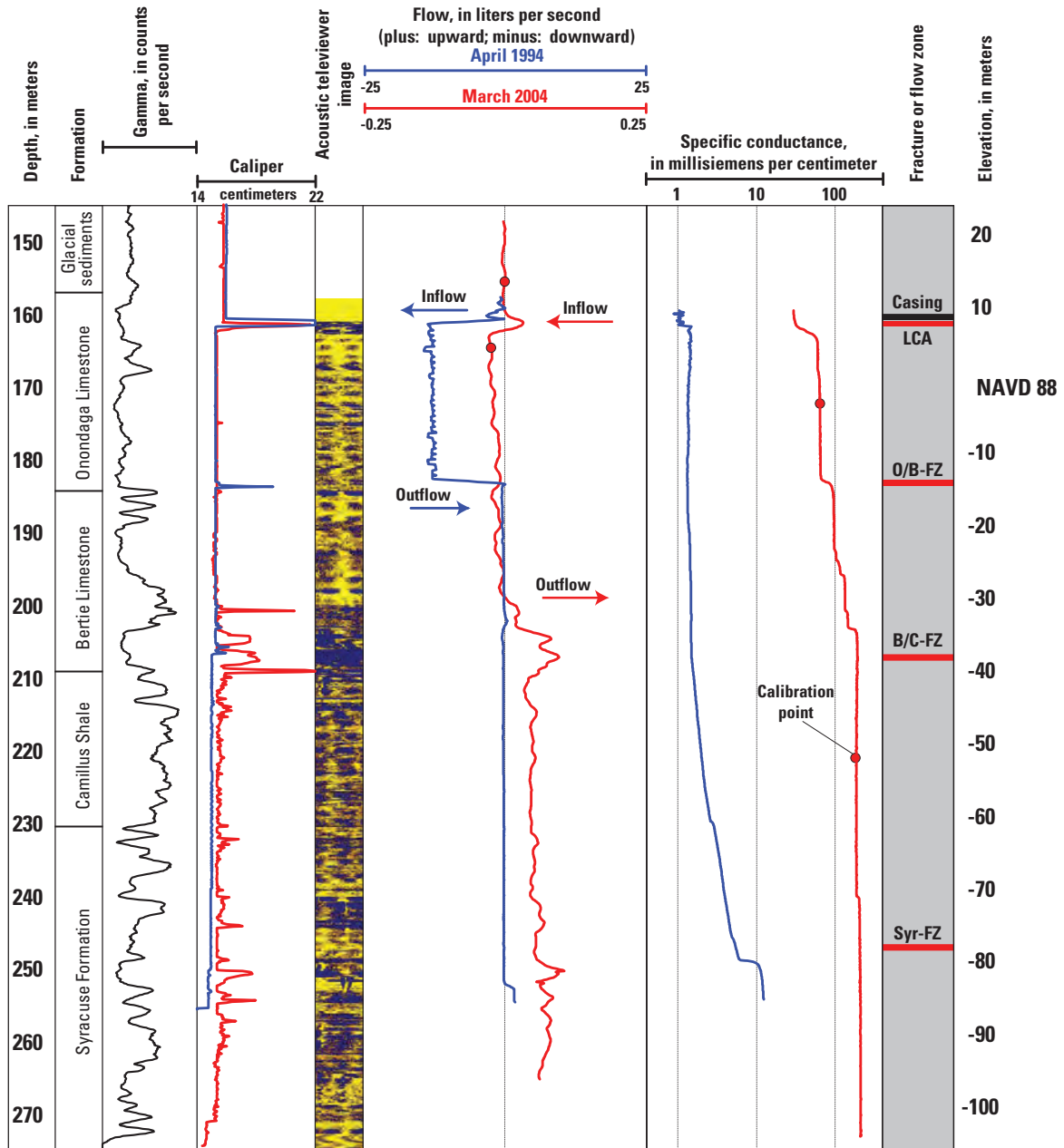
Figure 5.   Geophysical logs conducted in well Lv309 in April 1994 (blue lines) and March 2004 (red lines). Gamma log recorded in April 1994; acoustic televiewer image recorded in March 2004. LCA, lower confined aquifer. Fracture zones: O/B-FZ, Onondaga/Bertie contact; B/C-FZ, Bertie/Camillus contact; Syr-FZ, Syracuse Formation.

Water-Level Recovery and Migration of Brine

Water levels in the aquifer system began to recover after January 1996, and had largely returned to pre-collapse conditions by 2006, as predicted by simulations with the groundwater-flow model developed by Yager and others (2001) (fig. 6A). From 1996 through 2001, the average rate of land-surface subsidence above the mine ranged from 3 to 18 mm/yr, indicating that about 4.4 L/s of saturated brine was displaced from the mine as the cavity closed, with an estimated error of 50 percent (RE/SPEC, Inc., 2003). The brine level within the mine increased continuously after January 1996 as a result of the water-level recovery in the aquifer and the closure of the mine cavity, but at a declining rate (fig. 6B). By 2007, the increased formation pressure in the mine had slowed the land-surface subsidence rate to less than 2 mm/yr, displacing an estimated 1.6 L/s of brine from the mine (Alpha Geoscience, 2008).

Brine was displaced from the flooded mine after January 1996 as the mine cavity closed under the weight of overlying sediments (fig. 7). Freshwater in the LCA and saline water in the O/B-FZ continued to flow toward the collapse area until the natural northward hydraulic gradient was reestablished in 2006. The only known outlets for brine displaced from the mine are the rubble chimneys. Some of the upward-flowing brine could be diverted laterally into voids created by the collapse or fracture zones in the rocks that lie between the mine and LCA. The volume of these voids and the rate at which brine can enter these zones is unknown, however. Initially, the brine was expected to be diverted laterally into water-bearing fractures and, thus, never reach the bedrock surface (John T. Boyd Company, 1995). It is possible, however, that saline water from the O/B-FZ (29,000 mg/L chloride; Yager and others, 2001) could also enter the rubble chimney and migrate upward toward the LCA. The direction of the hydraulic gradient in the collapse area between bedrock fracture zones and the LCA during mine flooding and the recovery of the aquifer system is unknown, but an upward gradient was present between the O/B-FZ and the LCA at well Lv369, 15 km north of the collapse area.

Chloride concentrations were measured in groundwater sampled from wells Lv309 and Lv322 near the collapse area after January 1996 to detect the intrusion of saline water into the LCA (fig. 8). Water was collected with a Kemmerer sampling device to obtain grab samples at discrete depths (Alpha Geoscience, 2003). Several measured chloride concentrations were greater than the 3,000 to 5,000 mg/L initially measured in 1996, but these analyses were considered spurious. After chloride concentrations of 20,000 mg/L were measured in 2002, a review of the sampling technique led to the conclusion that most of the samples collected from 1996 to 2002 had been diluted through faulty seals in the sampling device. Subsequent measurements used an improved sampling method in which dedicated tubing was lowered to a specified depth and then pumped to obtain a water column with uniform density (Alpha Geoscience, 2005). These measurements revealed that the halite saturation of water in the LCA in the collapse area was 14 percent (corresponding to a chloride concentration of 25,000 mg/L) and that the top of the saturated brine column (greater than 90-percent halite saturation) had nearly reached the Bertie Limestone (fig. 9). The saturation of water decreased with increasing elevation and was diluted where fracture zones intersect the well in the Syr-FZ, at the B/C-FZ, and near the O/B-FZ. A comparison of saturation profiles (vertical profiles of halite saturation with depth) indicates that there was little movement in the position of the transition zone between saturated brine and saline water in the Bertie Limestone between August 2004 and September 2006 (fig. 10).

Interception of Brine and Saline Water

A brine-mitigation project was fully implemented in September 2006 to intercept saline water and brine in the collapse area and prevent further migration of saline water to the LCA (Alpha Geoscience, 2007). Water is pumped from five wells drilled east of the rubble chimneys in the collapse area (fig. 4) and then treated by an onsite thermal desalination plant to remove salt through a vacuum distillation process (Alpha Geoscience, 2006). The brine and saline-water mixture is pre-treated prior to distillation to remove hydrogen sulfide and methane. Water is pumped from three shallow wells completed in the Bertie Limestone (0.85 L/s) and two deep wells completed in the Camillus Shale (1.5 L/s) (fig. 11). The design flow rate is based on the estimated rate at which brine is displaced from the mine cavity. A total of 96,000 m³ of saline water and brine was pumped from September 2006 through February 2008, producing about 20 million kilograms of halite.

A Well Lv368 (lower confined aquifer)

B Wells Lv301 and Lv396 (flooded Retsof mine)
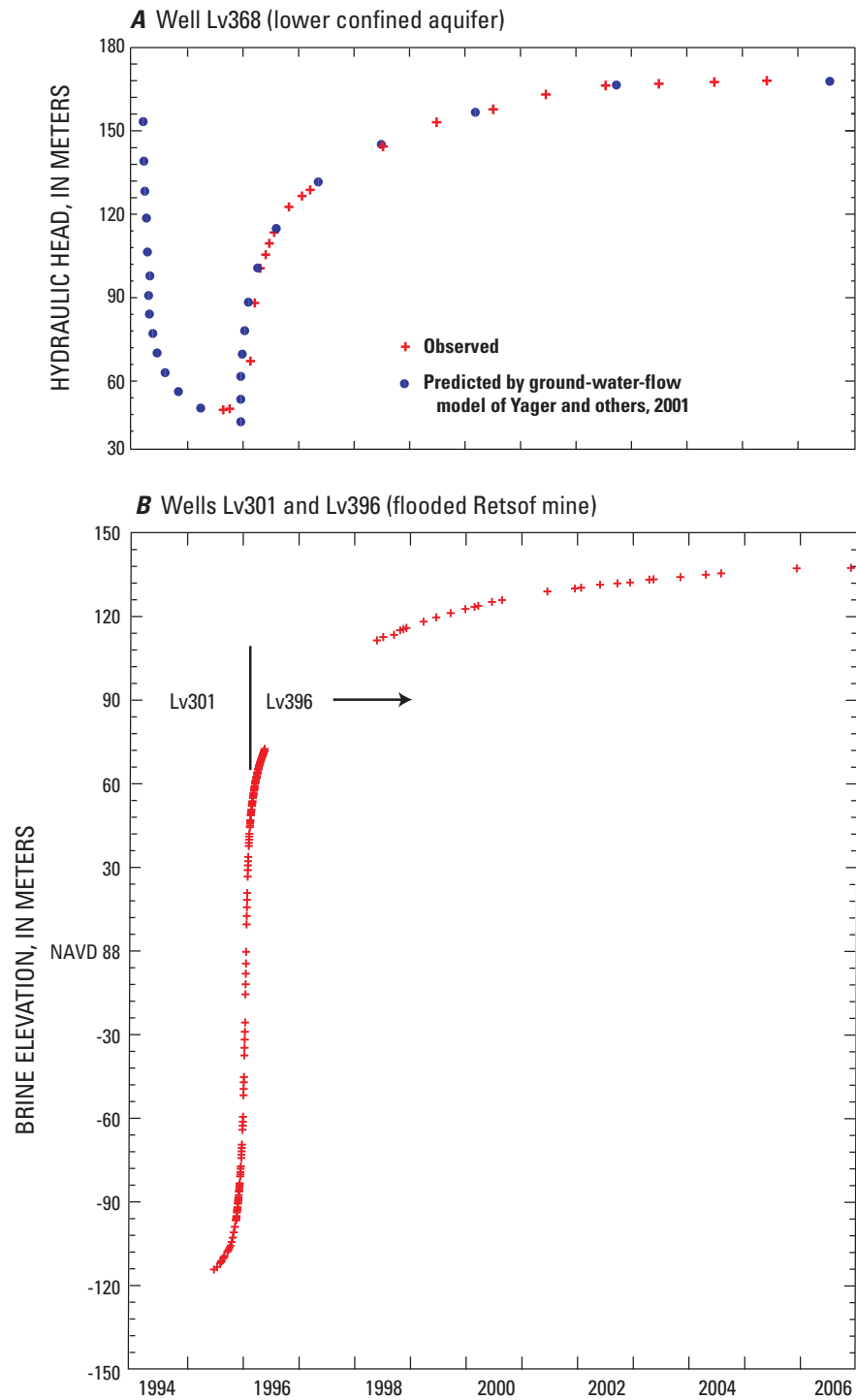
Figure 6. Drawdown and recovery of *(A)* water level in well Lv368 (lower confined aquifer) near the collapse area, and *(B)* brine level in wells Lv301 and Lv396 (flooded salt mine).
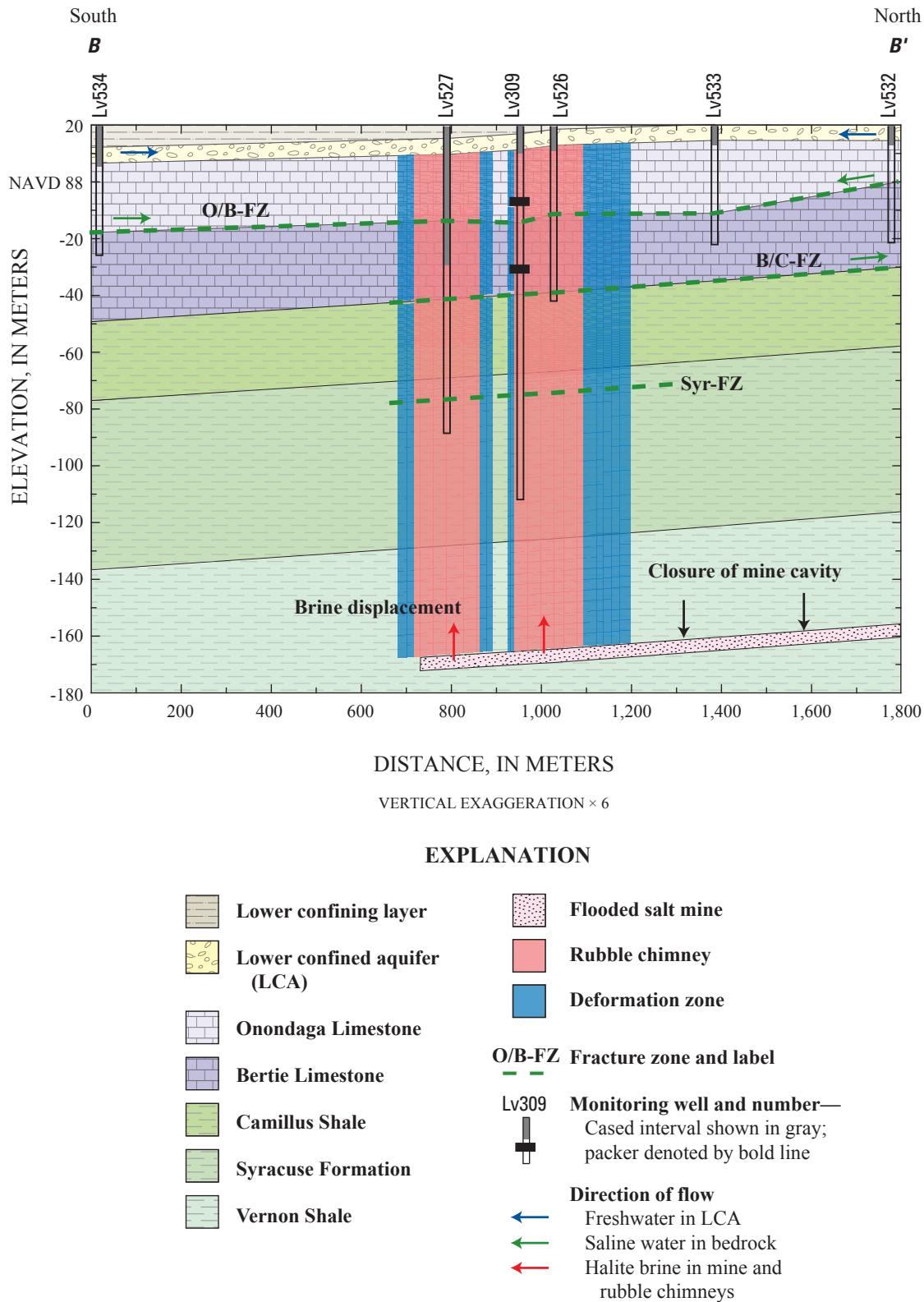
Figure 7. Stratigraphic section B-B' showing rubble chimneys and deformation zone in the collapse area above the flooded salt mine and direction of flow during water-level recovery, January 1996 through August 2006. Rubble chimneys and deformation zone are projected to section. Fracture zones: O/B-FZ, Onondaga/Bertie contact; B/C-FZ, Bertie/Camillus contact; Syr-FZ, Syracuse Formation. Location of section shown in figure 4.
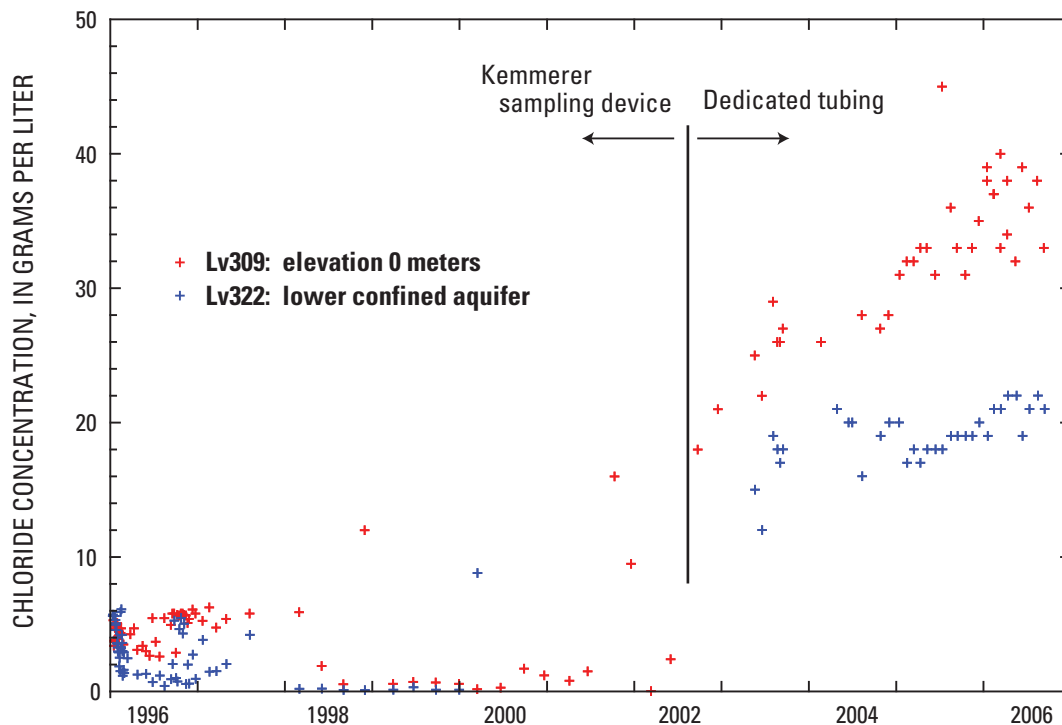
Figure 8. Chloride concentrations observed within the collapse area in well Lv309 (elevation 0 m) and well Lv322 (lower confined aquifer) after inundation of the salt mine, January 1996 through August 2006.

Geochemical Modeling

Water in the rubble chimneys was originally a mixture of freshwater from the LCA and saline water in fracture zones in the bedrock. After the mine filled and water levels in overlying aquifers began to recover, water in the rubble chimneys migrated upward as the mine cavity began to close, displacing halite brine. The changing chemical composition of waters in the rubble chimneys probably induced water-rock reactions during both the period of flooding from March 1994 through January 1996 and the subsequent period of upward migration from 1996 to the present (2008). In addition, brine from pre-existing cavities in the lower part of the Syracuse Formation penetrated by the collapse could also have entered the chimneys (Gowan and Trader, 2000a). Water that currently occupies the collapse area is, therefore, a complex mixture that has resulted from the hydraulic and chemical processes that occurred since mine flooding began in 1994.

Inverse geochemical models were developed using PHREEQC (Parkhurst and Appelo, 1999) to analyze the variation of chemical composition of water with depth in the collapse area. The inverse models were used to identify possible mixing proportions of initial waters and the water-rock reactions that could account for the observed water chemistry. The inverse models primarily considered mixtures

of three initial waters: saturated halite brine from the flooded mine, saline water from the O/B-FZ, and freshwater from the LCA. Some models included a fourth initial water to simulate hypothesized mixing with bromide-rich brine from cavities in the lower part of the Syracuse Formation. The bromide-rich brine was assumed to have a composition similar to that of other brines that formed following the precipitation of halite during the Silurian Period (D.O. Whittemore, Kansas Geological Survey, oral commun., 2008), using published analyses of waters from oil fields in the Smackover Formation in southwestern Arkansas (Carpenter and Trout, 1978). Forward geochemical models also were used to assess the potential for mineral dissolution and land subsidence that could result from further mixing of waters by pumping saline water and brine from the collapse area.

No samples of water have been obtained directly from the rubble chimneys because the instability of the rocks in these areas makes the installation of wells difficult. Water compositions in well Lv309 are probably most similar to those of waters in the rubble chimneys, however, because the well is between the chimneys and within the deformation zone that surrounds them (figs. 4 and 11). Well Lv309 is cased to bedrock, extends 123 m from the Onondaga Limestone to the Vernon Shale, and is instrumented with a dual-packer system that straddles a 22.5-m zone centered on the O/B-FZ. Five
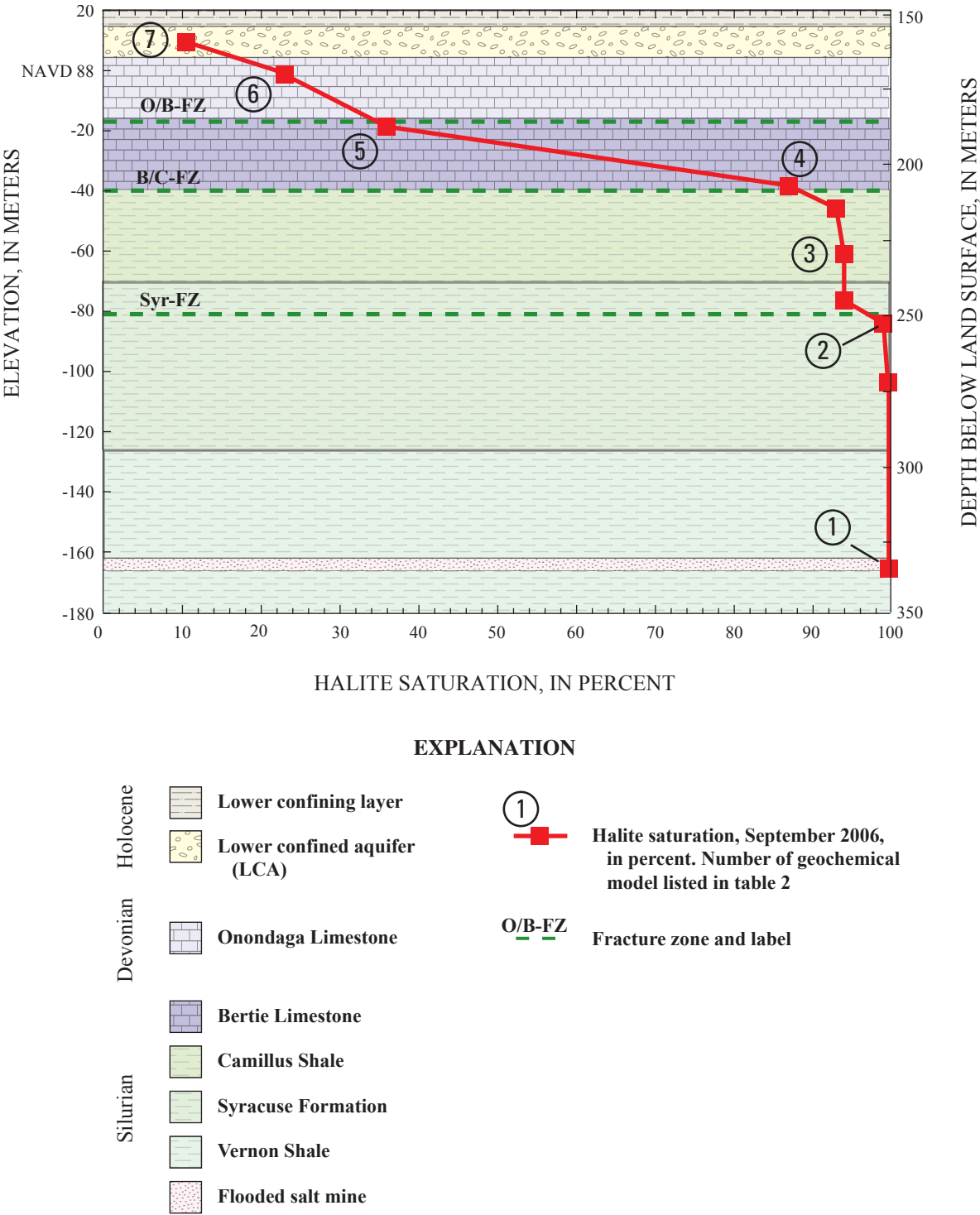
Figure 9. Vertical profile of halite saturation with depth measured in wells Lv309 and Lv322 in September 2006, showing stratigraphy and sample depths of final waters used in inverse geochemical models. Fracture zones: O/B-FZ, Onondaga/Bertie contact; B/C-FZ, Bertie/Camillus contact; Syr-FZ, Syracuse Formation.
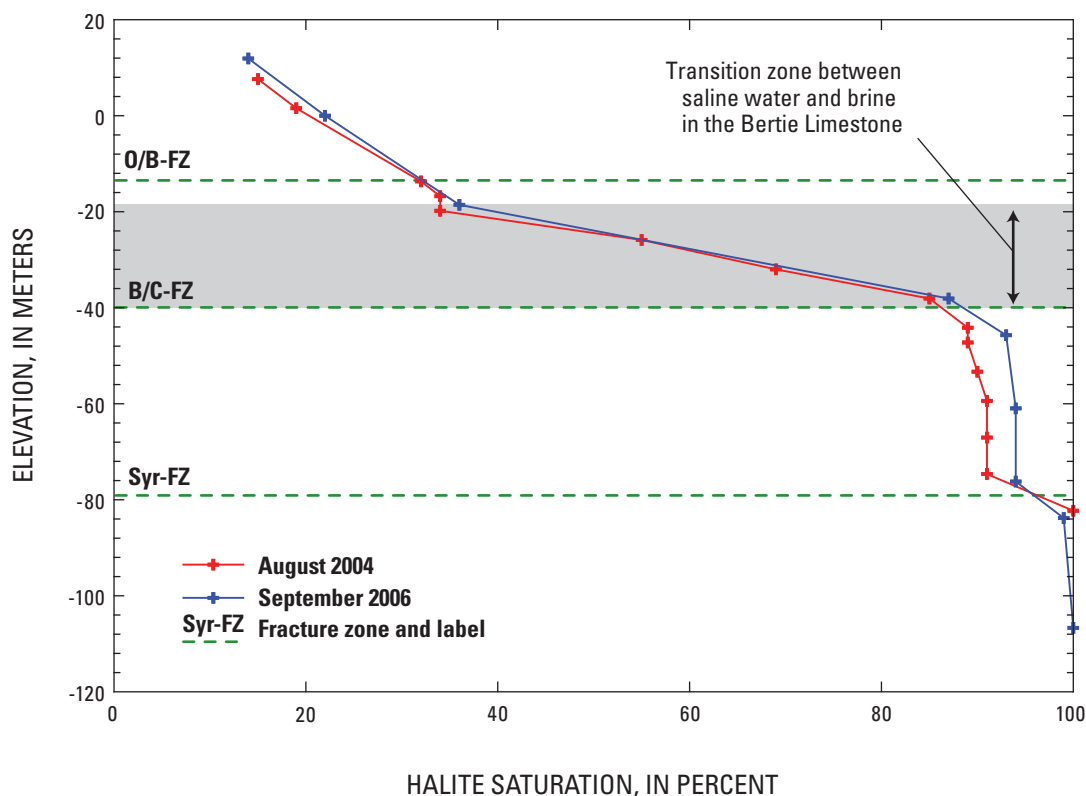
Figure 10. Vertical profiles of halite saturation with depth in well Lv309 measured in August 2004 and September 2006, showing transition zone between brine and saline water in the Bertie Limestone. Fracture zones: O/B-FZ, Onondaga/Bertie contact; B/C-FZ, Bertie/Camillus contact; Syr-FZ, Syracuse Formation.

water samples from Lv309 were included in geochemical models: one above, one between, and three below the two packers. The water was purged and then sampled through 19-mm high-density polyethylene (HDPE) tubing using a Waterra pump system after continuous measurement of the salinity of the water remained constant (Alpha Geoscience, 2005). Water also was sampled in a similar fashion at four other wells: two wells screened in the LCA (Lv322 and Lv368), one well connected to the flooded mine (Lv396), and one well completed in the lower part of the Bertie Limestone (Lv534) (fig. 4). The water samples were analyzed in the field for pH and then sent to a private laboratory for analysis of major ions (table 1). Salinity of water was determined in the field by measuring the density with a salometer that measures salt saturation using a salt conversion chart.

Inverse Models

Inverse models for seven water types in the collapse area were developed to determine whether mixtures of representative waters and hypothesized water-rock reactions could account for the changes in the observed geochemical composition of saline waters with depth in the collapse area (fig. 9 and table 2). The initial waters considered were (1) freshwater from the LCA (0-percent saturation) in well Lv368 (Lv368-LCA), (2) saline water from the O/B-FZ in well Lv534 (25-percent saturation) 630 m south of the collapse area (Lv534-O/B-FZ), (3) 100-percent-saturated halite brine in the flooded mine in well Lv396 (Lv396-mine), and (4) hypothesized bromide-rich brine based on analyses from the Smackover Formation, Arkansas (Br-brine). One inverse model was prepared for the halite brine in the flooded salt mine (no. 1), and six additional models were prepared for water sampled at different depths near the rubble chimneys in well Lv309 (nos. 2 to 6) and in well Lv322 (no. 7), where saline water has been detected in the LCA (table 2).

Aqueous speciation calculations indicated that charge imbalances ranged from 1 to 13 percent in the analyses of the sampled waters. Small charge imbalances of several percent can lead to large uncertainties in calculated mass transfer in geochemical mass-balance calculations involving highly saline fluids. Mass-balance errors were minimized by using an empirical relation between measured chloride concentrations
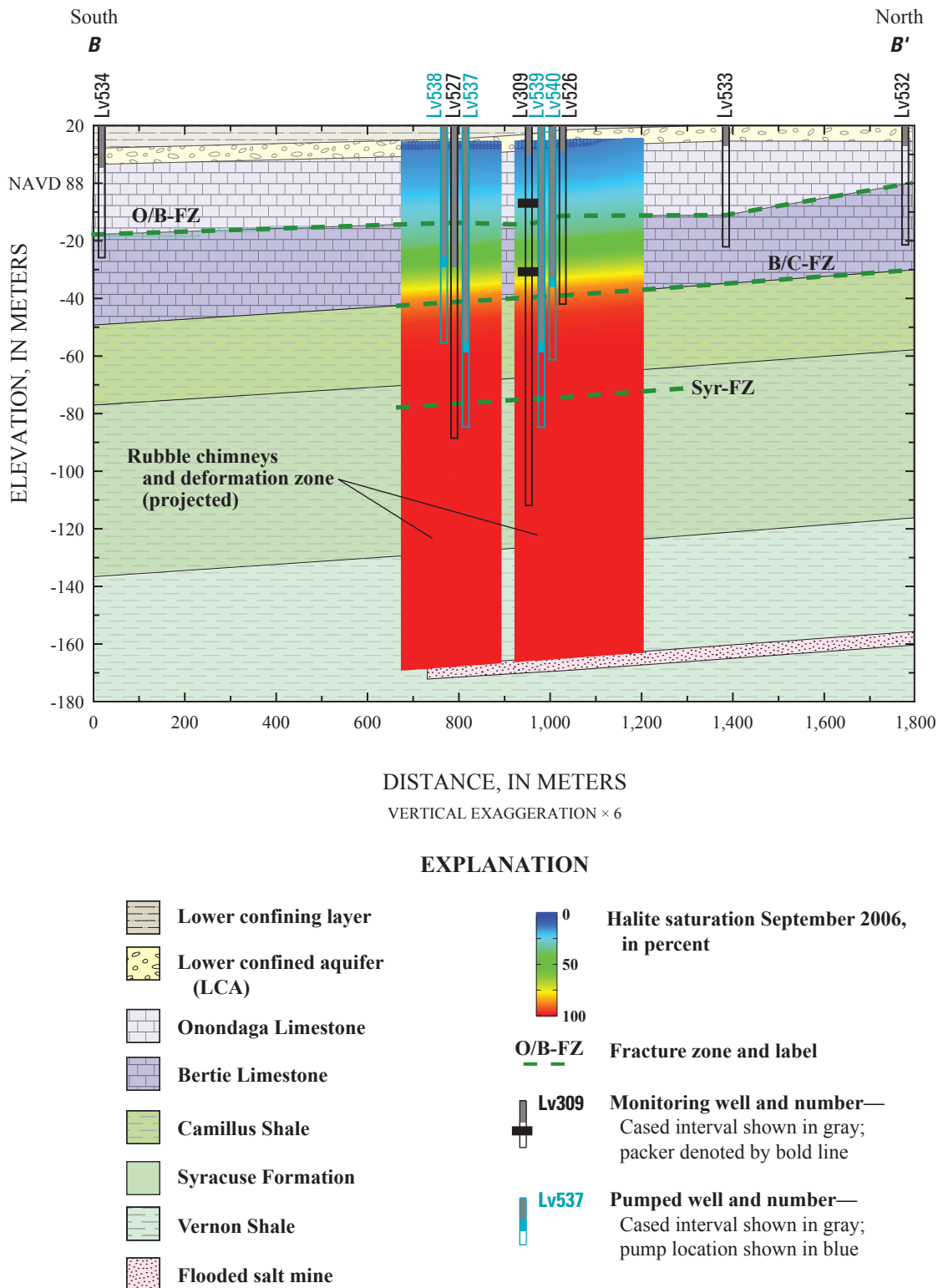
Figure 11. Stratigraphic section B-B′ depicting screened intervals of pumped and monitoring wells, and the distribution of halite saturation within the rubble chimneys and deformation zone in September 2006. Fracture zones: O/B-FZ, Onondaga/Bertie contact; B/C-FZ, Bertie/Camillus contact; Syr-FZ, Syracuse Formation.

Table 1. Chemical composition of brine and groundwater in November 2005 near collapse area above flooded Retsof mine, Livingston County, N.Y.

[Values in milligrams per liter unless noted. USGS, U.S. Geological Survey; m, meters; g, grams; cm, centimeters; Ca, calcium; Mg, magnesium; K, potassium; Na, sodium; Br, bromide; Cl, chloride; SO_4, sulfate; --, not reported; <, less than]

Well number[1]		Unit	Sampling elevation, m	pH	Density[3], g/cm	Halite saturation, percent	Ca	Mg	K	Na	Br	Cl	SO_4^{2-}	Alka-linity[2]	Dissolved solids
USGS	Local														
Lv396	9572	Flooded Retsof mine[3]	-88	6.0	1.200	100	3,660	396	748	101,000	240	190,000	1,400	76	330,000
Lv309e	9409e	Syracuse Formation	-84	6.4	1.200	100	9,340	1,010	1,350	102,000	440	200,000	710	<20	310,000
Lv309d	9409d	Camillus Shale	-61	6.4	1.190	95	13,300	1,550	1,970	80,300	810	170,000	540	<20	290,000
Lv309c	9409c	Bertie Limestone	-38	6.5	1.172	86	16,500	2,310	2,070	67,400	840	140,000	560	<20	250,000
Lv309b	9409b	Onondaga/Bertie contact (O/B-FZ)	-23	6.4	1.072	36	6,640	1,410	778	25,700	340	54,000	400	290	99,000
Lv534	0504	Onondaga/Bertie contact (O/B-FZ)	-23	6.6	1.050	25	8,820	1,780	503	15,200	400	46,000	680	270	76,000
Lv309a	9409a	Onondaga Limestone[4]	0	6.9	1.044	22	6,100	2,000	400	13,000	290	33,000	<2	160	59,000
Lv322	9422	Lower confined aquifer (LCA)	13	7.5	1.020	10	3,410	1,160	138	6,900	180	19,000	<3	88	41,000
Lv368	9568	Lower confined aquifer (LCA)	26	9.4	1.000	0	25.2	41.4	24.1	210	4	370	<3	160	1,000
--	--	Bromide-rich brine[5]	--	--	1.228	--	44,500	3,480	4,670	80,000	6,100	210,000	150	--	351,000

[1]Letter denotes relative position of discrete-depth sample.

[2]As $CaCO_3$.

[3]Sampled June 2006.

[4]Sampled September 2006.

[5]Jameson, Smackover Formation, Arkansas (Carpenter and Trout, 1978).

Table 2.   Inverse models of waters in the collapse area showing calculated percentages of initial waters and mole transfers for water-rock reactions.

[%, percent; m, meters; mmol, millimole; kg, kilogram; LCA, lower confined aquifer; O/B-FZ, Onondaga/Bertie fracture zone; Cl, chloride; Br, bromide; SO_4^{2-}, sulfate; Ca^{2+}, calcium; Mg^{2+}, magnesium; Na^+, sodium; K^+, potassium; CO_2, carbon dioxide; X, cation-exchange site]

Model	Final water[1]	Sampling elevation, m	Initial waters[1]	Percent of final water	Balances	Dissolution reactions		Precipitation reactions	
						Phase	Mole transfer, mmol per kg$_{water}$	Phase	Mole transfer, mmol per kg$_{water}$
1	Lv396-mine	-88	Lv368-LCA	81	Major ions[2]	Halite	4,560	Calcite	1.3
			Lv534-O/B-FZ	16		Anhydrite	15		
			Br-brine	3		Sylvite	14		
2	Lv309e-100%	-84	Lv396-mine	97	Cl/Br	$Ca^{2+}X$	130	Anhydrite	7.3
			Br-brine	3		$Mg^{2+}X$	23	Calcite	0.6
								Na^+X	300
								CO_2	1.1
3	Lv309d-95%	-61	Lv396-mine	81	Cl/Br	$Ca^{2+}X$	150	Anhydrite	7.3
			Lv534-O/B-FZ	10		$Mg^{2+}X$	33	Calcite	0.6
			Br-brine	9				Na^+X	410
								CO_2	1.1
4	Lv309c-86%	-38	Lv396-mine	70	Cl/Br	$Ca^{2+}X$	220	Anhydrite	6.5
			Lv534-O/B-FZ	21		$Mg^{2+}X$	72	Calcite	1.0
			Br-brine	9				Na^+X	550
								CO_2	1.7
5	Lv309b-36%	-23	Lv534-O/B-FZ	76	Cl/Br	Calcite	1.3	Anhydrite	3.5
			Lv396-mine	14		CO_2	2.1		
			Lv368-LCA	10					
6	Lv309a-22%	0	Lv534-O/B-FZ	82	Cl/Br	$Mg^{2+}X$	22	Anhydrite	5.9
			Lv368-LCA	18				Calcite	1.0
								Na^+X	44
								CO_2	2.0
7	Lv322-LCA-10%	13	Lv368-LCA	56	Cl/Br	$Mg^{2+}X$	14	Anhydrite	3.2
			Lv534-O/B-FZ	44				Calcite	1.5
								Na^+X	29
								CO_2	2.3

[1]Well number, unit, and halite saturation.

[2]Ca^{2+}, Mg^{2+}, K^+, Na^+, Cl^-, SO_4^{2-}, Br^-.

and halite saturation to compute chloride concentrations used in the inverse models (fig. 12A). The measured relation between halite saturation and specific gravity, the ratio of fluid density to that of water, is also shown in figure 12B. The error in measurement of saturation (salinity) is less than 3 percent, whereas errors in the measurement of chloride concentration in high-salinity waters can be higher than 10 percent. The initial and final solutions used in the inverse models were then adjusted by PHREEQC to ensure charge balance. All mole transfers are computed per kilogram of water.

Mixtures of waters were assumed to react with the principal minerals present in the collapse area: anhydrite, halite, calcite, and dolomite. Additional reactions considered included cation exchange (involving Ca^{2+} and Mg^{2+} for Na^+) and exsolution of CO_2 (as indicated by degassing of samples in the field). All models were constrained by measured concentrations of the elements chloride (Cl) and bromide (Br). Model no. 1 for the mine water was also constrained by measured concentrations of other major ions: Ca^{2+}, Mg^{2+}, K^+, Na^+, and SO_4^{2-}.

Reaction model no. 1 satisfied all the constraints and indicated that halite brine in the flooded mine (Lv396-mine) could have formed from a mixture of aquifer water (81 percent), bedrock water (16 percent), and bromide-rich brine (3 percent). Dissolution of halite, anhydrite, and sylvite were required to satisfy the major-ion constraints, and a small amount of calcite was precipitated (table 2). The calculated proportion of freshwater in the simulated mixture would be higher if some Br^- and Mg^{2+} were derived from impurities in the halite salt, rather than from bedrock water or bromide-rich brine.

The results for the remaining six inverse models that represent waters near the rubble chimneys are best presented from the bottom of the water column near the mine (no. 2) to the top of the water column at the bedrock surface (no. 7). Model no. 2 indicates that water near the bottom of the rubble chimneys (Lv309e-100%[1]) is nearly entirely derived from halite brine in the flooded mine (97 percent), diluted by a small amount of bromide-rich brine (3 percent). The water-rock reactions required to satisfy the model constraints included ion exchange (Ca^{2+} and Mg^{2+} for Na^+), precipitation of anhydrite and calcite, and exsolution of CO_2. The same reactions were included in models nos. 3 and 4 for the overlying samples, Lv309d-95% and Lv309c-86%. Both of these models involved mixtures of mine water, bedrock water, and bromide-rich brine. All four samples (Lv309c, Lv309d, Lv309e, and Lv396-mine) are at or near saturation with respect to anhydrite and calcite (table 3).

The last three models are for more dilute samples in the upper part of the water column, ranging from 36-percent to 10-percent saturation. The final water in model no. 5 (Lv309b-36%) was sampled in a zone isolated by packers that intersects the O/B-FZ. Model no. 5 indicates that this water is a mixture of three waters: bedrock water (76 percent),

___
[1] Number denotes halite saturation, in percent.

mine water (14 percent), and aquifer water (10 percent). The model requires a small amount of calcite and CO_2 dissolution and precipitation of anhydrite. Models nos. 6 and 7 for the waters above the packer assembly (Lv309-22% and Lv322-LCA-10%) indicate mixtures of just two waters: bedrock water and aquifer water. Both models require ion exchange (Mg^{2+} for Na^+), precipitation of anhydrite and calcite, and exsolution of CO_2. The simulated precipitation of anhydrite is consistent with the observed deposition of a $CaSO_4$-salt in pipes within the thermal desalination plant, which must be cleared regularly to prevent blockages (S.W. Gowan, Alpha Geoscience, oral commun., 2008).

Forward Models

Forward models of various mixtures of waters were developed to evaluate whether dissolution of minerals in the rubble chimneys could cause further land subsidence in the collapse area. The models considered mixtures of three initial waters, each ranging from 0 to 100 percent: (1) freshwater from the LCA (Lv368-LCA), (2) saline water from the bedrock fracture zone (Lv534-O/B-FZ), and (3) halite brine from the flooded mine (Lv396-mine). The mixtures were equilibrated with anhydrite, calcite, and dolomite in all of the models using solubilities consistent with the Pitzer aqueous model as implemented in PHREEQC (Version 2.12; Pitzer implementation from Plummer and others, 1988). Ion exchange also was considered in a second set of forward models because exchange reactions were identified in the inverse models presented above. One mole of exchange sites was specified in the models that included ion exchange, and the initial composition of the exchange sites was determined through equilibration with bedrock water (Lv534-O/B-FZ).

Anhydrite and dolomite were dissolved and calcite was precipitated in models without ion exchange, a process known as dedolomitization. The mole transfers for each reaction are presented per kilogram of water in ternary plots for mixtures of the three initial waters (fig. 13). The largest amount of anhydrite dissolution was predicted for mixtures of aquifer water and mine water, while the largest amount of dolomite dissolution was predicted for the 100-percent bedrock-water end-member. Calcite precipitation, which would offset void creation through dissolution reactions, was also largest for mixtures containing bedrock water.

Less dissolution of anhydrite was predicted in nearly all mixtures that included ion exchange because the exchange of Na^+ for Ca^{+2} provided an additional source of Ca^{+2} to the water mixtures. Rates of both dolomite dissolution and calcite precipitation increased with ion exchange because the exchange sites provided an additional sink for Mg^{+2}, enhancing dolomite dissolution. Anhydrite dissolution was largest for the 100-percent aquifer-water end-member, whereas both dolomite dissolution and calcite precipitation were largest for the 100-percent bedrock-water end-member.
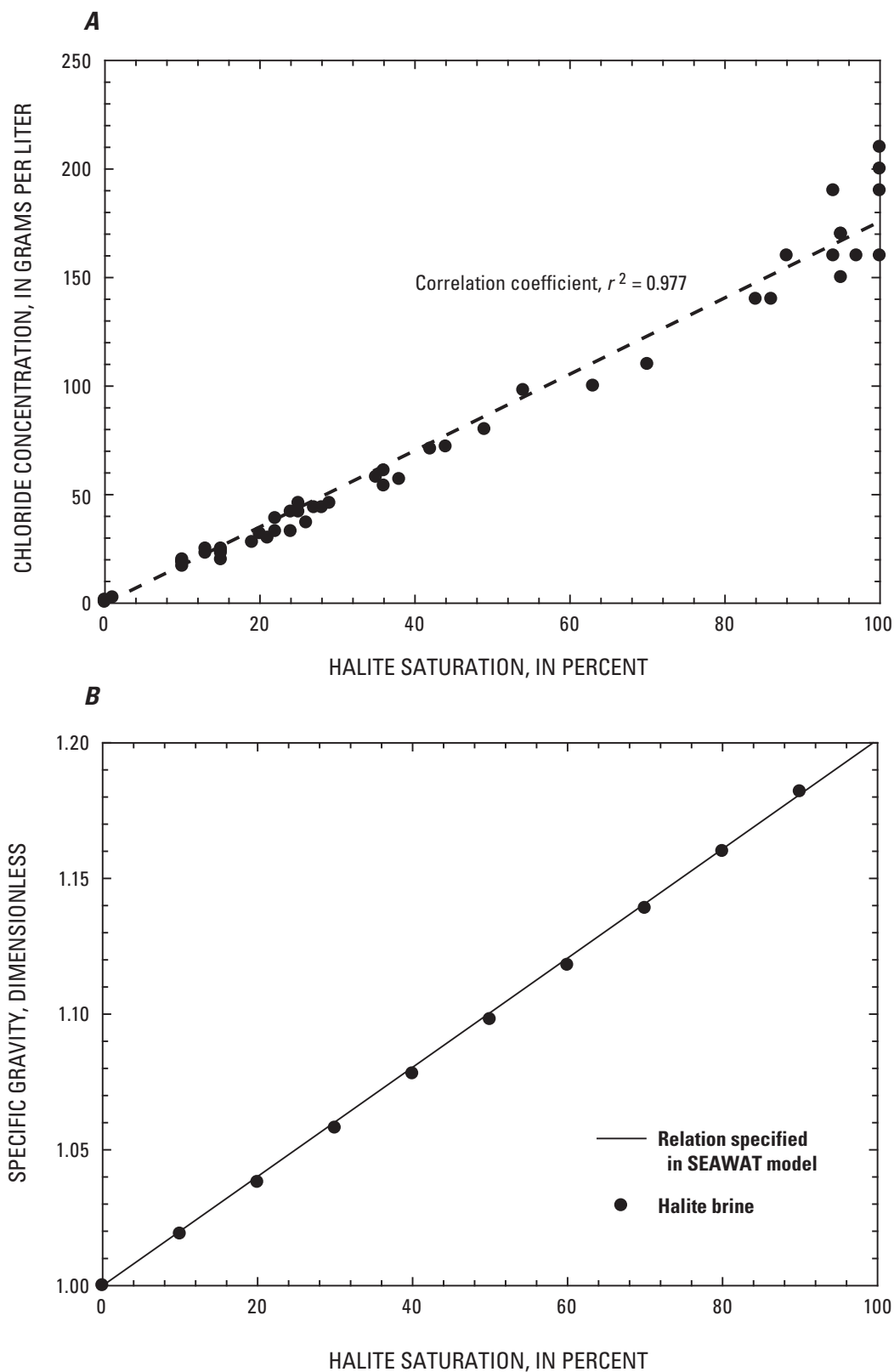
Figure 12.   Relation between halite saturation and *(A)* chloride concentration in samples of saline water and brine near the collapse area above the flooded salt mine, and *(B)* specific gravity of halite brine.

The potential subsidence that would occur as a result of water-rock reactions with the different water mixtures was computed using the molar volumes of the three minerals, and the mole transfers were predicted by the forward models (fig. 14). Subsidence was computed by assuming one pore volume of water in a rubble chimney (6.5×10^7 L) was displaced by each water mixture. In the pore-volume calculations, it was assumed that each rubble chimney is a cylinder 180 m in length and 91 m in diameter with a porosity value of 6 percent, as estimated from flow and transport simulations discussed later in this report. The time required to flush one pore volume of water from both rubble chimneys is 2.8 years, based on the estimated rate of brine displacement from the mine (1.6 L/s). The subsidence rate (centimeters per year) was then calculated by dividing the total subsidence per pore volume by 2.8 years.

Computed subsidence rates ranged from 0 to 1.1 cm/yr for water mixtures in which ion exchange was not considered. The maximum subsidence rate was predicted for mixtures of freshwater and halite brine. Computed subsidence rates were generally less (0 to 0.6 cm) with ion exchange because the increased calcite precipitation and decreased anhydrite dissolution offset the increased dolomite dissolution. One exception was the 100-percent aquifer-water end-member in which both anhydrite and dolomite dissolution increased with ion exchange, resulting in a computed subsidence rate of 1.4 cm/yr.

Discussion of Results from Geochemical Modeling

Geochemical modeling indicates that the brine in the flooded mine is derived from a mixture of freshwater from the LCA (81 percent), saline water from bedrock fracture zones (16 percent), and bromide-rich brine (3 percent). The proportions of the mixing waters are approximate because the concentrations used in modeling are subject to analytical error and the actual compositions of waters that flooded the mine from March 1994 through January 1996 are unknown. The simulated proportion of aquifer water could range from 74 to 90 percent as a result of analytical uncertainty, for example, and could be higher if some of the Mg^{2+} and Br^- in the brine were derived from impurities in the halite salt. The waters that flooded the mine likely dissolved halite, anhydrite, and sylvite exposed in the mine and in the rubble chimneys. As a result, the brine that currently fills the mine and the lower part of the rubble chimneys is near saturation with respect to anhydrite. Although these waters appear supersaturated for calcite and dolomite, the computed supersaturation may be due in part to degassing of CO_2 observed during sampling.

The water columns in the rubble chimneys were displaced upward after the mine was filled in January 1996 and closure of the mine cavity began to displace the halite brine. Halite brine (saturation greater than 90 percent) has migrated upward to the bottom of the Bertie Limestone

Table 3. Saturation indices calculated with the Pitzer aqueous model for sampled waters in the collapse area.

[%, percent; LCA, lower confined aquifer; O/B-FZ, Onondaga/Bertie fracture zone]

Sample	Water[1]	Saturation index		
		Anhydrite	Calcite	Dolomite
1	Lv309a-22%	-3.11	0.71	1.26
2	Lv309b-36%	-0.83	0.49	0.65
3	Lv309c-86%	-0.25	0.41	0.41
4	Lv309d-95%	-0.15	0.32	0.18
5	Lv309e100%	0.08	0.44	0.44
6	Lv322-LCA	-2.97	0.74	1.34
7	Lv368-LCA	-3.38	0.09	0.26
8	Lv396-mine	0.1	1.18	1.91
9	Lv534-O/B-FZ	-0.48	0.74	1.12

[1]Well number, unit, and halite saturation.

(fig. 9) and has been diluted with bedrock water. The Br content of the halite brine in samples from the Bertie Limestone and Camillus Shale is elevated above concentrations present in bedrock water (table 1), indicating that the halite brine was exposed to a source of Br in the rubble chimneys, possibly a Br-rich brine similar to that present in oil fields in southwestern Arkansas. Saline water at the O/B-FZ (saturation 36 percent) appears to be a mixture of bedrock water that has been enriched with mine water and diluted by aquifer water. The water above the O/B-FZ appears to be solely a mixture of bedrock water and aquifer water, indicating that water from the flooded mine has not reached the LCA.

The inverse models indicate that dissolution reactions are not presently occurring in the rubble chimneys, and that the principal water-rock reaction that affects the chemical composition of water is ion exchange (Ca^{2+} and Mg^{2+} for Na^+), accompanied by precipitation of anhydrite and calcite and exsolution of CO_2. These results indicate that additional land subsidence in the collapse area as a result of anhydrite dissolution was not a concern under pre-pumping (2005) conditions. The forward models indicate that subsidence could occur, however, if certain mixtures of waters formed in the rubble chimneys and the volume of voids created by dissolution of anhydrite and dolomite were not filled by calcite precipitation. Mixtures containing large proportions of freshwater from the LCA or saline water from the O/B-FZ, which are undersaturated with respect to anhydrite, have the greatest potential to create subsidence. Although the introduction of these waters into the lower part of the rubble chimneys where anhydrite and dolomite are present could result in subsidence, the upward flow of brine through the rubble chimneys under current (2008) pumping conditions

A Anhydrite dissolution (-) and precipitation (+)
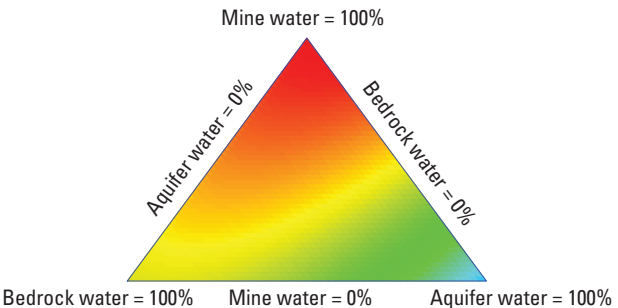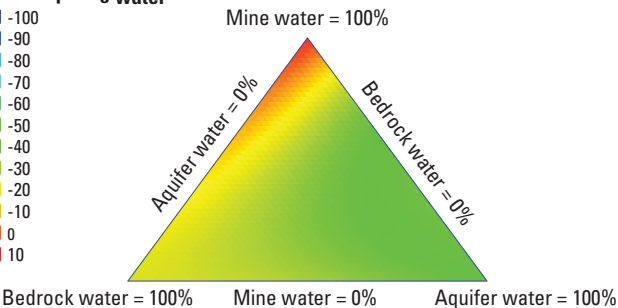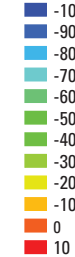
B Calcite precipitation (+)
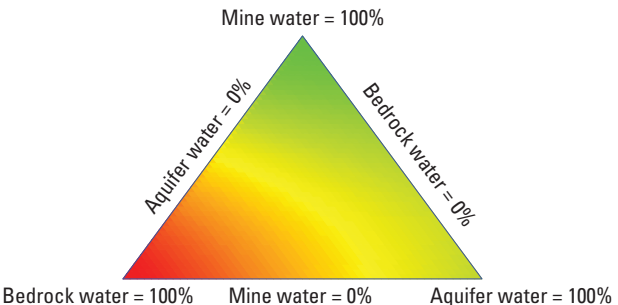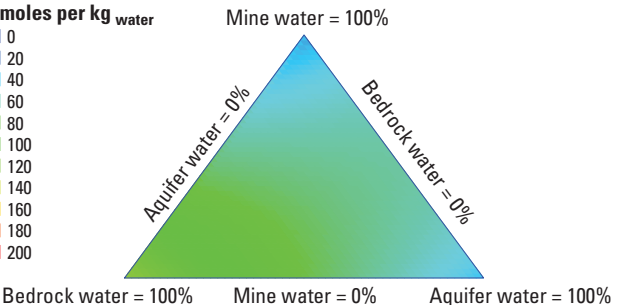
C Dolomite dissolution (-)
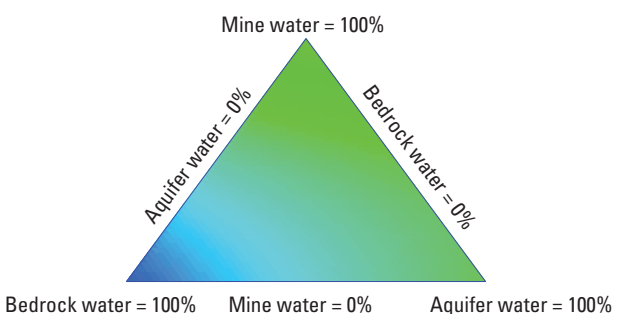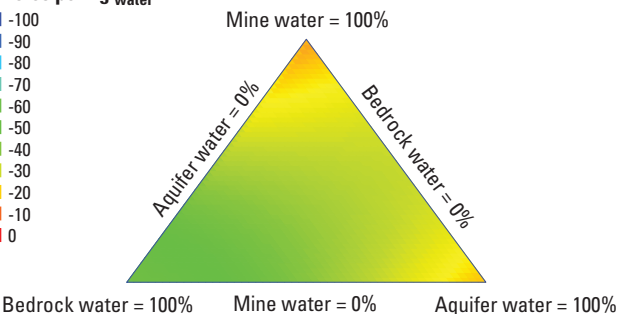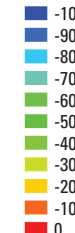
Figure 13.   Ternary diagrams showing water-rock reactions for different mixtures of waters in the collapse area without and with ion exchange. Percentages of aquifer water (Lv368), bedrock water (Lv534) and mine water (Lv396) are indicated by trilinear axes (water compositions are listed in table 1). Shading indicates mole transfer, the amount of mineral precipitated (+) or dissolved (-), in millimoles per kilogram of water (mmol/kg$_{water}$): *(A)* dissolution or precipitation of anhydrite, *(B)* precipitation of calcite, and *(C)* dissolution of dolomite.

A Without ion exchange

Mine water = 100%

Aquifer water = 0%

Bedrock water = 0%

Bedrock water = 100%   Mine water = 0%   Aquifer water = 100%

EXPLANATION

Subsidence rate, in centimeters per year

- 0
- 0.3
- 0.6
- 0.9
- 1.2
- 1.5

B With ion exchange

Mine water = 100%

Aquifer water = 0%

Bedrock water = 0%

Bedrock water = 100%   Mine water = 0%   Aquifer water = 100%
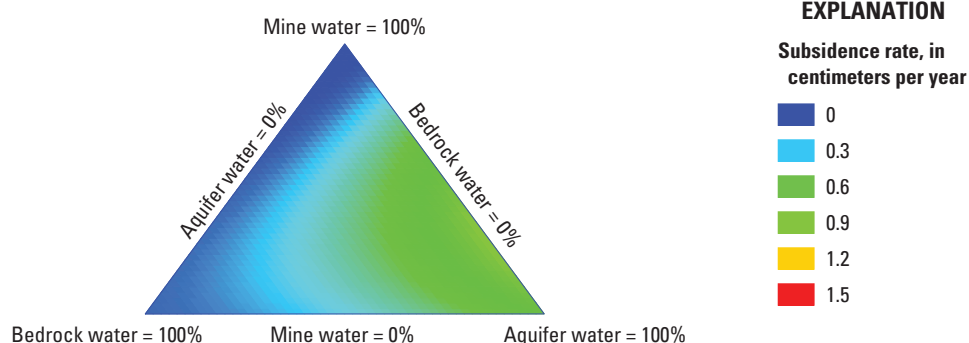
Figure 14. Ternary diagrams showing subsidence rates resulting from water-rock reactions for different mixtures of waters in the collapse area: *(A)* without ion exchange, *(B)* with ion exchange.

makes this scenario unlikely. Continued interception of brine through pumping could alter the current hydraulic conditions, but the potential for further subsidence can be minimized by maintaining a lower rate of pumping than the rate of upward flow of halite brine from the flooded mine.

The subsidence rates computed by the forward models are conservative because the water mixtures were assumed to interact with the entire volume of the rubble chimneys. The maximum predicted subsidence rates (0.6 to 1.1 cm/yr) were computed for mixtures containing more than 40 percent aquifer water. When ion-exchange reactions were considered, these predicted subsidence rates decreased to 0.1 to 0.6 cm/yr. One exception was the 100-percent aquifer-water end-member for which subsidence increased to 1.4 cm/yr in the presence of ion exchange. Ion-exchange reactions, therefore, can be considered as a geologic safeguard that reduces the potential for subsidence. The ion-exchange capacity of the materials in the rubble chimneys is limited, however. The source of Ca^{+2} represented by the exchange sites will be depleted with time, and thereafter, ion-exchange reactions will have no further effect on water-rock interactions.

Simulated Migration of Brine and Saline Water During Water-Level Recovery

The movement of aquifer water, bedrock water, and halite brine within the rubble chimneys and the surrounding deformation zone during the 10.7-year period following flooding of the salt mine (January 1996 through August 2006) was simulated with analytical and numerical models. The numerical models were constructed using SEAWAT (Langevin and others, 2007), a computer program that simulates flow using a modified version of MODFLOW-2000 (Harbaugh and others, 2000) and simulates transport with a version of MT3DMS (Zheng and Wang, 1998). Both one-dimensional (1D) and three-dimensional (3D) models were constructed. The 1D models simulated upward flow of brine through a single rubble chimney toward the LCA and were used to estimate the upward rate of brine migration and the longitudinal dispersivity of the rubble material. The 3D

models simulated flow through both rubble chimneys and the surrounding deformation zone, and also represented mixing of brine with bedrock water where fracture zones intersect the rubble chimneys. The 1D simulations ran quickly (less than 1 hour) and were used to determine the number of model layers that were required in more time-consuming 3D simulations that were subsequently used to simulate more accurately the movement of the transition zone between saline water and brine during the 10.7-year recovery period. The 3D models described in this section were later used to simulate movement of aquifer water, bedrock water, and brine in response to pumping from the collapse area beginning in September 2006, as discussed later in this report.

SEAWAT was selected to simulate variable-density flow because multiple solutes could be represented in the model and a wide range of boundary conditions could be specified and changed during the transient simulations. The SEAWAT program solves the variable-density flow equation by formulating the matrix equations in terms of fluid mass, with the assumption that the fluid density is a linear function of solute concentration (Guo and Langevin, 2002; Langevin and others, 2003). Transport simulations used a migrating tracer to represent halite saturation, which was related to density using a linear function between saturation and specific gravity (Hilderbrand, 1999), the ratio of fluid density to that of water (fig. 12B). The advection part of the transport equation was solved using the total-variation-diminishing (TVD) method with a courant number of 1.0 in order to minimize numerical dispersion. Remaining terms of the transport equation were solved using an implicit finite-difference method. The flow and transport equations were explicitly coupled and solved alternately; the flow solution was updated whenever the maximum change in density at a single cell exceeded 5×10^{-3} g/cm^3, about 2.5 percent of the range in density. The effect of variable fluid viscosity on flow was represented using the data and procedures described in Thorne and others (2006) and Langevin and others (2007).

One-Dimensional Flow

A single rubble chimney was represented in 1D models as a 180-m-long column, and solute was introduced through a constant concentration boundary at the bottom of the column to represent brine displaced from the flooded mine. Computed concentrations (saturations) along the length of the column after 10.7 years of transport were compared to halite saturations measured in wells Lv309 and Lv322 in September 2006. Although the 1D models neglect the effect of density variations on flow, the effect of density-driven flow is minor for the case of upward flow through a vertical column. Results from 1D models, therefore, were consistent with those obtained from 3D variable-density flow models configured to simulate one-dimensional flow.

One-dimensional flow was initially simulated using an analytical solution to the 1D advection-dispersion

equation with a constant concentration boundary given by Ogata (1970). The two variables required by this equation, groundwater velocity and longitudinal dispersivity, were estimated by fitting the computed saturations to the saturation profile observed at well Lv309 (table 4; fig. 15). The simulated saturations closely match those observed in the lower part of the profile, but measured saturations exceed those simulated near the top of the profile. This result indicates that the saturations greater than 10 percent near the top of the profile cannot be explained by simple one-dimensional advective transport and dispersion of brine from the flooded mine. The portion of the saturation profile where the observed saturations exceed simulated saturations corresponds to the Onondaga Limestone, which overlies the O/B-FZ. Inflow of saline water from this fracture zone during the 10.7-year recovery period could have entered the rubble chimney and migrated upward in front of the brine. This hypothesis is consistent with the results of inverse geochemical models that indicate saline water near the top of the saturation profile is derived from mixtures of freshwater from the LCA and saline water discharged from the O/B-FZ, and not from brine discharged from the mine cavity. The 3D models described in the following section were designed to simulate this mixing process.

Several 1D numerical models were constructed with different levels of resolution to assess the effect of numerical dispersion on simulated saturations. Hydraulic-conductivity and porosity values were specified for the rubble-chimney material in these models (table 4), and brine displacement from the mine was represented by a constant-flux boundary. Both steady-state and transient simulations were conducted, but there was little difference in simulated concentrations at the end of 10.7 years of transport. In steady-state simulations, the groundwater velocity was adjusted by specifying a constant hydraulic gradient along the column. In transient simulations, the specified hydraulic head at the top of the column was adjusted annually to reflect measured water levels in well Lv346, screened within the top 6 m of bedrock near the western edge of the collapse area (fig. 4). Simulation results with 4-m-layer spacing closely approximate those obtained with the analytical solution, whereas those obtained with 7-m-layer spacing display the effects of numerical dispersion, which widens the simulated transition zone between brine and saline water (fig. 15). The 4-m-layer spacing was, therefore, initially used in the construction of 3D models of the collapse area.

Three-Dimensional Flow

The 3D models represented a 4.7-km^2 area surrounding the rubble chimneys with northern and southern boundaries that coincided with the location of wells Lv532 and Lv534, respectively. The modeled area was divided into 75 rows and 52 columns, with cell dimensions ranging from 10 m to 300 m. The 3D models simulated flow through the LCA, the

Table 4.   Values of hydraulic and transport properties used in one-dimensional simulations.

[m/d, meters per day; m, meters]

Hydraulic property	Value
Hydraulic conductivity, m/d	3
Transport property	
Velocity, m/d	0.04
Porosity	0.1
Longitudinal dispersivity, m	0.6
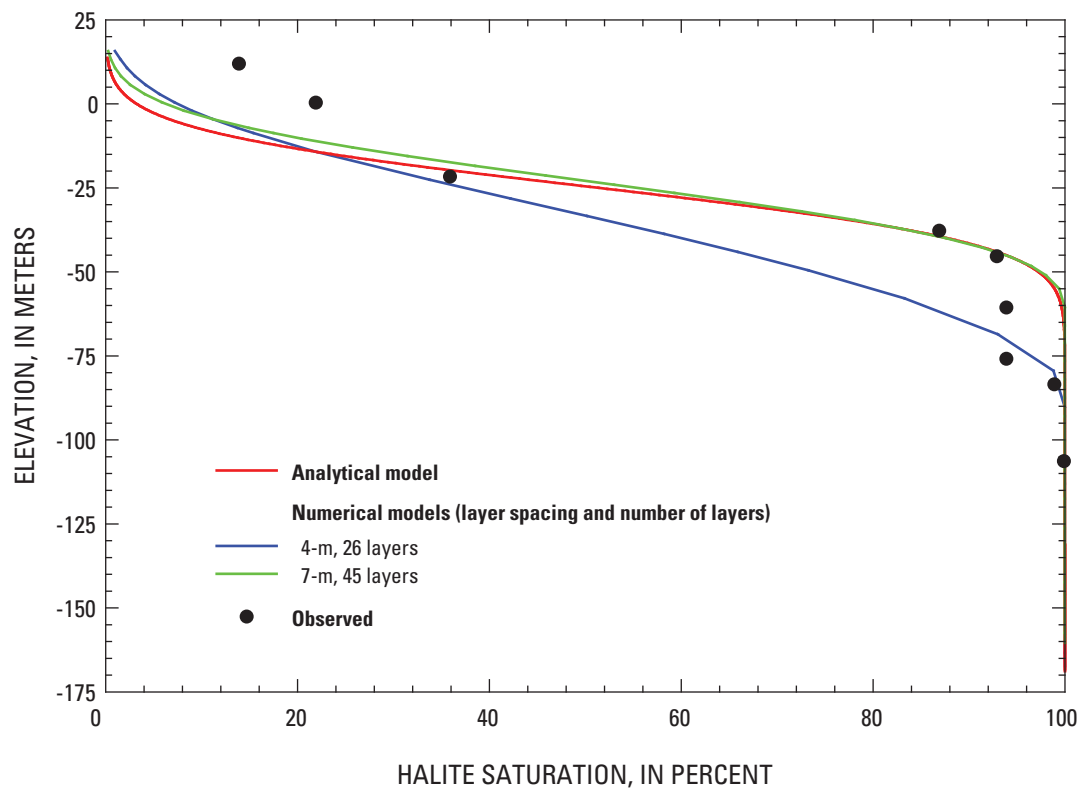
Figure 15.   Comparison of vertical profiles of halite saturations observed in wells Lv309 and Lv322 with those simulated in one-dimensional simulations with different layer spacings.

two rubble chimneys and surrounding deformation zone, and a part of the flooded salt mine (fig. 16). The 4-m-layer spacing produced a model with 45 layers and 82,177 active cells. Initial results with the 45-layer 3D model indicated that finer resolution was required in the vertical dimension to minimize numerical dispersion, so the layer spacing was reduced to 0.6 m in the upper half of the domain, producing a model with 159 layers and 283,558 active cells.

Two nearly identical 3D models were constructed (model A and model B). The primary difference between the models is that one fracture zone (O/B-FZ) was represented in model A, whereas three fracture zones were represented in model B, which also included the B/C-FZ and the Syr-FZ (fig. 17). The O/B-FZ was assumed to extend both northward and southward beyond the modeled area below the bedrock valley, and to pinch out beneath the uplands. The B/C-FZ was assumed to only extend northward of the modeled area above the flooded mine. Borehole geophysical logs (fig. 5B) indicate that within the deformation zone, the B/C-FZ likely consists of connected voids and broken zones and was, therefore, considered highly transmissive with a larger porosity than either the O/B-FZ or Syr-FZ. The extent of the Syr-FZ was assumed to be limited to the deformation zone; the Syr-FZ could either have developed in response to the collapse or have been a pre-existing cavity, as hypothesized by Gowan and Trader (2000b).

Model Design

The extent of the LCA within the model domain was taken from the previous groundwater-flow model of Yager and others (2001). The two models were not coupled, however, because the previous model did not represent the rubble chimneys and deformation zone, which were the focus of this study. A 5-m thickness was assumed for the LCA throughout the model domain and the elevation of the top of bedrock was based on data from Alpha Geoscience (2005). Model layers are inclined from north to south at less than 1° to represent the bedding dip of bedrock, and are parallel to elevations measured in the salt mine (John Nadeau, Alpha Geoscience, written commun., 2006). A 4-m thickness was assumed for the flooded mine. Thicknesses of fracture zones represented in 159-layer 3D models were arbitrary and based on the layer spacing at the depth of each specified zone. A 0.6-m thickness was specified for the O/B-FZ, whereas thicknesses of the B/C-FZ and the Syr-FZ were specified as 1.3 and 5.4 m, respectively. The elevation of O/B-FZ was interpolated from borehole geophysical logs in wells Lv532 and Lv534, north and south of collapse area, respectively (fig. 4). As a result, the O/B-FZ simulated by the model intersects the rubble chimneys at a higher elevation (-10 m) than that detected by the borehole geophysical log of well Lv309 (-14 m), which is in the area of greatest bedrock subsidence. The elevations of the B/C-FZ and the Syr-FZ were based on borehole geophysical logs and the saturation profile at Lv309 (figs. 5 and 10).

The 10.7-year transient simulation was divided into annual periods and preceded by a steady-state simulation with a nominal length of 1 day to provide the initial head distribution. A constant head based on the measured brine levels in well Lv396, screened in the flooded salt mine, was specified in the steady-state period for the bottom model layer. The initial concentration (saturation) of water in the rubble chimneys and deformation zone was specified as zero and a constant saturation of 100 percent was specified for the bottom model layer (flooded mine). Constant heads at the northern and southern boundaries in the top model layer (LCA) were varied annually during the 10.7-year period, based on measured water levels in well Lv346, at the western edge of the collapse area. A source of brine at 100-percent saturation was injected into the bottom model layer during the 10.7-year period to represent brine displaced from the flooded mine. The specified brine-displacement rates were estimated through model calibration and declined from 6.9 L/s at the beginning of the simulation to 1.6 L/s at the end. The specified rates were consistent with the mean rate estimated through subsidence surveys from 1996 through 2001 (4.4 L/s) and the rate estimated in 2007 (1.6 L/s).

Underflow of saline water through the O/B-FZ was represented in both models A and B at the northern and southern boundaries in model layer 37 (fig. 17). The actual inflow rates are unknown but are assumed to have diminished during the 10.7-year period as the hydraulic head within the LCA and rubble chimneys increased. Vertical-pressure gradients were negligible between the O/B-FZ and the LCA in September 2006 (based on water levels measured at wells Lv532 and Lv534), indicating no potential for inflow at the end of the simulated period. Specified inflow rates were estimated through model calibration to decline during the first 9 years of the simulation period from 5.9 to 0.0 L/s in model A, and from 3.0 to 0.0 L/s in model B, yielding mean inflow rates of 1.9 and 1.0 L/s, respectively (table 5). Constant heads were specified at the northern and southern boundaries of the O/B-FZ during the last 1.7 years of the simulation, using measured heads in well Lv346 and assuming a zero vertical-pressure gradient between the O/B-FZ and the LCA. Constant saturations of 16 and 30 percent (based on values measured in September 2006) were specified at the northern and southern boundaries, respectively, and the initial saturation distribution varied linearly from north to south.

Underflow through the B/C-FZ was represented in model B through a head-dependent boundary specified at the northern edge of model layer 83. The heads were computed on an annual basis with the same method used to compute heads for the O/B-FZ, as described above. The hydraulic conductivity of the head-dependent boundary was specified as 1.5 m/d to limit outflow. Lateral boundaries of the Syr-FZ (model layers 137 and 138) were specified as no-flow. The initial saturations within the B/C-FZ and Syr-FZ were specified as 30 and 0 percent, respectively, under the assumptions that the B/C-FZ is hydraulically connected to a saline-water source, and that the Syr-FZ was filled with freshwater during mine flooding.
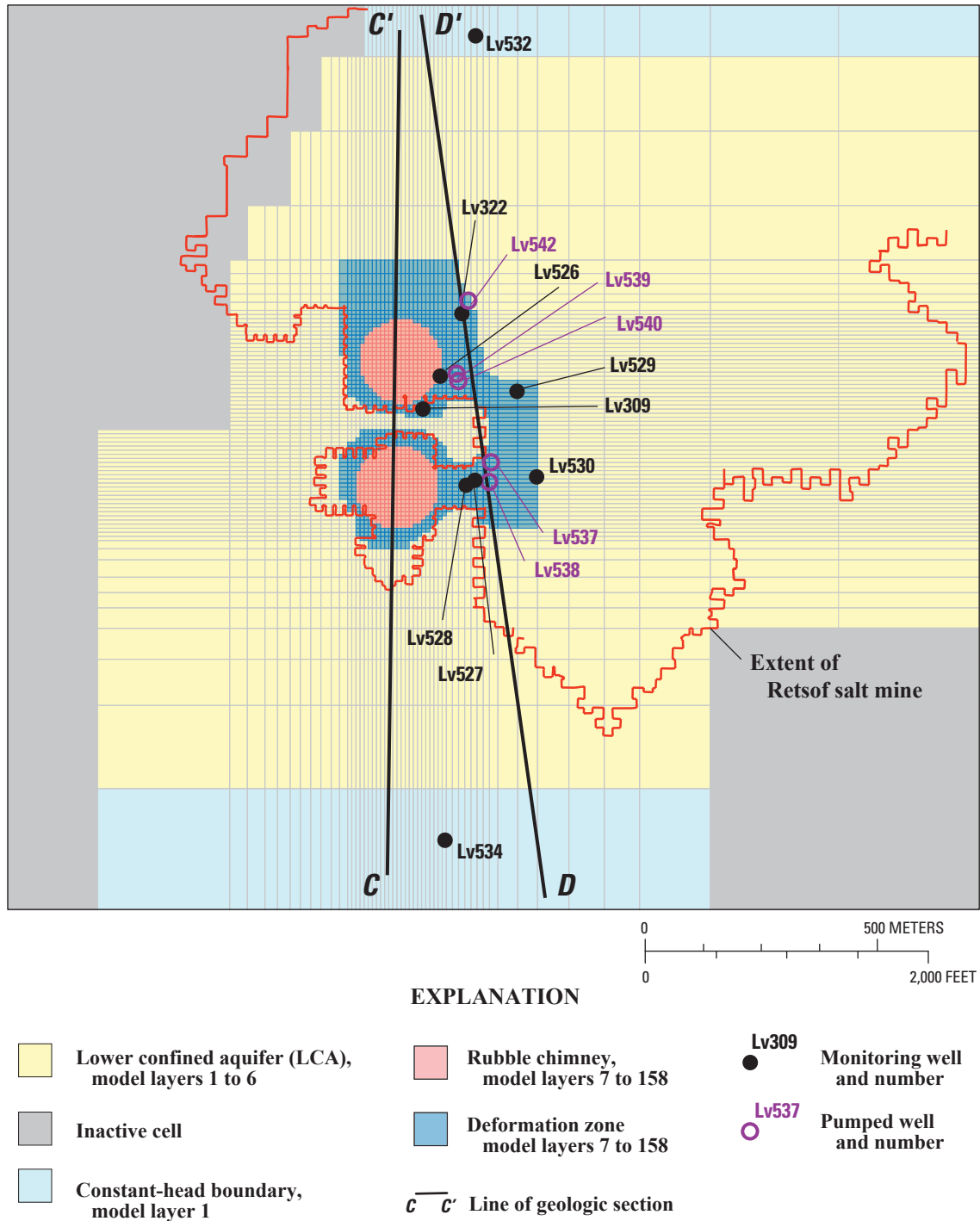
Figure 16. Boundaries of three-dimensional model showing extent of flooded salt mine, and locations of rubble chimneys, deformation zone, and wells.
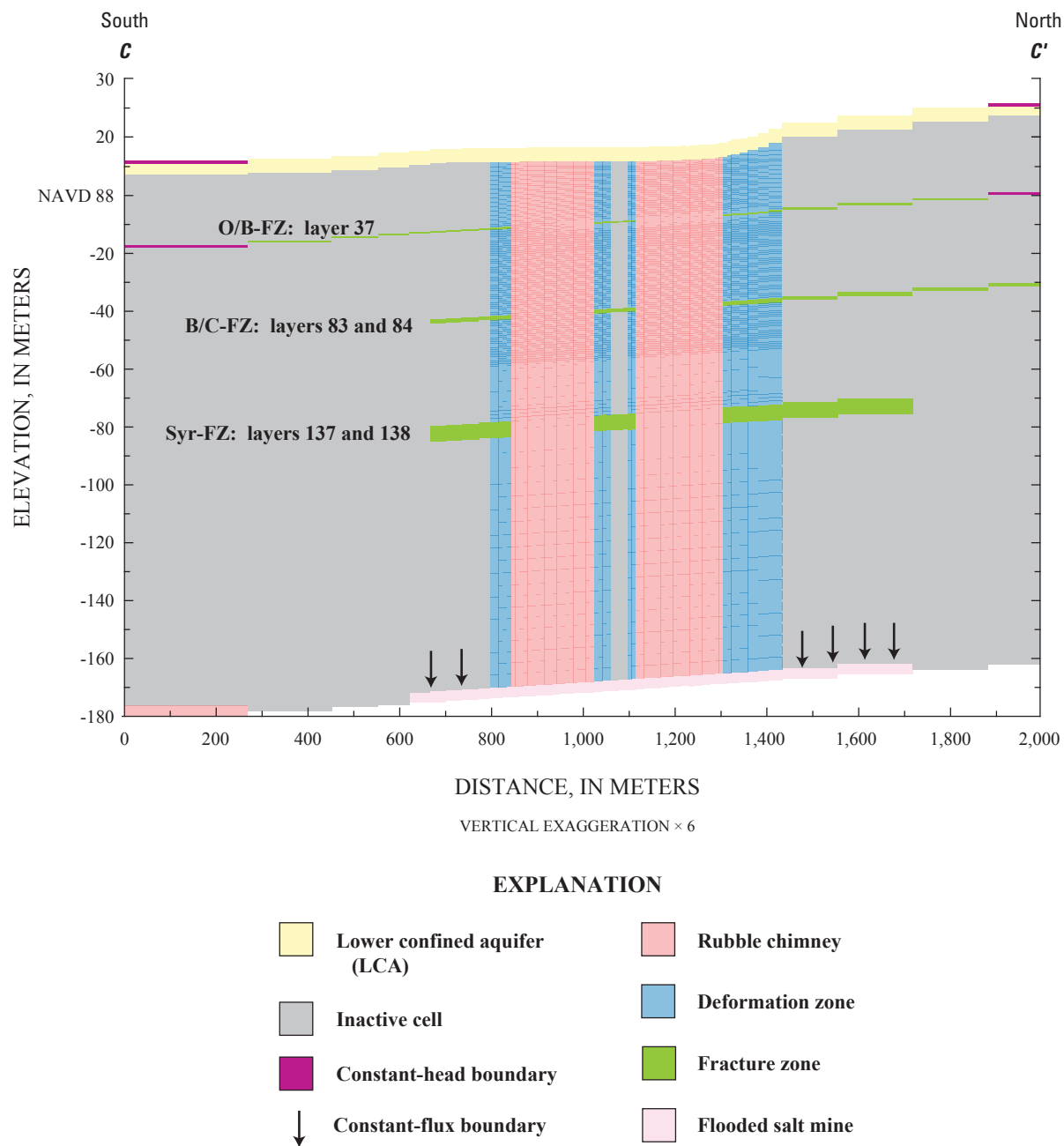
Figure 17. Section C-C′ showing boundary conditions specified in three-dimensional model, and depths and extents of fracture zones. Fracture zones: O/B-FZ, Onondaga/Bertie contact; B/C-FZ, Bertie/Camillus contact; Syr-FZ, Syracuse Formation. Location of section shown in figure 16.

Table 5.   Values of hydraulic and transport properties used in three-dimensional simulations of saline water and brine migration during recovery of aquifer system.

[Shading indicates different values used in model A and B; L/s, liters per second; m/d, meters per day; --, not used; fracture zones: O/B-FZ, Onondaga/Bertie contact; B/C-FZ, Bertie/Camillus contact; Syr-FZ, Syracuse Formation]

	Model	
	A	**B**
Fracture zones	O/B-FZ	O/B-FZ, B/C-FZ, Syr-FZ
Boundary flow rates, L/s		
Brine displacement from mine	6.9 to 1.6	6.9 to 1.6
Mean saline-water inflow from O/B-FZ	1.9	1
Hydraulic conductivity[1], m/d		
Lower confined aquifer	150	150
Rubble chimneys	3	3
Deformation zone	3[2]	3[2]
O/B-FZ	15	15
C/B-FZ	--	230
Syr-FZ	--	6
Porosity, percent		
Lower confined aquifer	25	25
Rubble chimneys	10	6
Deformation zone	1	1
O/B-FZ	1	1
C/B-FZ	--	50
Syr-FZ	--	5
Longitudinal dispersity, m	0.6	1.5

[1]Isotropic unless otherwise noted.

[2]10:1 ratio of horizontal to vertical hydraulic conductivity.

Model Calibration

Simulated saturations were visually compared with time-series plots of saturation observed in well Lv309 and well Lv322 from January 1996 through September 1996 (fig. 8), and with the saturation profile observed in September 2006 (fig. 9). The length of the simulations (2 to 5 days) precluded the application of parameter estimation, so model parameters were adjusted by trial and error and later assessed through sensitivity analyses in simulations of pumping described later in this report. The resulting models were intended to illustrate important processes controlling transport, rather than as calibrated representations of the flow system.

Values were specified for hydraulic conductivity, porosity and longitudinal dispersivity (table 5). The 3D models were largely insensitive to values of specific storage, which were taken from the literature and ranged from 6×10^{-6} to

$6 \times 10^{-7} \, \mathrm{m}^{-1}$. The porosity value for the rubble chimneys was the most sensitive parameter because it determined the velocity of brine migration and the position of the transition zone between brine and saline water at the end of the 10.7-year simulation. Different porosity values were estimated for model A (10 percent) and model B (6 percent) to match the saturation profile measured in well Lv309 in September 2006 (fig. 18). Porosity values taken from the literature were specified for sand and gravel in the LCA (25 percent) and fractured rock in the O/B-FZ (1 percent). Porosity values for the B/C-FZ (50 percent) and the Syr-FZ (5 percent) in model B are larger to reflect the assumed presence of voids in these lower fracture zones, and were determined through trial and error; these values are arbitrary, however, because they reflect the model-layer spacing (as described above) rather than the actual thicknesses of the fracture zones. A porosity value of 100 percent was specified for layer 159, which represented the flooded
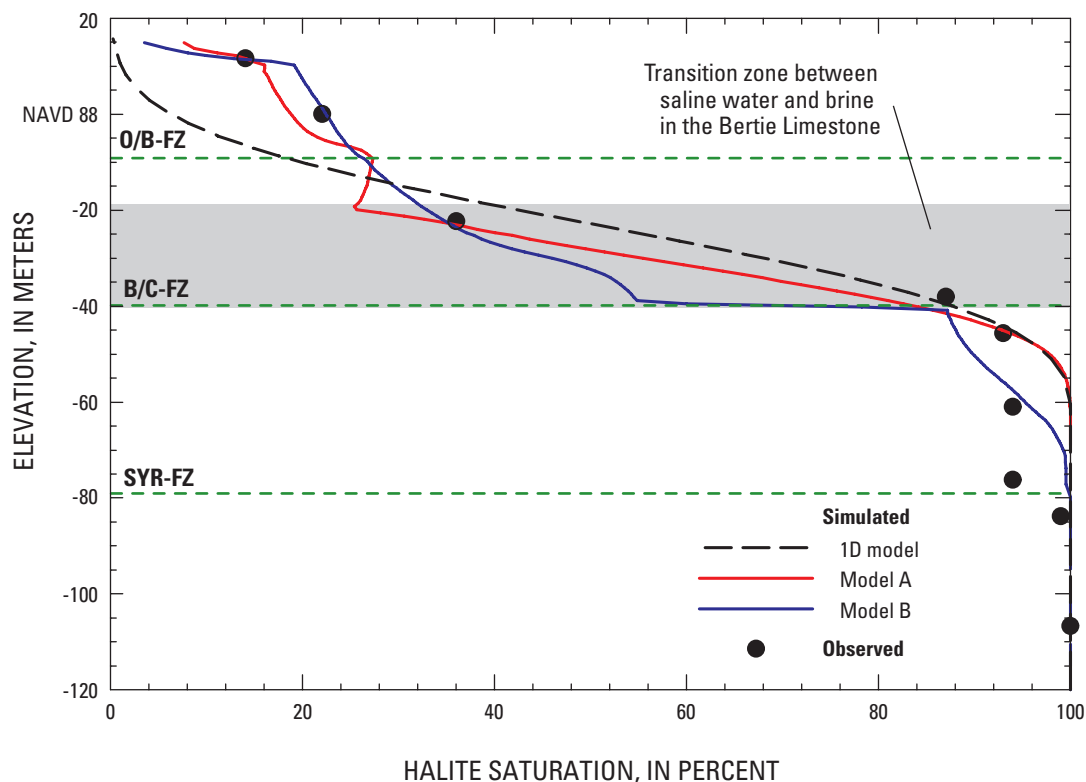
Figure 18. Comparison of vertical profiles of halite saturations observed in wells Lv309 and Lv322 with those simulated by one-dimensional simulation and by three-dimensional simulations with models A and B.

mine. The longitudinal-dispersivity value estimated for the rubble chimneys in 1D simulations (0.6 m) was specified for all materials in model A but was increased to 1.5 m in model B to better match the saturation profile measured in well Lv309.

The hydraulic-conductivity value for the LCA (150 m/d) was based on the transmissivity value (700 m²/d) estimated with the groundwater-flow model of the aquifer system in the Genesee Valley described in Yager and others (2001). The hydraulic-conductivity value for the rubble chimneys and deformation zone (3 m/d) was the same as that specified in 1D models discussed previously. The rubble chimneys were assumed to be isotropic, but an anisotropy ratio of 10:1 (ratio of horizontal to vertical hydraulic conductivity) was specified for the deformation zone to represent preferential horizontal flow parallel to fractures created by the roof collapses in the mine. The 3D models were largely insensitive to hydraulic-conductivity values specified for the rubble chimneys and deformation zone because the velocity of the brine was determined by the brine-displacement rate and the porosity of the rubble chimneys. A sufficiently large hydraulic-conductivity value (3,000 m/d) was specified for the flooded

mine to minimize the hydraulic gradient within the model layer that represented the mine. The hydraulic-conductivity values for the three fracture zones were arrived at through trial and error and ranged from 6 to 230 m/d. The hydraulic conductivity assigned to the O/B-FZ (15 m/d) is slightly lower than that estimated for a fractured zone near the top of the Onondaga Limestone (23 m/d) at well Lv346 (Alpha Geoscience, 1996). The B/C-FZ was assigned the highest hydraulic conductivity (230 m/d) to reflect the assumed transmissivity of this high-porosity zone. The lowest hydraulic conductivity (6 m/d) was assigned to the Syr-FZ, which is assumed to be a rubble-filled zone in shale bedrock.

Model Results

The saturation profile simulated with model A is similar to that simulated by the 1D model presented earlier, but better matches the lower saturations (between 10 and 40 percent) observed in the upper part of the saturation profile above the transition zone from brine to saline water in the Bertie

Limestone (fig. 18). In the 1D simulation, salinity in the rubble chimney is derived solely from the advection and dispersion of brine from the flooded mine. In contrast, part of the salinity in the upper part of the chimney above the transition zone simulated by model A is derived from the inflow of saline water from the O/B-FZ during recovery of water levels in the aquifer system. The saturation profile simulated with model B also matches the observed profile, but unlike in model A, the effects of mixing among aquifer water, bedrock water, and brine at the B/C-FZ and the Syr-FZ also are represented. Some of the brine in model B displaces less dense water in the Syr-FZ, and some brine and saline water are diverted laterally through the B/C-FZ. Mixing associated with the movement of brine through these flow paths lifts saline water derived from the mine water higher in the rubble chimney than in model A. Consequently, some of the salinity above the transition zone in model B is derived from brine, rather than from bedrock water.

Differences in the compositions of water simulated with models A and B were evaluated by comparing the results of transport simulations that included three additional solutes, which act as tracers that track the movement of mine water, bedrock water, and aquifer water. Water density computed by the simulations was solely dependent on the solute that tracked halite saturation, as in the single-solute simulations presented earlier. The simulated mixture of water was derived from three sources (mine water, bedrock water, and aquifer water), each with concentrations that ranged from 0 to 100 percent. Simulated concentrations for the three-component mixtures sum to 100 percent (plus or minus 5 percent, because no mass-balance constraints were imposed on the simulations). For initial conditions in model A (1996), the flooded mine was assumed to be filled with brine, whereas aquifer water occupied the LCA, the rubble chimneys and the deformation zone, and bedrock water occupied the O/B-FZ. For model B, the B/C-FZ and Syr-FZ were assumed to be filled with bedrock water and aquifer water, respectively.

Differences in the sources of salinity in the upper parts of the saturation profiles simulated by models A and B are apparent in time-series plots that illustrate changes in the simulated composition of waters at wells Lv309 and Lv322 from 1996 through 2006 (fig. 19). In model A, bedrock water intrudes the -23-m elevation in well Lv309 in 1999, displacing aquifer water and increasing the salinity of water. A similar pattern is evident at well Lv322, and the increase in simulated salinity at both wells tracks the observed changes reasonably well. In contrast, part of the salinity at both wells in model B is derived from mine water, which has been transported upward through mixing with waters at the B/C-FZ and Syr-FZ. This process is described in the following paragraph.

The development of saturation profiles simulated by models A and B from 1998 through 2006 is illustrated by sequences of images that show changes in halite saturation (fig. 20A) and changes in flow directions (fig. 20B). In model A, saline water from the O/B-FZ enters the rubble chimneys and moves downward, where it forms a pool above brine migrating upward from the flooded mine (fig. 20A). The

brine continues upward and pushes the saline water ahead of it, forming a diffuse front above the transition zone between the brine and saline water. The level of brine (greater than 90-percent saturation) is nearly horizontal in both chimneys by 2006. The initial development of the saturation profile simulated by model B is similar to that of model A, but less saline water flows from the O/B-FZ into the rubble chimneys. After 1998, the transition zone in the northern chimney becomes more diffuse than in the southern chimney as mixing with waters from the B/C-FZ and Syr-FZ transports mine water higher in the water column. Brine levels in both chimneys slope northward by 2006, reflecting the lateral diversion of about 0.2 L/s of mine water into the B/C-FZ.

Flow directions simulated by models A and B are shown in figure 20B. In both simulations, closure of the mine cavity displaces brine from the flooded mine, causing upward flow through the rubble chimneys and deformation zone, and outflow to the LCA. Water in the O/B-FZ flows into the rubble chimneys during both simulations, but the flow direction reverses at the end of the simulation period (September 2006), when water from the rubble chimneys flows outward into the O/B-FZ. The simulated flow direction in the B/C-FZ is outward from the collapse area in model B. The divergence of flow vectors from uniform flow near the bottom of the rubble chimneys causes mixing within the water column in both simulations. The degree of mixing is greater in model B than in model A and strongest at depths where fracture zones intersect the rubble chimneys.

The simulated movement of mine water, bedrock water, and aquifer water in model A from 1996 through 2006 is shown in figure 21. Each type of water was treated as a conservative tracer that ranged in concentration from 0 to 100 percent. The assumed concentration distributions within the model domain are indicated at the start of the simulation in January 1996. Mine water is pushed upward in the center of the rubble chimneys by the downward flow of bedrock water from the O/B-FZ but does not reach the LCA. The bedrock water forms a pool at the periphery of the deformation zone that remains intact as it is displaced upward by the mine water. The distribution of aquifer water created by these flow patterns is complex, and some aquifer water remains in the rubble chimneys below the O/B-FZ in 2006. Mine water moves higher in the rubble chimneys in model B than in model A and displaces some bedrock water in the O/B-FZ (fig. 22). The pool of bedrock water is smaller in model B than in model A, and more bedrock water is displaced from the O/B-FZ. As a result, less aquifer water is displaced upward in model B than in model A, particularly within and around the northern rubble chimney. Animations showing the movement of saline water, mine water, bedrock water, and aquifer water during the 10.7-year simulations with models A and B can be viewed online at http://ny.water.usgs.gov/projects/Coram/seawat/seawat.html
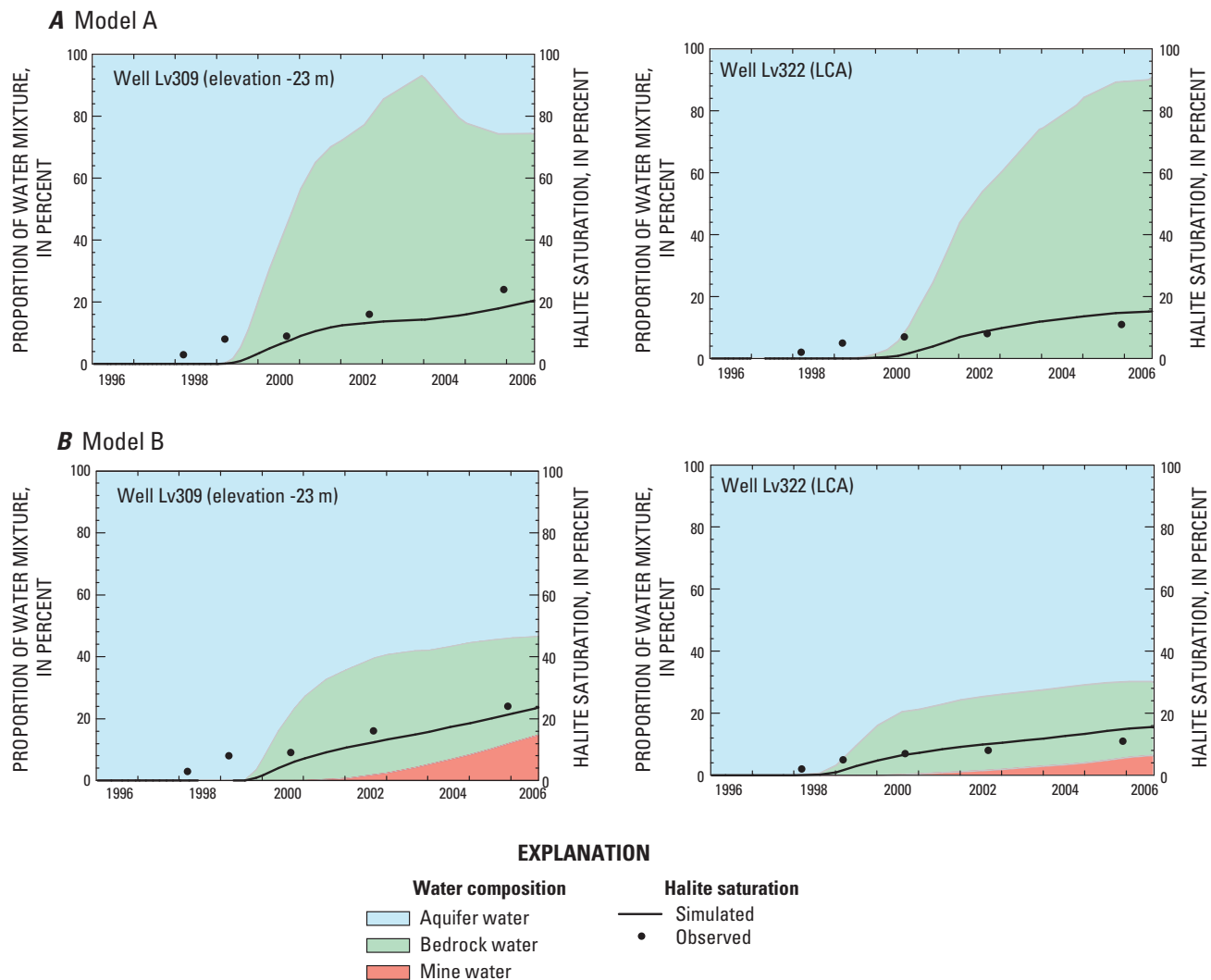
Figure 19.   Changes in water compositions in wells Lv309 (elevation -23 m) and Lv322 from January 1996 through August 2006 in four-solute simulations with: *(A)* model A and *(B)* model B. Shading indicates proportions of aquifer water, bedrock water, and mine water in simulated mixtures. Observed and simulated halite saturation reference right-hand scale.
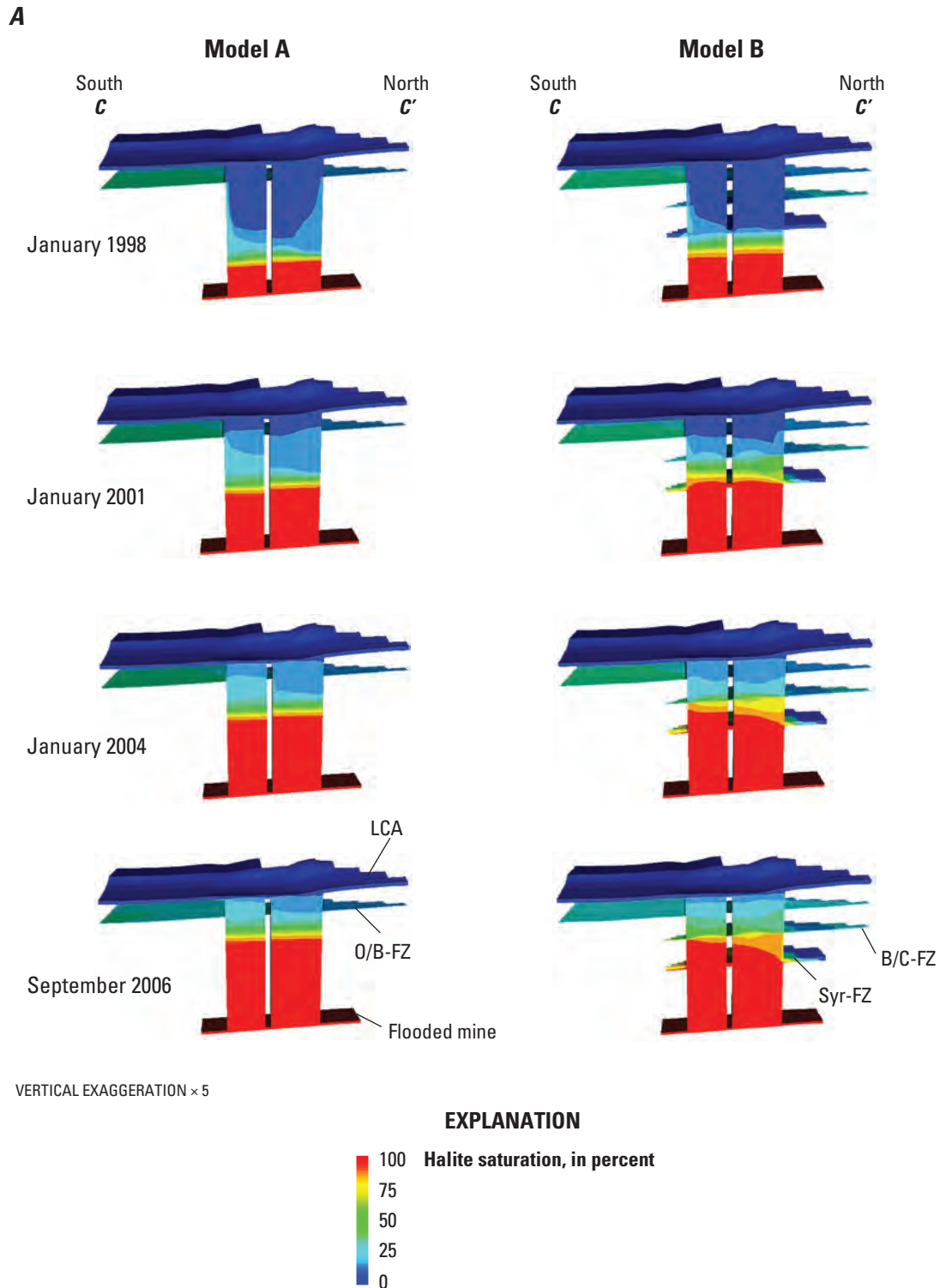
A

Figure 20.   Block diagrams along section C-C′ in the collapse area showing simulation results from January 1998 through September 2006 with model A and model B: *(A)* changes in spatial distribution of halite saturation, and *(B)* changing directions of groundwater flow. LCA, lower confined aquifer; fracture zones: O/B-FZ, Onondaga/Bertie contact; B/C-FZ, Bertie/Camillus contact; Syr-FZ, Syracuse Formation. Location of section shown in figure 16.

B
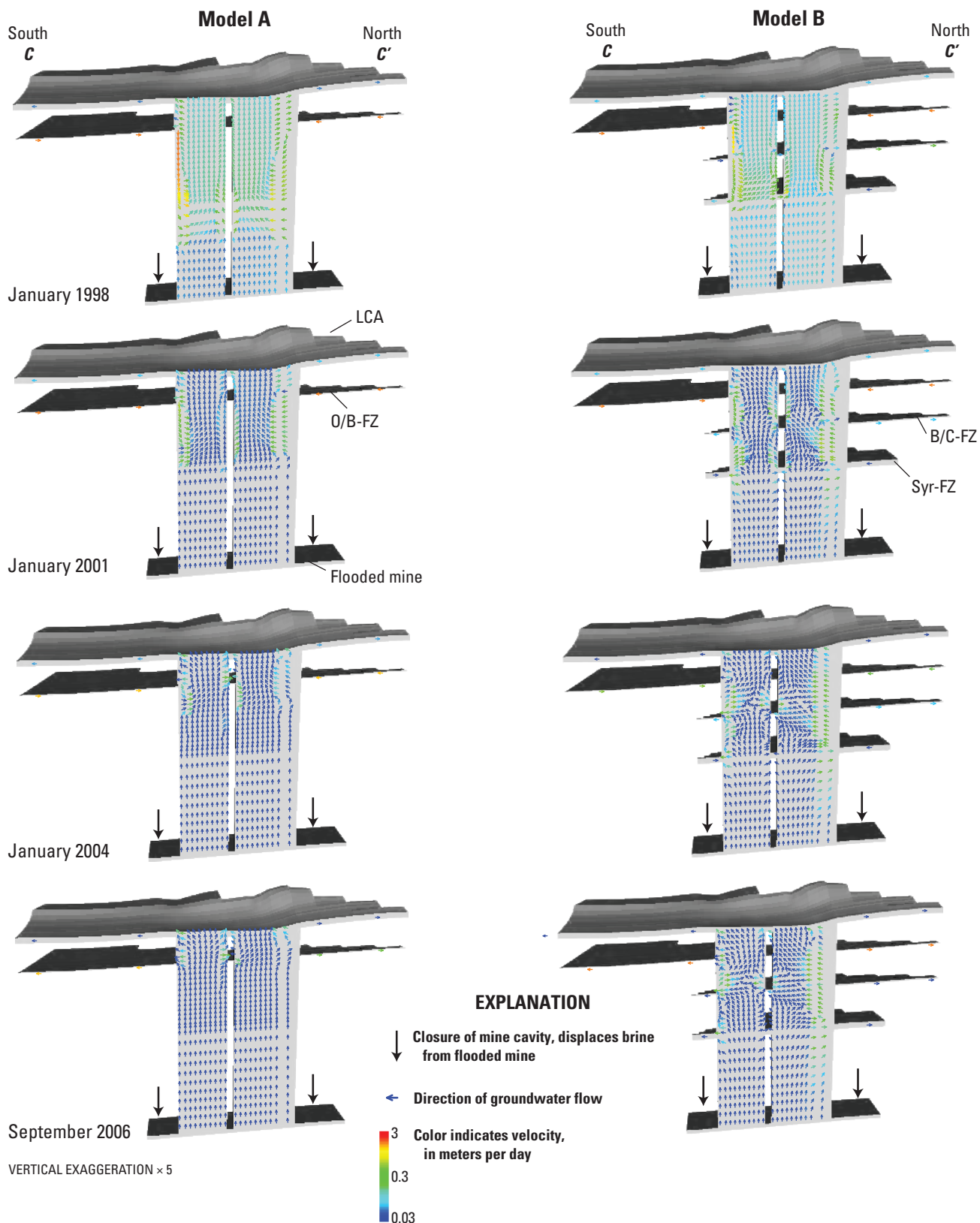
Figure 20.   Block diagrams along section C-C' in the collapse area showing simulation results from January 1998 through September 2006 with model A and model B: *(A)* changes in spatial distribution of halite saturation, and *(B)* changing directions of groundwater flow. LCA, lower confined aquifer; fracture zones: O/B-FZ, Onondaga/Bertie contact; B/C-FZ, Bertie/Camillus contact; Syr-FZ, Syracuse Formation. Location of section shown in figure 16.—Continued
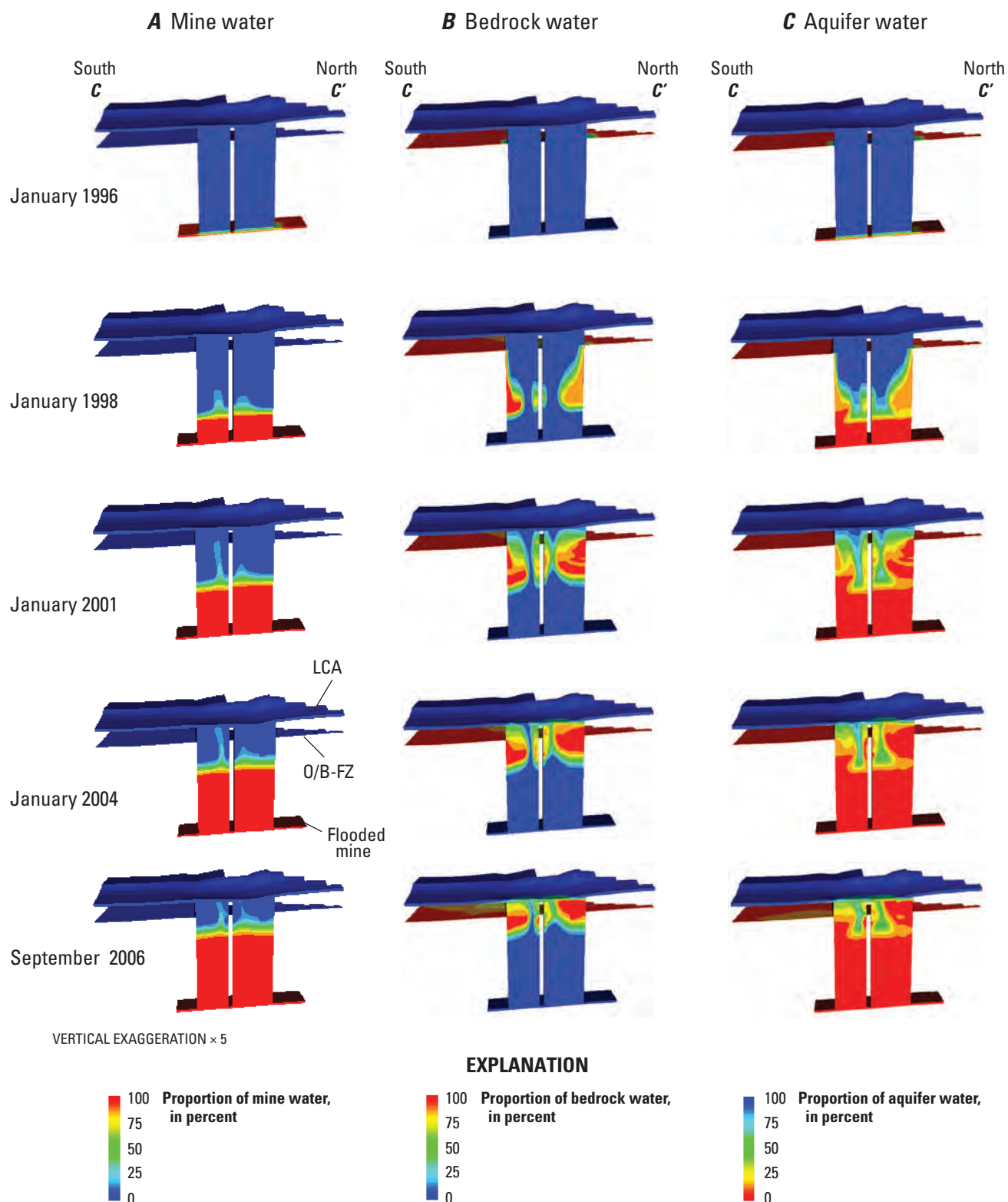
Figure 21. Block diagrams along section C-C′ showing changes in the composition of water in the collapse area from January 1996 through September 2006 in simulations with model A. Color scale indicates proportion of water mixture derived from: *(A)* mine water, *(B)* bedrock water and *(C)* aquifer water (note color scale is reversed). LCA, lower confined aquifer; O/B-FZ, fracture zone at Onondaga/Bertie contact. Location of section shown in figure 16.
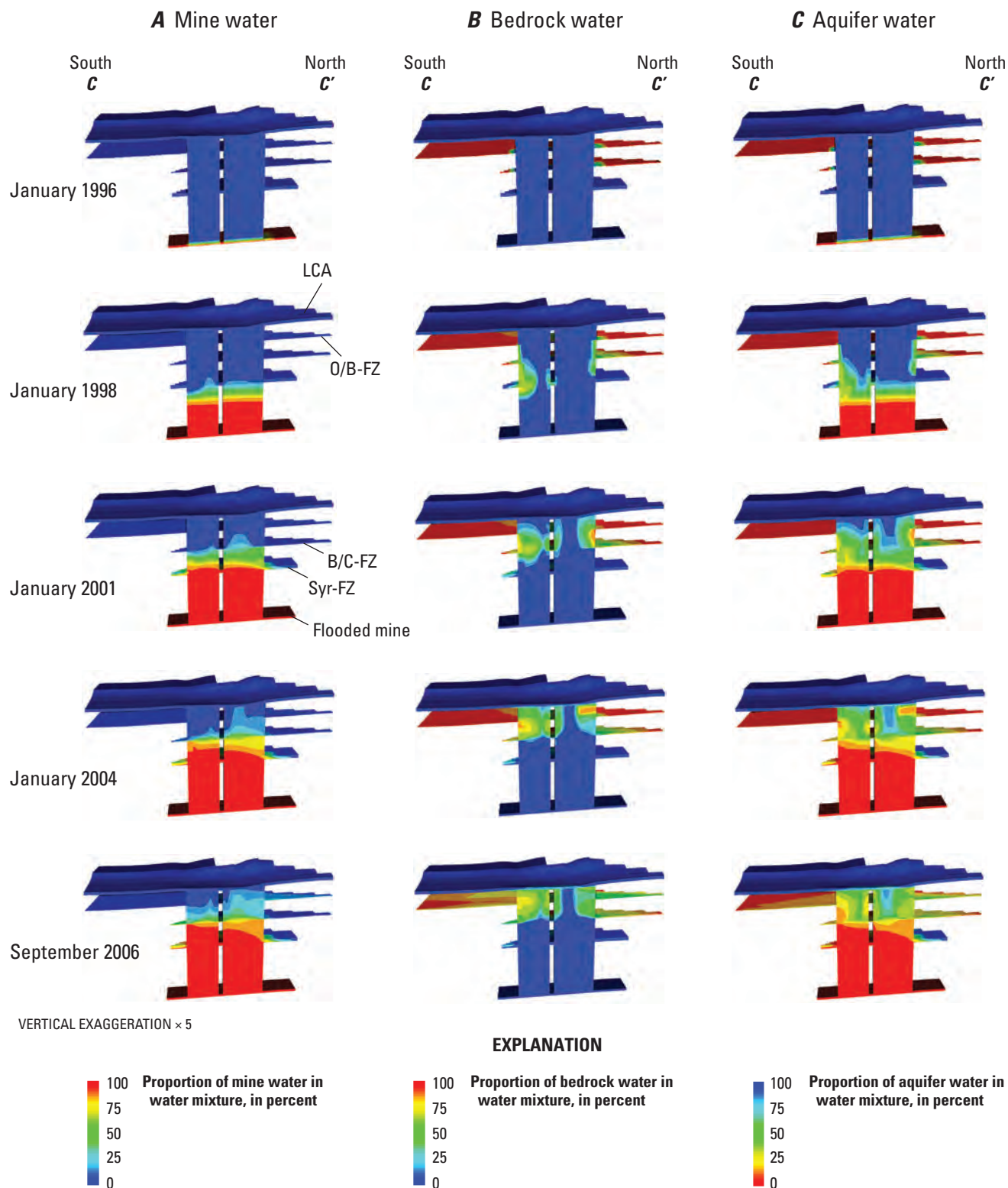
Figure 22. Block diagrams along section C-C' showing changes in the composition of water in the collapse area from January 1996 through August 2006 in simulations with model B. Color scale indicates proportion of water mixture derived from: *(A)* mine water, *(B)* bedrock water, *(C)* aquifer water (note color scale is reversed). LCA, lower confined aquifer; fracture zones: O/B-FZ, Onondaga/Bertie contact; B/C-FZ, Bertie/Camillus contact; Syr-FZ, Syracuse Formation. Location of section shown in figure 16.

Discussion of Results

Both models A and B reproduce the saturation profile measured in September 2006 in wells Lv309 and Lv322 reasonably well, and neither model indicates that saline water had migrated beyond the collapse area by that time. Model A (one fracture zone) indicates that saline water in the LCA is derived primarily from upward migration of bedrock water from the O/B-FZ, which is consistent with results from inverse geochemical models (table 2). The simulated distribution of aquifer water, bedrock water, and mine water in the collapse area is complex, however, and it is possible that saline water in parts of the LCA that were not sampled could contain mine water. Model B (three fracture zones) indicates lateral diversion of mine water into the O/B-FZ, the B/C-FZ, and the Syr-FZ. The resultant mixing of mine water with aquifer water and bedrock water could induce upward transport of mine water to the LCA. The simulated outflow of mine water from the rubble chimneys to the B/C-FZ in model B is consistent with the original predictions of geotechnical studies (John T. Boyd Company, 1995) and with flowmeter surveys conducted in Lv309 in 2004 (fig. 5).

It is not possible on the basis of available information to assess whether model A or model B better represents conditions in the collapse area from January 1996 through August 2006. No wells have been completed below the bottom of the Bertie Limestone outside the collapse area, so the lateral extents of the B/C-FZ and Syr-FZ cannot be delineated. As a result, it cannot be determined whether either or both of these lower fracture zones affected the transport of brine and saline water during water-level recovery (as in model B), or whether transport was only affected by the O/B-FZ (as in model A).

Boundary conditions specified for the flooded mine, the O/B-FZ, and the B/C-FZ during the 10.7-year simulation period also are uncertain. The boundary conditions affect both the estimated values of model parameters and the simulated movement of water. Porosity values estimated with both models for the rubble chimneys and deformation zone are correlated with specified rates of brine displacement from the flooded mine. Porosity determines both the volume of void space filled by migrating brine and the velocity of brine migration, so a lower rate of brine displacement can be compensated for in either model by decreasing the porosity value, thereby increasing the velocity of migration. The mean inflow rate of bedrock water from the O/B-FZ during water-level recovery also is uncertain. The simulated proportion of salinity derived from bedrock water in either model would be less if the inflow rate was lower, for example. This change can be compensated for by decreasing the porosity value to increase the upward extent of brine migration and, thereby, match the observed saturation profile. Similarly, the outflow rate through the B/C-FZ simulated in model B also affects the saturation profile—for example, increasing the rate of outflow also requires an increase in the velocity of brine migration (decrease in porosity) to maintain salinity in the simulated water column.

As a result of these and other sources of uncertainty, both models A and B are nonunique, and it is likely that other sets of parameter values and boundary conditions could be selected that match the observed saturations equally well. The 1D and 3D simulations of brine and saline-water migration discussed in this section are not, therefore, intended as accurate representations of flow and transport in the collapse area. Simulation results can, however, be used to identify important processes that probably contributed to the migration of brine and saline water. The primary source of salinity in the collapse area is halite brine that was displaced from the flooded mine and transported upward by advection and dispersion through the rubble chimneys and deformation zone. Depth profiles of both the simulated distribution of salinity (fig. 18) and the simulated geochemical composition of waters (table 2), however, indicate the presence of a second source of salinity, most likely the O/B-FZ. The observed saturation profile can be reproduced by combining inflow of bedrock water from this fracture zone with advection and dispersion of brine from the flooded mine (as in model A). In addition to these processes, the lateral diversion of brine into the B/C-FZ and Syr-FZ (as in model B) promotes the upward migration of mine water. The relative contributions of mine water, bedrock water, and aquifer water to the observed salinity within the collapse area are controlled by the rates of flow to and from the three fracture zones.

Simulated Pumping of Brine and Saline Water

Changes in water levels and halite saturation produced by pumping for the brine-mitigation project were computed with 5-year transient simulations conducted with both models A and B. Simulated results were compared with water levels and saturations observed from September 2006 through February 2008 and the total mass of halite produced by the desalination plant. The transport of four solutes (saturation, mine water, bedrock water, and aquifer water) was simulated so that the composition of water produced by each pumped well could be calculated. A sensitivity analysis was conducted with both models A and B to identify the important model parameters and quantify the uncertainty in model predictions.

Model Design

The 5-year transient simulations covered the period from September 2006, when pumping for the brine-mitigation project began, through August 2011. The 5-year simulation was divided into six periods with four time steps each to represent two periods when pumping was halted in January and April 2007 and the pumped intervals and rates in some wells were changed. The final 4.4 years were divided into

two periods to enable the comparison of model results with observations made in February 2008.

The initial conditions for the 5-year simulations of pumping were obtained from the water levels and concentrations computed by the 10.7-year simulations of water-level recovery discussed previously. The boundary conditions specified in the bedrock fracture zones (O/B-FZ and B/C-FZ) for the 5-year simulations were the same as those in the 10.7-year simulations. Heads at the northern and southern boundaries of the LCA were adjusted in the 5-year simulations, however, to reflect a 0.3-m decline in head across the model domain under the current (2008) northward hydraulic gradient.

Median pumping rates from five pumped wells during the period September 2006 through February 2008 were used to represent withdrawals during the 5-year simulations (table 6). Although the pumps are all in open boreholes, the pumped intervals correspond to 3-m intervals surrounding the pumps, based on the assumption that most of the water withdrawn by pumping is derived from the rubble zone through a limited interval around each pump (John Nadeau, Alpha Geoscience, oral commun., 2007).

Model Results

Saturation profiles simulated by both models A and B reflect the influence of pumping, with brine levels (greater than 90-percent saturation) decreasing and aquifer water entering the top of the collapse area during the 5-year simulations (fig. 23). Simulated brine levels fall only slightly in model A, but saturations decrease substantially in the upper part of the collapse area. There is a greater decline in saturation simulated in model B because the porosity of the rubble chimneys (6 percent) is lower than in model A (10 percent). Some brine and saline water also are diverted through the B/C-FZ in model B. Both simulations indicate that current pumping rates are sufficient to reverse the upward migration of brine and saline water through the collapse area.

Saturations simulated at elevations corresponding to the O/B-FZ with both models A and B indicate a downward trend that is generally more gradual than that observed from September 2006 through February 2008 (fig. 24). The simulated decline of saturations in the LCA at well Lv322 (fig. 24F) is also lower than the observed decline. Initial simulated saturations match the observed saturations in September 2006 reasonably well, with the exception of that in well Lv527 (fig. 24C), where simulated saturations underpredict observed saturations by 30 percent. Well Lv527 is near the southern rubble chimney and was sampled in the transition zone from saline water to brine in the Bertie Limestone. Errors in the simulated saturation profile are magnified at this elevation because saturations in the transition zone increase rapidly with depth. It is also possible that heterogeneity within the collapse area causes higher saturations at this location.

Simulated water levels reflect the observed upward trend as lower salinity (less dense) water intrudes the collapse area and replaces saline water and brine removed by pumping (fig. 25). The water levels rise in response to pumping because a greater depth of low-density water is required to balance the weight of high-density water remaining in the collapse area. Simulated water levels match observed water levels reasonably well, with the exceptions of those in well Lv527 (fig. 25C), where simulated saturations are less than observed, as noted above, and well Lv526 (fig. 25A), located near the

Table 6.   Average halite saturation in water pumped by brine-mitigation project in February 2008, and simulated saturation and composition of pumped water with models A and B.

[L/s, liters per second]

Well	Median pumped rate, L/s	Halite saturation, percent			Water composition, percent						
						Model A			Model B		
		Observed	Model A	Model B	Mine water	Bedrock water	Aquifer water	Mine water	Bedrock water	Aquifer water	
Lv537	0.71	93	99	95	97	1	1	91	0	8	
Lv538	0.36	77	47	42	17	72	11	24	40	36	
Lv539	0.74	97	100	98	100	0	0	97	0	3	
Lv540	0.38	53	66	53	60	28	12	52	12	36	
Lv542	0.11	65	82	63	78	16	6	69	7	25	
Influent to desalination plant	2.30	78	86	80	78	17	4	75	9	16	
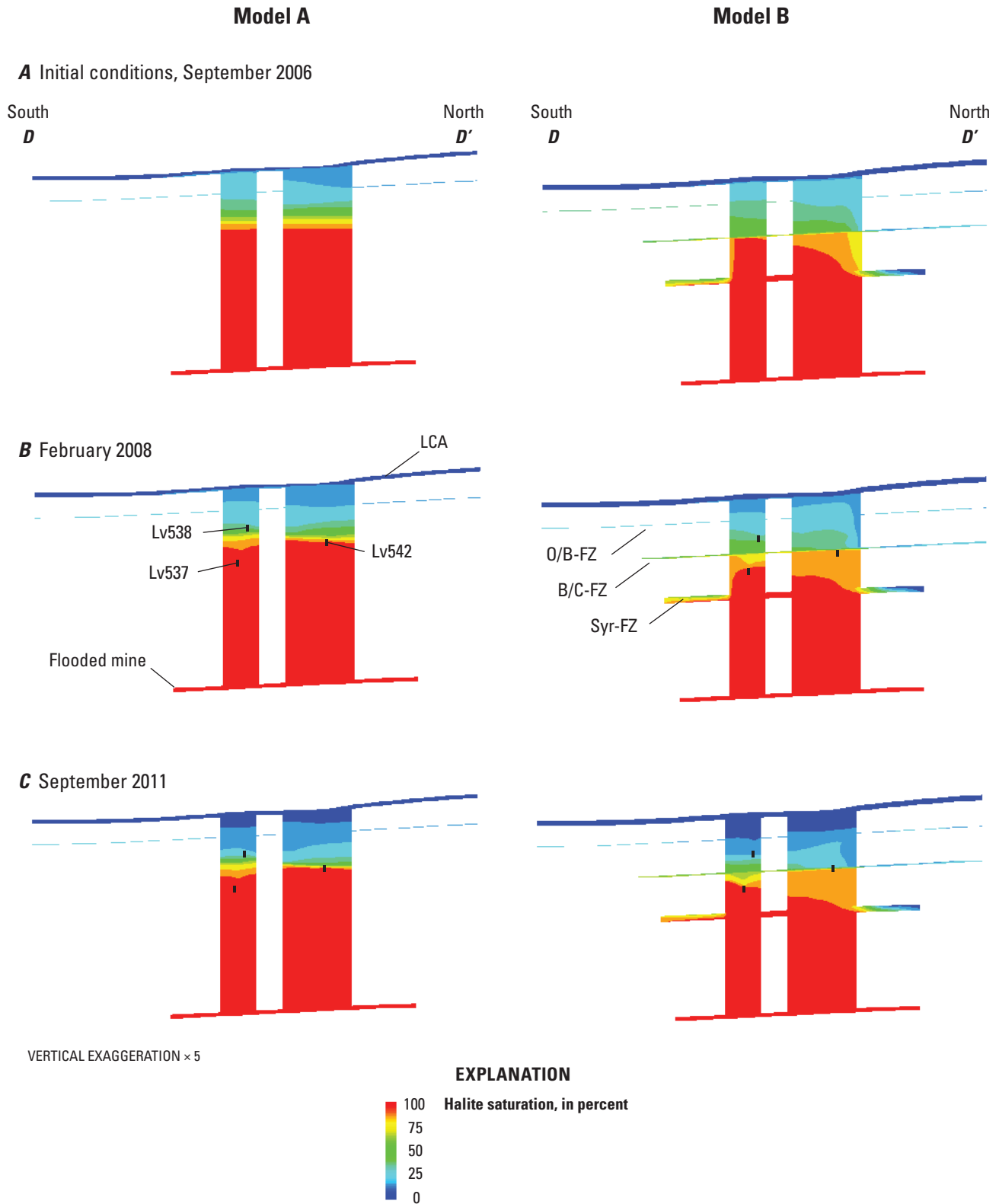
Figure 23.   Section D-D′ showing changes in halite saturations simulated by models A and B in response to pumping from the collapse area: *(A)* initial conditions, September 2006; *(B)* February 2008; and *(C)* September 2011. LCA, lower confined aquifer; fracture zones: O/B-FZ, Onondaga/Bertie contact; B/C-FZ, Bertie/Camillus contact; Syr-FZ, Syracuse Formation. Location of section shown in figure 16.
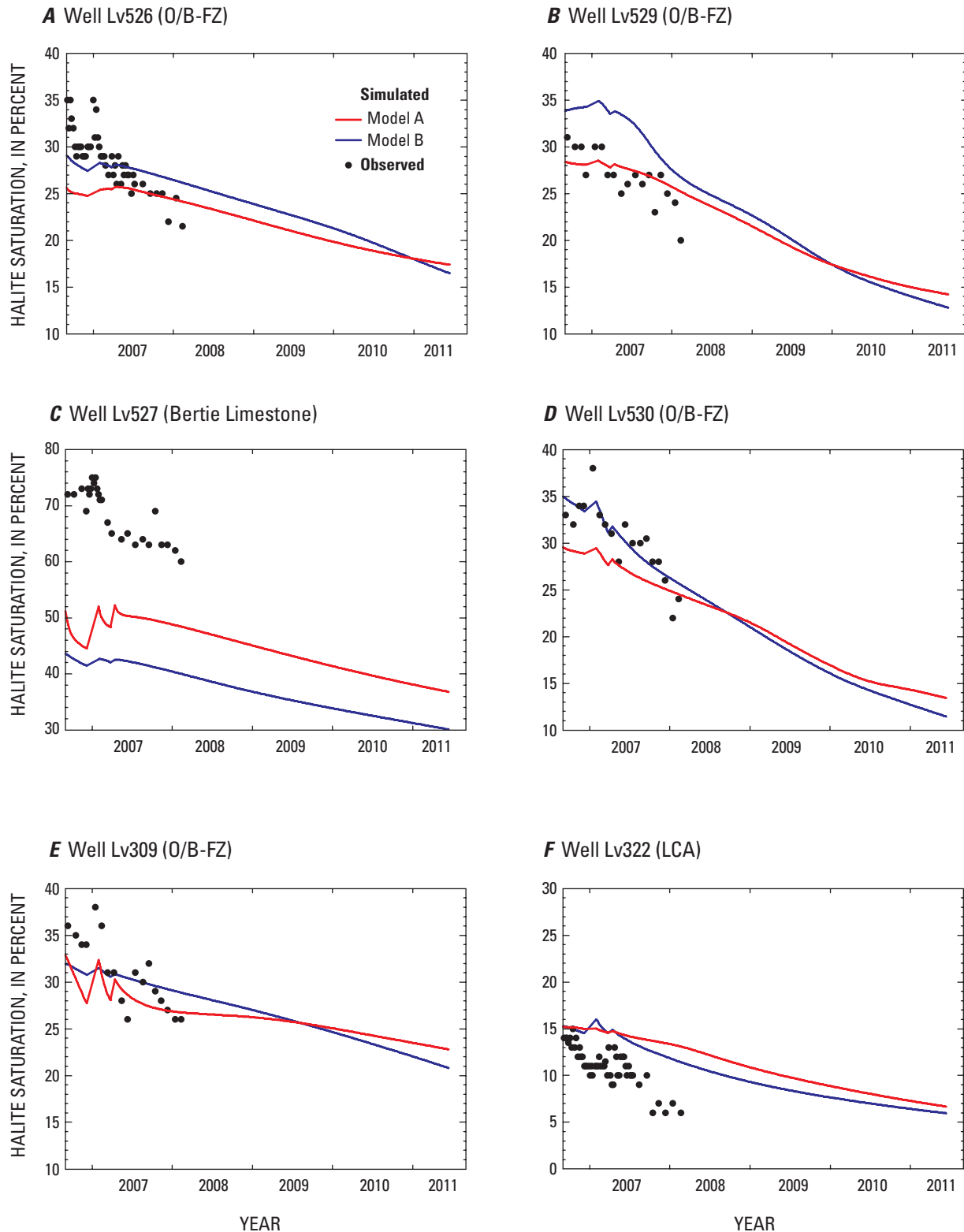
Figure 24.   Changes in halite saturation in the collapse area during pumping from September 2006 through February 2008, and those simulated by models A and B from September 2006 through September 2011: *(A)* well Lv526, *(B)* well Lv529, *(C)* well Lv527, *(D)* well 530, *(E)* well Lv309, and *(F)* well Lv322. Sampled depths correspond to O/B-FZ (Onondaga/Bertie contact fracture zone), with the exception of well Lv527 (Bertie Limestone) and well Lv322 (lower confined aquifer). Note difference in scale in C.
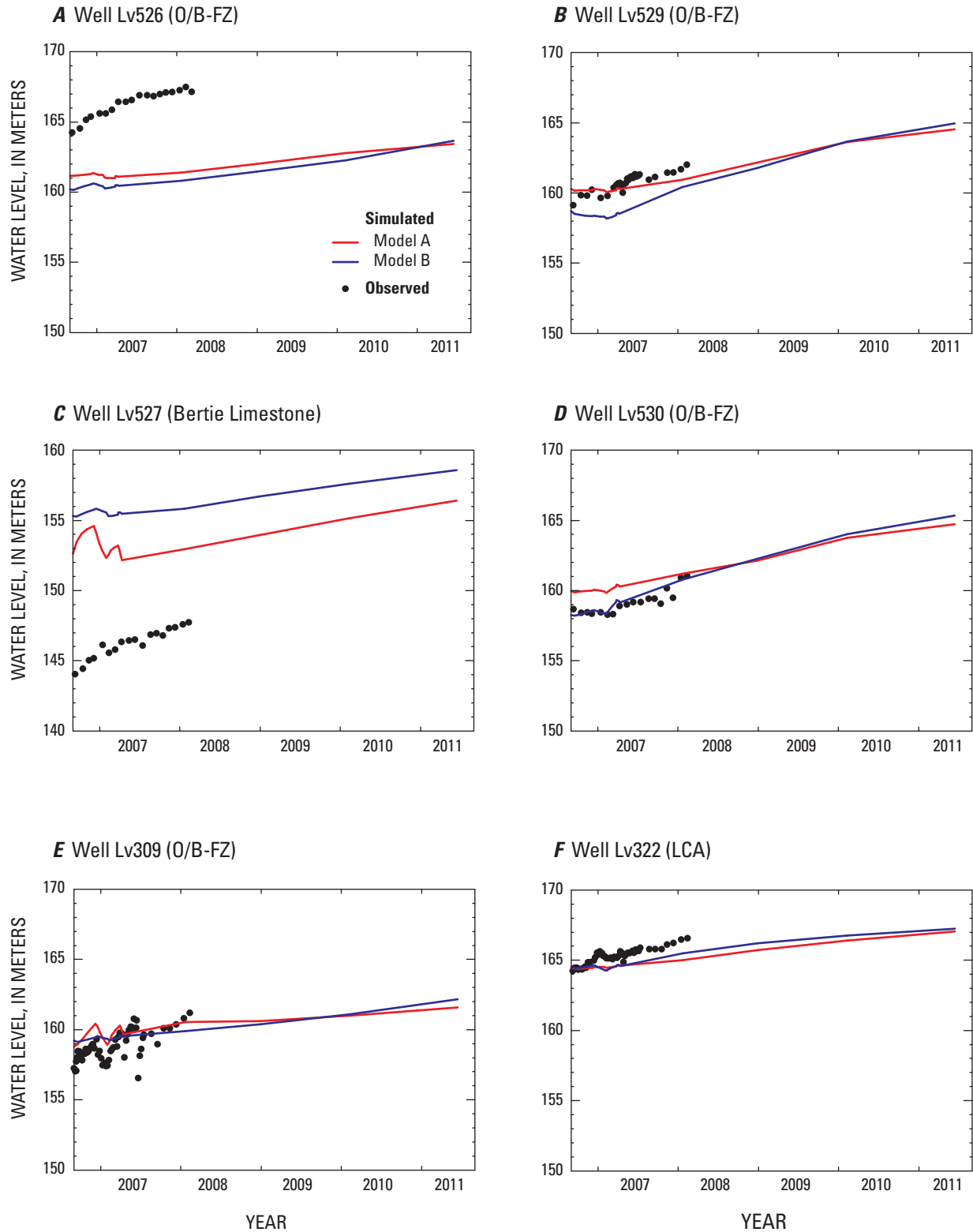
Figure 25.   Changes in water levels in the collapse area during pumping from September 2006 through February 2008, and those simulated by models A and B from September 2006 through September 2011: *(A)* well Lv526, *(B)* well Lv529, *(C)* well Lv527, *(D)* well 530, *(E)* well Lv309, and *(F)* well Lv322. Measurement depths correspond to O/B-FZ (Onondaga/ Bertie contact fracture zone), with the exception of well Lv527 (Bertie Limestone) and well Lv322 (lower confined aquifer).

northern rubble chimney. Observed water levels at well Lv526 are nearly 2 m higher at this elevation than in surrounding areas, indicating the presence of lower salinity water. Both models simulate a larger thickness of low-salinity water above the brine in this area as a result of flow through fracture zones (fig. 23), but still underpredict the observed water levels.

The average halite saturation influent to the desalination plant in February 2008 (78 percent) is better matched by model B (80 percent) than by model A (86 percent). Halite saturations produced by each pumped well also are more closely matched by model B than by model A (table 6), with the exception of that produced by well Lv538 located near the southern rubble chimney, where saturations are underpredicted. These results indicate that the transition zone from saline water to brine is relatively diffuse (as simulated by model B) and not as sharp as that simulated by model A. Both models A and B indicate that water produced by the deeper wells (Lv537 and Lv539) is predominantly brine, but model B predicts that more aquifer water than bedrock water is produced from the shallower wells, which is opposite the pattern predicted by model A (table 6).

Model Sensitivity

The sensitivity of simulated saturations to changes in model parameter values was assessed through two series of eight 5-year simulations conducted with both models A and B. Changes were considered to the specified values of four parameters: (1) hydraulic conductivity of the rubble chimneys and deformation zones (K), (2) porosity of the rubble chimneys (n), (3) brine-displacement rate (Q_{brine}), and (4) pumping rates (Q_{pump}). Values of K and n were both increased by a factor of 2 and decreased by a factor of 10; values of Q_{brine} and Q_{pump} were both doubled and set to zero. Results are shown for simulated saturations at the O/B-FZ in well Lv530, which are best matched by model B. Two other simulations were conducted in which the transverse dispersivity was doubled in model A (to 1.5 m) and halved in model B (to 0.6 m), but these changes had little effect on the simulated saturations and are not shown.

Increasing and decreasing the values of hydraulic conductivity K and porosity n through the range considered had a slight effect on simulated saturations at Lv530 (figs. 26A and B), although the effect was greater for changes in n, especially during the latter part of the simulation. Only the results for model B are shown because the effects of parameter changes were similar for both models. Saturations decreased more slowly with larger n (because the mass of halite in the modeled domain was increased), and decreased more rapidly with smaller n. Changes in the rates of brine displacement Q_{brine} and pumping Q_{pump} caused much greater changes in simulated saturations. These changes had nearly equal, but opposite effects. Doubling Q_{brine} (fig. 26C) caused the simulated saturations to rise from 35 to 60 percent during the 5-year simulation, whereas setting Q_{pump} to zero (fig. 26D) caused simulated saturations to increase to 56 percent. These results are expected because Q_{pump} (2.3 L/s) is slightly greater than Q_{brine} (1.6 L/s), so a cessation of pumping is roughly equivalent to continued pumping with a doubled rate of inflow Q_{brine}.

Decreasing the brine-displacement rate to zero or doubling the pumping rate also had similar effects, reducing the simulated saturations at Lv530 to less than 5 percent within 5 years. These results indicate that the actual brine-displacement rate could be lower than that specified in models A and B because simulated declines in saturations under predict the observed decline at most wells from September 2006 through February 2008. In simulations with Q_{brine} set to zero, the mass of halite produced through February 2008 declined slightly in both models A and B, and the simulated composition of pumped water contained more bedrock water in model A and more aquifer water pumped in model B (table 7). Doubling Q_{pump} doubled the mass of halite produced, and the simulated composition of pumped water was nearly the same as in the simulation with Q_{brine} set to zero.

Discussion of Results

Analysis of the simulated saturations in response to pumping in the collapse area indicates that model B (three fracture zones) better matches the influent saturation to the desalination plant, the amount of halite produced, and the observed declines in saturations than does model A (one fracture zone). This result indicates that the transition zone from saline water to brine is relatively diffuse and has been affected by flow through fracture zones that intersect the collapse area. The composition of saline water in the upper part of the collapse area simulated by model A better matches the results of geochemical models, however. This result indicates that the salinity in the LCA is derived primarily from a mixture of aquifer water and bedrock water, rather than aquifer water and mine water as in model B. Actual conditions in the collapse area, therefore, display some aspects of both models. These results indicate that more than one fracture zone affects the migration of saline water and brine in the collapse area, but that the amount of mixing and rate of fracture flow is less than the amount and rate simulated by model B.

Both models predict that current rates of pumping will cause saturations to decrease in the collapse area and prevent further upward migration of saline water to the LCA. More saline water is removed by pumping in model B, and the simulated level of brine declines further than in model A. The difference in specified porosity of the rubble chimneys in models A and B (10 percent and 6 percent, respectively) accounts for the slightly faster decline in saturations predicted by model B.
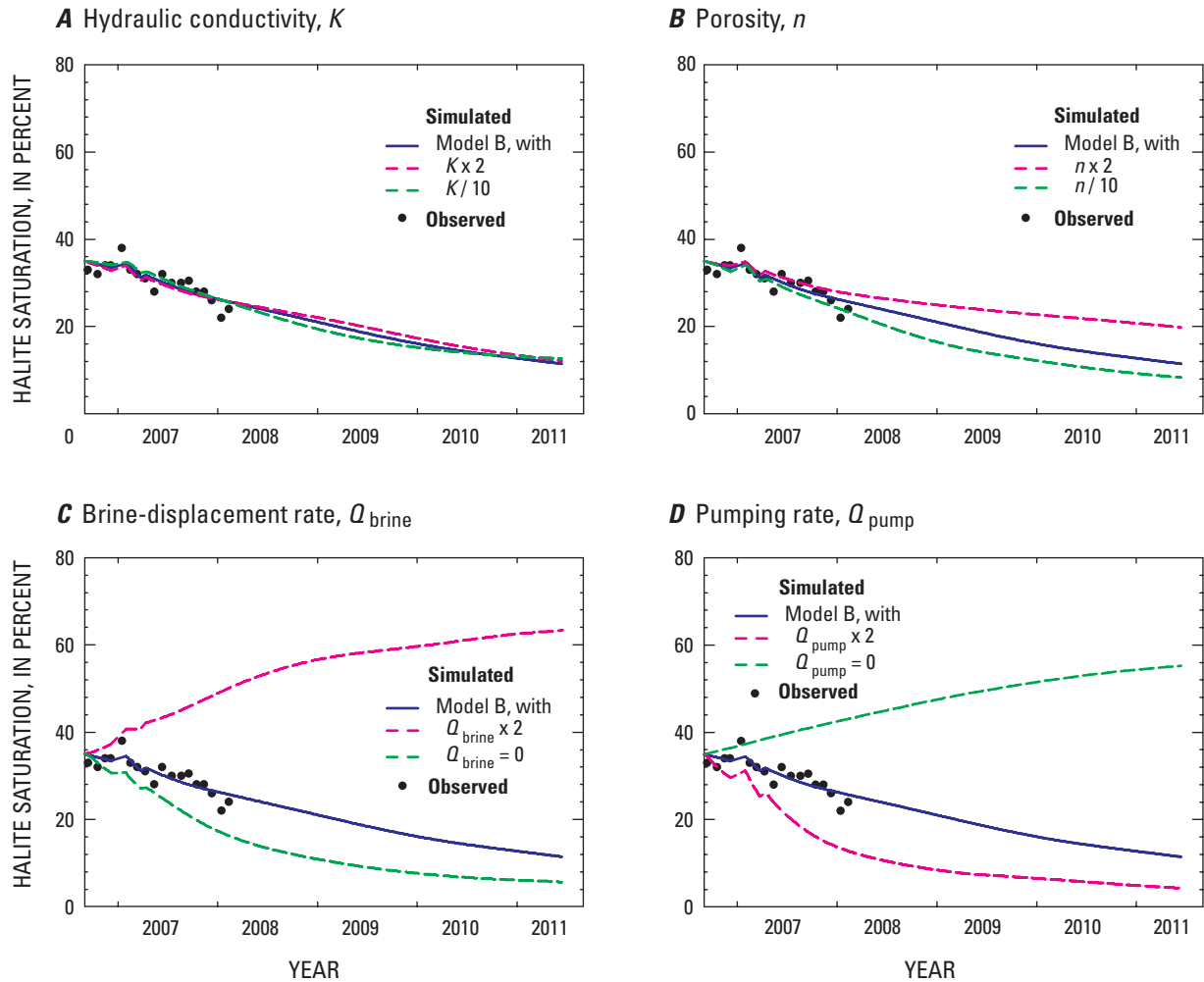
Figure 26. Halite saturations simulated by model B at well Lv530 from September 2006 through September 2011 with different values of *(A)* hydraulic conductivity, *(B)* porosity, *(C)* brine-displacement rates, and *(D)* pumping rates.

Table 7.   Sensitivity of simulated concentrations in February 2008 and mass of halite produced from September 2006 through February 2008 in models A and B to changes in rates of brine displacement (Q_{brine}) and pumping ($Q_{pumping}$).

[kg, kilogram; --, not computed]

	Halite saturation, percent	Water composition, percent			Mass of halite produced, kg
		Mine water	Bedrock water	Aquifer water	
Observed	78	[1]84	[2]16	--	1.97E+07
Model A					
Reported rates	86	78	17	4	2.31E+07
$Q_{brine} = 0$	78	65	29	6	2.15E+07
$Q_{pumping} \times 2$	78	66	25	9	4.29E+07
Model B					
Reported rates	80	75	9	16	2.14E+07
$Q_{brine} = 0$	72	64	11	25	1.99E+07
$Q_{pumping} \times 2$	74	66	10	24	4.04E+07

[1]Volumetric estimate from changes in halite saturation from October 2006 through March 2008 (Alpha Geoscience, 2008).

[2]Saline water composed of both bedrock water and freshwater.

Implications for Future Mitigation Efforts

Current Conditions in the Collapse Area

Simulations of water-level recovery (1996 through 2006) and pumping (2006 through 2011) indicate that the rate of brine displacement from the flooded mine is currently (2008) no more than 1.6 L/s, and that as much as 0.3 L/s could be diverted laterally into the B/C-FZ. Simulations of water-level recovery also indicate that saline water has probably not moved beyond the collapse area, whereas simulations of pumping indicate that further upward migration of brine and saline water has been prevented by groundwater withdrawals under the brine-mitigation project. Salinity within the upper parts of the rubble chimneys and deformation zone is expected to decrease over the next few years if the current rates of pumping are maintained.

Additional 10-year simulations were conducted with model A to predict changes in halite saturation that would occur within the O/B-FZ and the LCA if the brine-mitigation project was shut down in September 2008 after 2 years of pumping. These simulations were similar to the 5-year simulations discussed earlier, with the exception that constant-concentration boundaries in model layer 37 (O/B-FZ) were replaced by constant-head boundaries. The constant heads were computed using reference densities that correspond to saturations of 16 and 30 percent at the northern and southern

boundaries, respectively. This change prevented the simulation of a concentration gradient near the model boundaries and increased the simulated outflow of high-salinity water through the O/B-FZ.

Simulation results indicate that in the absence of pumping, saturated brine will nearly reach the O/B-FZ by September 2011 and that saline water will migrate southward from the collapse area in the LCA (fig. 27). The predicted saturation in the LCA at the southern model boundary in September 2011 is about 10 percent. Saturated brine is predicted to extend throughout the O/B-FZ within the model domain by September 2016 and continue to rise toward the LCA. A plume of saline water extends southward from the collapse area in the LCA to the southern model boundary, where the predicted saturation is about 20 percent. Decreasing the hydraulic conductivity of the O/B-FZ in model A from 15 to 7.5 m/d reduces the flow of saturated brine into the O/B-FZ and results in higher predicted salinities in the LCA. Under this scenario, predicted saturations at the southern model boundary increase to 30 percent in September 2016. In simulations of a shutdown with model B, brine is diverted laterally into the lower two fracture zones. As a result, the level of saturated brine only reaches the B/C-FZ by September 2016, when the predicted saturation at the southern model boundary in the LCA is 12 percent.

Continued monitoring of changes in saturation within the collapse area and fracture zones in the bedrock in response to pumping will provide data that could be used to refine these model predictions. Additional test holes could be drilled to
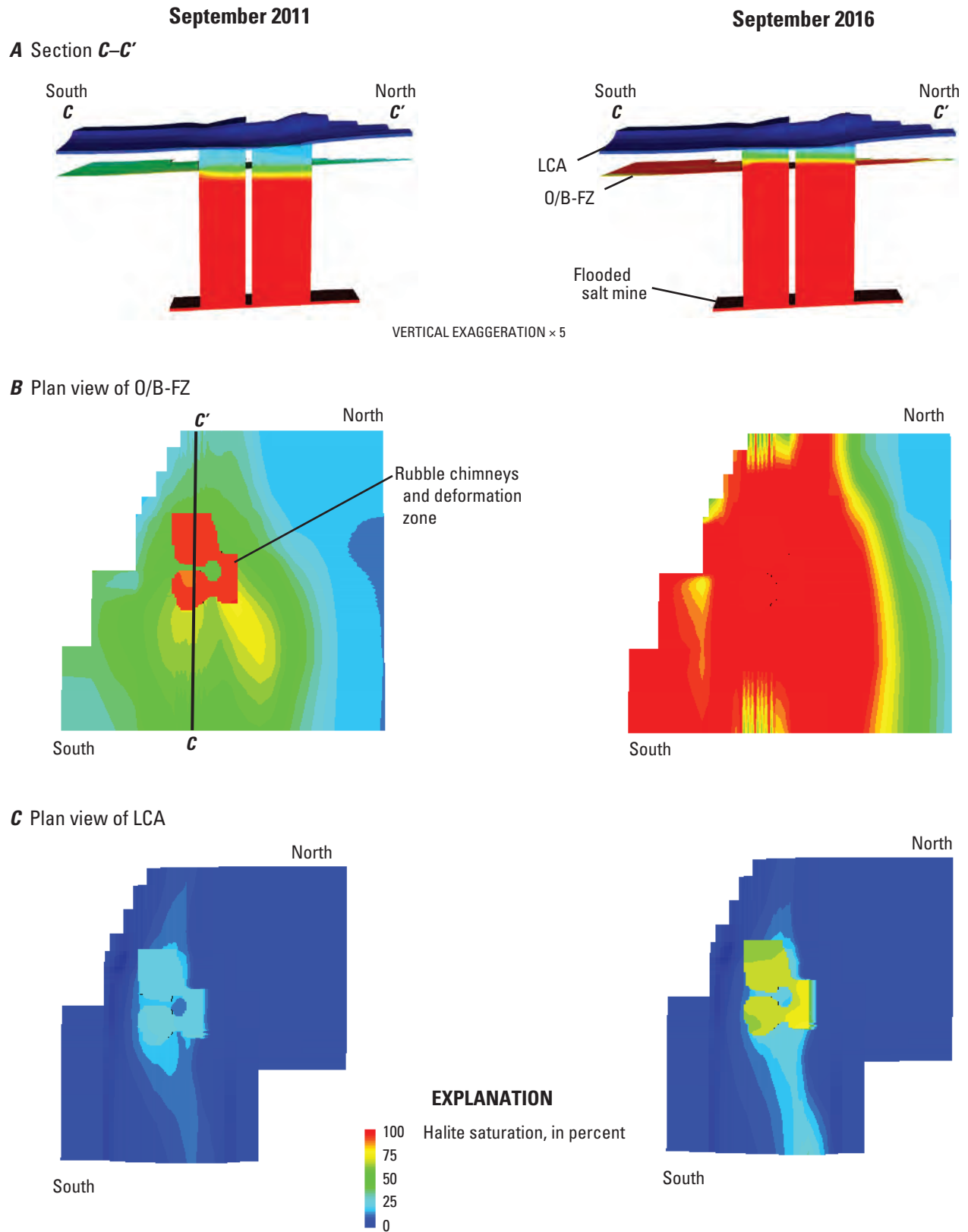
Figure 27. Simulated halite saturations in 2011 and 2016 following shutdown of brine-mitigation project after 2 years of pumping from September 2006 through August 2008: *(A)* along section C-C' through the collapse area, *(B)* in plan view of fracture zone at Onondaga/Bertie contact (O/B-FZ), and *(C)* in plan view of lower confined aquifer (LCA). Location of section shown in figure 16.

the Syracuse Formation outside the collapse area to delineate the extent of the fracture zones and provide additional access points for groundwater sampling. Measurement of groundwater levels in these fracture zones would allow the determination of the hydraulic gradients to better define boundary conditions specified in model simulations. Borehole flowmeter surveys also could be conducted during pumping to provide information on flow contributions from, and the hydraulic properties of, the fracture zones.

Model simulations indicate that saline water will continue to flow upward to the LCA if the brine-mitigation project is terminated. Whether brine eventually reaches the LCA depends upon the assumed properties of fracture zones that intersect the rubble chimneys, which are unknown. Dense, saline water will migrate southward in the LCA along the sloping bedrock surface to its lowest point near Sonyea (fig. 1). A pool of saline water will form in this depression and begin to extend northward and southward upslope as saline water continues to accumulate; however, the large relative density of the saline water will likely prevent it from reaching overlying aquifers. The fate of brine in the bedrock fracture zones is uncertain. Some brine could possibly emerge updip to the north where the subcrop area of the Bertie Limestone intersects the bedrock surface near Avon, but the time of travel cannot be determined on the basis of current information.

The LCA in the Genesee Valley is not currently utilized as a source of groundwater, with the exception of a few residential wells southwest of Avon (fig. 1). The volume of water within the LCA is estimated as 140 million cubic meters, more than twice the volume of brine expected to be displaced from the flooded mine. The water in the LCA is generally potable (chloride concentration less than 250 mg/L), although higher salinity water has been detected north of the collapse area. Steady-state simulations with the groundwater-flow model of the regional aquifer system developed by Yager and others (2001) indicate that the potential yield of the LCA is about 11,000 m^3/d. The total value of this resource includes the volume of water it contains, as well as its value as a storage reservoir.

Considerations for Future Mitigation

The objectives of the brine-mitigation project are to (1) reduce the salinity of water in the upper part of the collapse area and (2) prevent further upward migration of brine through the rubble chimneys (Alpha Geoscience, 2006). Implementation of the plan requires specification of pumping rates and pumped intervals in each of the five wells in the collapse area, which are subject to two constraints. The pumping rate is set less than or equal to the brine-displacement rate to prevent additional upward flow of brine from the flooded mine, which could induce leakage of unsaturated water into the mine and cause further salt dissolution and land subsidence. In addition, water supplied to the desalination plant must be sufficiently saturated to allow for the efficient

production of salt. The distribution of pumping, therefore, must strike a balance between controlling upward brine migration and sustaining the plant operation. The variable-density models described in this report could be used to predict the water composition produced by each pumped well under different pumping scenarios.

The brine-mitigation project implemented in 2006 can be considered a success because pumping controls the upward migration of both brine and saline water within the collapse area, and the desalination plant produces potable water and salt that can be offered for sale. The value of these products is less than the cost of the plant operation, however, and this difference will likely increase as the price of natural gas used to fuel the plant continues to rise (S.W. Gowan, Alpha Geoscience, oral commun., 2008). Moreover, brine displacement from the flooded mine is expected to continue for hundreds of years (John T. Boyd Company, 1995), which will necessitate continued operation of the plant for the indefinite future. The decision whether to continue operation of the plant will likely take into account both the costs of mitigation and the value of the groundwater resource.

The cost of the brine-mitigation operation could be reduced significantly if saline water and brine produced by pumping were utilized directly, thereby saving the cost of desalination. Several areas within the United States are utilizing brine as a de-icing agent for roadways (Donahey and Burkheimer, 1996). De-icing brine also is used in New York State by the New York State Thruway Authority and in some smaller communities, such as the Town of LaFayette, near Syracuse (W.M. Kappel, U.S. Geological Survey, oral commun., 2008). Salt brine offers advantages over dry salt that is commonly used to clear roads of ice and snow because it clings to the road surface and continues to melt ice at temperatures below freezing. As a result, less salt is required, which decreases both the cost of salt and the potential damage to the environment. The use of the saline water and brine produced by the desalination plant as a de-icing agent is under consideration and would likely necessitate the construction of additional storage facilities (S.W. Gowan, Alpha Geoscience, oral commun., 2008).

Summary

Roof collapses in the Retsof salt mine in upstate New York in the spring of 1994 triggered flooding by water from a confined glacial-drift aquifer overlying the mine. Groundwater flowed downward through two rubble chimneys that had propagated upward from the mine through 180 m of shale and carbonate bedrock following the roof collapses. The mine was completely flooded by January 1996 and about 60 billion L of saturated halite brine are currently (2008) present in the mine cavity. The mine cavity is expected to close over the next several hundred years, and as much as 80 percent of the brine could be displaced and migrate upward to the aquifer.

The chloride concentration of water sampled from the aquifer near the collapse area in 2002 was about 20,000 mg/L, indicating that saline water migrating through the rubble chimneys had reached the aquifer. Two possible sources of salinity include (1) saline water flowing through carbonate rocks between the mine and the aquifer, and (2) halite brine displaced from the flooded mine cavity. A brine-mitigation project that includes pumping and desalination of saline water and brine from the collapse area was begun in 2006 to limit further contamination of the confined aquifer. The U.S. Geological Survey began a study in 2006 using geochemical and variable-density flow models to assess the potential sources of salinity and to identify factors that control the movement and mixing of waters in the collapse area. Model simulations were conducted to predict the effect of pumping on salinity within the collapse area in support of the brine-mitigation project. The potential for anhydrite dissolution and land subsidence as a result of pumping and migration of saline water also were assessed.

The collapse area overlying the flooded salt mine is within a bedrock valley that was deepened and widened by ice and filled with more than 150 m of glacial drift. The glacial-drift sediments comprise an aquifer system that contains three aquifers separated by two confining layers. The bottom aquifer (referred to herein as the lower confined aquifer, or LCA) was the source of most of the water that flooded the mine. About 180 m of Silurian and Devonian rock separates the mined salt bed from the bedrock surface in the collapse area. Bedrock units are largely undeformed with bedding that dips to the south at less than 1°.

The roof collapses in the salt mine propagated upward in stages from March through April 1994, forming two rubble chimneys until the bedrock surface was breached, allowing as much as 76 m³/min (1,300 L/s) of freshwater to flow from the LCA to the mine. Two large sinkholes appeared at land surface in April and May 1994 after glacial-drift sediments subsided into cavities created by the collapses. The rubble chimneys are surrounded by a zone of fracturing within the bedrock (the deformation zone) that formed as the rock layers sagged toward the mine cavity after the collapses. Borehole geophysical surveys conducted in April 1994 indicated that water also flowed toward the rubble chimneys through two fracture zones at stratigraphic contacts in the bedrock: an upper zone at the contact between the Onondaga and Bertie Limestones (O/B-FZ), and a lower zone between the Bertie Limestone and the Camillus Shale (B/C-FZ). Subsequent borehole logs conducted in 2004 indicated that the collapse caused increased fracturing in carbonate rock and formed or exposed cavities in the Syracuse Formation (Syr-FZ).

Water levels in the aquifer system began to recover after January 1996 and had nearly returned to pre-collapse conditions by 2006. The closure rate of the mine cavity was estimated from land-surface subsidence above the mine, which ranged from 3 to 18 mm/yr from 1996 through 2001, corresponding to a brine-displacement rate of 4.4 L/s. The brine level in the mine continued to rise through 2007,

increasing the hydrostatic pressure and lowering the rates of subsidence to less than 2 mm/yr and brine displacement to 1.6 L/s. The only outlets for brine displaced from the mine are through the rubble chimneys, although some of the upward-flowing brine could be diverted laterally into voids created by the collapse or fracture zones in the rocks that lie between the mine and the LCA.

Seven inverse geochemical models were developed using PHREEQC to identify mixing proportions of initial waters and water-rock reactions that explain the observed water chemistry in the collapse area. Three initial waters were considered: halite brine from the flooded mine, saline water from the O/B-FZ, and freshwater from the LCA. Some models also included hypothesized bromide-rich brine that was assumed to have formed following precipitation of halite during the Silurian Period. Model results indicate that halite brine in the flooded mine is derived from a mixture of aquifer water (81 percent), bedrock water (16 percent), and bromide-rich brine (3 percent). The simulated mixtures indicate that halite brine flowing upward through the rubble chimneys has been diluted with bedrock water, and that saline water at the O/B-FZ (saturation 36 percent) is a mixture of bedrock water that has been enriched with mine water and diluted by aquifer water. Saline water above the O/B-FZ is a mixture of bedrock water and aquifer water, indicating that water from the flooded mine has not reached the LCA. The principal water-rock reactions included in the inverse models were ion exchange (Ca^{2+} and Mg^{2+} for Na^+), accompanied by the precipitation of anhydrite and calcite, and exsolution of CO_2.

Forward geochemical models were used to quantify mineral dissolution and land subsidence that could result from further mixing of waters induced by pumping from the brine-mitigation project. The models considered mixtures of mine water, bedrock water, and aquifer water, each ranging from 0 to 100 percent, with and without ion exchange. Anhydrite and dolomite were dissolved and calcite was precipitated in forward models, which indicated that subsidence could occur if the volume of voids created by dissolution were not filled by calcite precipitation. Under current (2008) conditions, this situation is unlikely to occur unless either aquifer water or bedrock water that is undersaturated with respect to anhydrite is introduced into the lower part of the rubble chimneys. Maximum predicted subsidence rates (0.6 to 1.1 cm/yr) were computed for mixtures containing more than 40 percent aquifer water, but these predicted subsidence rates decreased to 0.1 to 0.6 cm/yr when ion-exchange reactions were considered. Ion-exchange reactions can, therefore, generally be considered as a geologic safeguard that reduces the potential for subsidence.

The movement of aquifer water, bedrock water, and mine water within the rubble chimneys and surrounding deformation zone during the 10.7-year period following flooding of the salt mine (January 1996 through August 2006) was simulated with a 1D analytical advection-dispersion model, as well as 1D and 3D variable-density, transient groundwater-flow models constructed using SEAWAT. Transport simulations accounted for the effect of variable fluid viscosity on flow and

used a migrating tracer to represent halite saturation, which is linearly related to density. The advection part of the transport equation was solved using the total-variation-diminishing (TVD) method with a courant number of 1.0 to minimize numerical dispersion. The flow and transport equations were explicitly coupled and solved alternately.

One-dimensional models were used to simulate upward flow of brine to the LCA through a single 183-m column, representing a rubble chimney, and were used to estimate the upward rate of brine migration and the longitudinal dispersivity of the rubble material. Saturations computed with a 1D analytical model with a constant concentration boundary closely matched those observed in the lower part of the profile, but underpredicted those measured at the top of the profile. This result indicates that saturations greater than 10 percent at the top of the profile are not derived from simple 1D advective transport and dispersion of brine from the flooded mine. Subsequent 3D models were designed to assess the hypothesis that salinity in the upper part of the profile is derived from inflow of bedrock water from the O/B-FZ, as indicated by inverse geochemical models.

Three-dimensional models were used to simulate the flow of mine water, bedrock water, and aquifer water through the rubble chimneys and surrounding deformation zone, the LCA, and a part of the flooded mine. The 3D models represented a 4.7-km^2 area that was divided into 75 rows and 52 columns, with cell dimensions ranging from 10 m to 300 m. The models contained 159 layers that dip from north to south parallel to the flooded salt mine with layer spacings that range from 4 m in the bottom half of the domain to 0.6 m in the upper half. Two 3D models were constructed: Model A represented one fracture zone (O/B-FZ), whereas three fracture zones were represented in model B, which also included the B/C-FZ and the Syr-FZ.

The 10.7-year transient simulation was preceded by a 1-day steady-state simulation with constant heads specified in the LCA and the flooded mine to provide an initial head distribution. A declining source of brine (6.9 to 1.6 L/s at 100-percent saturation) was injected as recharge into the bottom model layer that represented the flooded mine. Head and concentration boundaries were specified at the northern and southern edges of the model domain in the LCA. A declining rate of saline-water underflow was represented through the O/B-FZ in both models A and B, and underflow through the B/C-FZ was represented in model B through a head-dependent boundary with a relatively low hydraulic conductivity that limited outflow. To simulate initial conditions, the flooded mine was filled with brine; aquifer water occupied the LCA, the rubble chimneys, the deformation zone, and the Syr-FZ, and bedrock water filled the O/B-FZ and the B/C-FZ.

Models A and B were calibrated through trial and error to match halite saturations in time-series plots and a profile observed in September 2006, but were intended to illustrate processes controlling transport, rather than as calibrated representations of the flow system. Values were specified for porosity, longitudinal dispersivity, and hydraulic conductivity

for the following materials: rubble chimneys, deformation zone, LCA, flooded mine, and three fracture zones (O/B-FZ, B/C-FZ, and Syr-FZ). The porosity value for the rubble chimneys was the most sensitive parameter because it determined the velocity of brine migration and the position of the transition zone between brine and saline water in the Bertie Limestone at the end of the 10.7-year simulation. Different values were used in models A and B for porosity (10 and 6 percent, respectively), longitudinal dispersivity (0.6 and 1.5 m, respectively), and mean inflow from the O/B-FZ (1.9 and 1.0 L/s, respectively); all other parameter values were identical.

The saturation profiles simulated with models A and B were similar to that simulated by the 1D model, but better matched the lower saturations (10 to 40 percent) in the upper part of the profile. In model A simulations, saline water from the O/B-FZ entered the rubble chimneys and formed a pool above brine migrating upward from the flooded mine. The brine displaced saline water ahead of it, forming a nearly horizontal brine level in both chimneys with a diffuse front above the transition zone from brine to saline water. Some mine water was displaced upward in the center of the rubble chimneys by the downward flow of bedrock water, but did not reach the LCA. In model B simulations, the rate of saline-water inflow from the O/B-FZ was lower, and mixing with waters from the Syr-FZ and B/C-FZ transported mine water higher in the water column than in model A. Simulated brine levels in both chimneys sloped northward, reflecting lateral diversion of brine into the B/C-FZ. The pool of bedrock water was smaller and more bedrock water was displaced from the O/B-FZ and B/C-FZ, so less aquifer water was displaced from the collapse area in model B than in model A.

Neither model A nor model B indicated that saline water had migrated beyond the collapse area. The origin of salinity in the upper part of the collapse area simulated with model A is consistent with results from inverse geochemical models, whereas the origin of salinity simulated with model B is consistent with original predictions of geotechnical studies and flowmeter surveys that predicted outflow of brine through the B/C-FZ. It is not possible to assess whether model A or model B better represents conditions in the collapse area because the lateral extents of the B/C-FZ and Syr-FZ have not been delineated beyond the collapse area. Boundary conditions specified during the 10.7-year simulation period are uncertain, and estimates of rubble-chimney porosity are correlated with the specified brine-displacement rate. As a result of this uncertainty, both models A and B are nonunique, and may not be accurate representations of flow and transport in the collapse area. The models, however, do simulate the important processes that contributed to the migration of brine and saline water—advection and dispersion of halite brine through the rubble chimneys and deformation zone, and mixing with bedrock water in fracture zones. The relative contributions of mine water, bedrock water, and aquifer water to the simulated salinity within the collapse area are controlled by the rates of flow to and from the three fracture zones.

Changes in water levels and halite saturation produced by pumping for the brine-mitigation project from September 2006 through February 2008 were computed with 5-year transient simulations using both models A and B. Initial and boundary conditions were taken from the 10.7-year simulations of water-level recovery, with the exception of heads at the northern and southern boundaries of the LCA that were adjusted to reflect the 0.3-m decline in head under the northward hydraulic gradient. Groundwater withdrawals were represented by median pumping rates at five wells from September 2006 through February 2008.

Both models indicated that current pumping rates are sufficient to reverse the upward migration of brine and saline water through the collapse area and prevent contamination of the LCA. The simulated decline in saturation was greater in model B, however, because the porosity of the rubble chimneys was lower (6 percent compared to 10 percent in model A), and some brine and saline water were diverted through the B/C-FZ. Model B better matched the influent saturation to the desalination plant, the amount of halite produced, and the observed declines in saturations than model A. This result indicates that a diffuse transition zone from saline water to brine was formed by mixing of waters near fracture zones that intersect the collapse area, as simulated by model B. Sensitivity analyses indicate that rates of brine displacement and pumping are the most important parameters controlling simulated saturations and water levels, and that the actual brine-displacement rate could be lower than the estimated rate because simulated declines in saturations underpredict the observed decline at most wells from September 2006 through February 2008.

Simulations of water-level recovery (1996 through 2006) and pumping (2006 through 2011) indicate that the rate of brine displacement from the flooded mine is currently (2008) 1.6 L/s or less, and that as much as 0.3 L/s could be diverted laterally into the B/C-FZ. Simulations of water-level recovery also indicate that saline water has not moved beyond the collapse area, whereas simulations of pumping indicate that further upward migration of brine and saline water has been prevented by the brine-mitigation project. Halite saturations within the upper part of the collapse area are expected to decrease over the next few years if the current rates of pumping are maintained. Simulations of a shutdown of the brine-mitigation project indicate that further upward migration of brine through the rubble chimneys and into the O/B-FZ would occur. Under this scenario, saline water would reach the southern model boundary within 10 years—the predicted salinity depends on the assumed properties of fracture zones that intersect the rubble chimneys, which are unknown. If the project is terminated, dense saline water will probably migrate southward along the sloping bedrock surface and form a pool within the LCA in a depression near Sonyea. Some brine that enters bedrock fracture zones could possibly emerge updip to the north where the subcrop area of the Bertie Limestone intersects the bedrock surface near Avon, but the time of travel is unknown.

References Cited

Alpha Geoscience, 1996, Geologic and hydrogeologic investigation of the Genesee River Valley: Albany, NY, Alpha Geoscience, 31 p.

Alpha Geoscience, 2003, Conceptual brine management plan for the collapse area of the former Retsof mine: Clifton Park, NY, Alpha Geoscience, 19 p.

Alpha Geoscience, 2005, Comprehensive summary report, Retsof brine mitigation project: Clifton Park, NY, Alpha Geoscience, 45 p.

Alpha Geoscience, 2006, Pumping test and monitoring plan, Retsof brine mitigation project: Clifton Park, NY, Alpha Geoscience, 26 p.

Alpha Geoscience, 2007, December 2006 quarterly report for the Akzo brine mitigation project: Clifton Park, NY, Alpha Geoscience, 9 p.

Alpha Geoscience, 2008, April 2008 quarterly report for the Akzo brine mitigation project: Clifton Park, NY, Alpha Geoscience, 12 p.

Berest, P., Brouard, B., and Feuga, B., 2004, Dry mine abandonment: Wichita, KS, Proceedings of Spring 2004 Conference, Solution Mining Research Institute, p. 1–28.

Carpenter, A.B., and Trout, M.L., 1978, Geochemistry of bromide-rich brines of the Dead Sea and Southern Arkansas, in Johnson, K.S., and Russell, J.A., eds., Oklahoma Geological Survey Circular 79, Proceedings of the 13th Annual Meeting of the Forum on the Geology of Industrial Minerals, May 12–14, 1977, Norman, OK, p. 78–88.

Dobecki Earth Sciences, Inc., 1994, Phase III seismic survey above 11 West panel, Akzo Nobel Retsof mine: Houston TX, Dobecki Earth Sciences, Inc., 20 p.

Donahey, T.J., and Burkheimer, Dennis, 1996, Prewetting with salt brine: Semisequicentennial Transportation Conference Proceedings, May 1996, Iowa State University, Ames, IA, accessed May 15, 2008, at http://www.ctre.iastate.edu/pubs/semisesq/session1/donahey/index.htm.

Gowan, S.W., and Trader, S.M., 2000a, Mine failure associated with a pressurized brine horizon—Retsof salt mine, western New York: Environmental & Engineering Geoscience, v. 6, no. 1, p. 57–70.

Gowan, S.W., and Trader, S.M., 2000b, The mechanism of sinkhole formation above the collapse of a small yield-pillar panel in the Retsof salt mine: Encinitas, CA, Proceedings of 2000 Fall Meeting, Solution Mining Research Institute, p. 313–328.

Guo, Weixing, and Langevin, C.D., 2002, User's guide to SEAWAT: A computer program for simulation of three-dimensional variable-density groundwater flow: U.S. Geological Survey Techniques of Water-Resources Investigations, book 6, chap. A7, 77 p.

Harbaugh, A.W., Banta, E.R., Hill, M.C., and McDonald, M.G., 2000, MODFLOW-2000, the U.S. Geological Survey modular groundwater model—user guide to modularization concepts and the groundwater flow process: U.S. Geological Survey Open-File Report 00–92, 121 p.

Hilderbrand, K.S., Jr., 1999, Preparation of salt brines for the fishing industry: ORESU-H-99-002 (formerly SG22), accessed January 15, 2008, at http://seagrant.oregonstate.edu/sgpubs/onlinepubs/h99002.pdf

John T. Boyd Company, 1995, Impact analysis—Retsof Mine, Akzo Nobel Salt, Inc.: Pittsburgh, PA, John T. Boyd Company, 50 p.

Langevin, C.D., Shoemaker, W.B., and Guo, Weixing, 2003, MODFLOW-2000, the U.S. Geological Survey modular groundwater model—Documentation of the SEAWAT-2000 version with the variable-density flow process (VDF) and the integrated MT3DMS transport process (IMT): U.S. Geological Survey Open-File Report 03–426, 43 p.

Langevin, C.D., Thorne, D.T., Jr., Dausman, A.M., Sukop, M.C., and Guo, Weixing, 2007, SEAWAT Version 4: A computer program for simulation of multi-species solute and heat transport: U.S. Geological Survey Techniques and Methods book 6, chap. A22, 39 p.

New York State Department of Environmental Conservation, 1997, Collapse and flooding of Akzo Nobel's Retsof salt mine, Livingston County, N.Y.: Albany, NY, Division of Mineral Resources, 113 p.

Ogata, Akio, 1970, Theory of dispersion in a granular medium: U.S. Geological Survey Professional Paper 411–I, 34 p.

Parkhurst, D.L., and Appelo, C.A.J., 1999, User's guide to PHREEQC (Version 2)—A computer program for speciation, batch-reaction, one-dimensional transport, and inverse geochemical calculations: U.S. Geological Survey Water-Resources Investigations Report 99–4259, 310 p.

Plummer, L.N., Parkhurst, D.L., Fleming, G.W., and Dunkle, S.A., 1988, Computer program incorporating Pitzer's equations for calculation of geochemical reactions in brines: U.S. Geological Survey Water-Resources Investigations Report 88–4153, 310 p.

RE/SPEC, Inc., 2003, Calculation of brine squeeze rate from Retsof, NY, mine: Rapid City, SD, RE/SPEC Consulting & Services, 9 p.

Richard F. Langill and Associates, 1990, Subsidence and groundwater inflow at the Sterling Mine: Germantown, MD, Richard F. Langill and Associates, 23 p.

Rolleke, F.J., 2000, Subsidence and sinkholes over flooded potash mines in northern Germany: San Antonio, TX, Proceedings of 2000 Fall Meeting, Solution Mining Research Institute, p. 87–101.

Runnells, D.D., 1969, Diagenesis, chemical sediments and the mixing of natural waters: Journal of Sedimentary Petrology, v. 39, no. 3, p. 1,188–2,101.

Thoms, H., and Gehle, R.M., 1994, The Jefferson Island mine flooding revisited: Houston, TX, Proceedings of 1994 Spring Meeting, Solution Mining Research Institute.

Thorne, D.T., Langevin, C.D., and Sukop, M.C., 2006, Addition of simultaneous heat and solute transport and variable fluid viscosity to SEAWAT: Computer and Geosciences, v. 32, no. 10, p. 1,758–1,768.

Van Sambeek, L.L., and Thoms, R., 2000, Pre- and post-flooding surface subsidence rates at the Retsof, Belle Isle, Jefferson Island salt mines: San Antonio, TX, Proceedings of 2000 Fall Meeting, Solution Mining Research Institute, p. 75–85.

Williams, J.H., 1996, Application of borehole geophysics at the Retsof salt-mine collapse site, western New York, *in* Bell, R.S., and Cramer, M.H., eds., Proceedings of Symposium on the Application of Geophysics to Engineering and Environmental Problems, Environmental and Engineering Geophysical Society, Keystone, CO, p. 813–822.

Yager, R.M., and Fountain, J.C., 2001, Effect of natural gas exsolution on specific storage in a confined aquifer undergoing water-level decline: Ground Water, v. 39, no. 4, p. 517–525.

Yager, R.M., Miller, T.S., and Kappel, W.M., 2001, Simulated effects of 1994 salt-mine collapse on groundwater flow and land subsidence in a glacial aquifer system, Livingston County, New York: U.S. Geological Survey Professional Paper 1611, 85 p.

Zheng, Chunmiao, and Wang, P.P., 1998, MT3DMS: A modular three-dimensional multi-species transport model for simulation of advection, dispersion, and chemical reactions of contaminants in groundwater systems: Vicksburg, MS, U.S. Army Corps of Engineers, Waterways Experiment Station, 191 p.

Appendix.   Wells and boreholes in and near the collapse area above the flooded Retsof salt mine.

[USGS, U.S. Geological Survey]

| Well number | | | Type | Monitored or pumped interval |
USGS	API[1]	Local		
Lv301	21508	9401	Monitoring well	Flooded mine
Lv305	21510	9405	Borehole	None
Lv309	21516	9409	Monitoring well	Onondaga Limestone to Syracuse Formation
Lv322	21528	9422	Monitoring well	Lower confined aquifer
Lv326	21532	9426	Borehole	None
Lv328	21534	9428	Borehole	None
Lv343	21557	9443	Borehole	None
Lv346	21561	9446	Monitoring well	Onondaga Limestone
Lv368	21602	9568	Monitoring well	Lower confined aquifer
Lv396	21620	9572	Monitoring well	Flooded mine
Lv526	23103	0401	Monitoring well	Onondaga Limestone to Camillus Shale
Lv527	23106	0402	Monitoring well	Onondaga Limestone to Syracuse Formation
Lv528	23107	0403	Monitoring well	Onondaga Limestone to Bertie Limestone
Lv529	23108	0404	Monitoring well	Onondaga Limestone to Bertie Limestone
Lv530	23109	0405	Monitoring well	Onondaga Limestone to Bertie Limestone
Lv531	23194	0501	Monitoring well	Lower confined aquifer
Lv532	23195	0502	Monitoring well	Onondaga Limestone to Bertie Limestone
Lv533	23196	0503	Monitoring well	Onondaga Limestone to Bertie Limestone
Lv534	23197	0504	Monitoring well	Onondaga Limestone to Bertie Limestone
Lv535	23198	0505	Monitoring well	Lower confined aquifer
Lv536	23199	0506	Monitoring well	Onondaga Limestone to Bertie Limestone
Lv537	23209	0507	Pumped well	Camillus Shale
Lv538	23204	0508	Pumped well	Bertie Limestone
Lv539	23205	0509	Pumped well	Syracuse Formation
Lv540	23206	0510	Pumped well	Bertie Limestone
Lv541	23206	0511	Pumped well	Syracuse Formation
Lv542	23208	0512	Pumped well	Camillus Shale

[1]American Petroleum Institute; well-identification number assigned by New York State Department of Environmental Conservation.

USGS